Investigation into the Reinforcement Effect of Filler Nanoparticles in Polymer-Silica Nanocomposites and the Effects of Physical Aging on SAN Nanocomposites

Amy Louise Bremner

Thesis Submitted to Heriot Watt University for the degree of:

Masters of Research in Materials Chemistry

Project Supervisor: Dr Valeria Arrighi

Department of Engineering and Physical Sciences

Heriot Watt University

May 2019

Research Thesis Submission

Please note this form should be bound into the submitted thesis.

Name*:*	Amy Louise Bremner		
School:	EPS		
Version: *(i.e. First, Resubmission, Final)*	First	Degree Sought:	MRes Materials Chemistry

Declaration

In accordance with the appropriate regulations I hereby submit my thesis and I declare that:

1. The thesis embodies the results of my own work and has been composed by myself
2. Where appropriate, I have made acknowledgement of the work of others
3. Where the thesis contains published outputs under Regulation 6 (9.1.2) these are accompanied by a critical review which accurately describes my contribution to the research and, for multi-author outputs, a signed declaration indicating the contribution of each author (complete Inclusion of Published Works Form – see below)
4. The thesis is the correct version for submission and is the same version as any electronic versions submitted*.
5. My thesis for the award referred to, deposited in the Heriot-Watt University Library, should be made available for loan or photocopying and be available via the Institutional Repository, subject to such conditions as the Librarian may require
6. I understand that as a student of the University I am required to abide by the Regulations of the University and to conform to its discipline.
7. Inclusion of published outputs under Regulation 6 (9.1.2) shall not constitute plagiarism.
8. I confirm that the thesis has been verified against plagiarism via an approved plagiarism detection application e.g. Turnitin.

* *Please note that it is the responsibility of the candidate to ensure that the correct version of the thesis is submitted.*

Signature of Candidate*:*	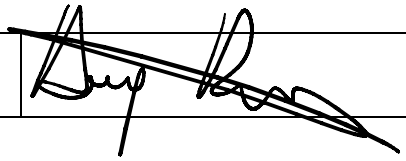	Date:	18/05/2019

Submission

Submitted By *(name in capitals):*	AMY LOUISE BREMNER
Signature of Individual Submitting:	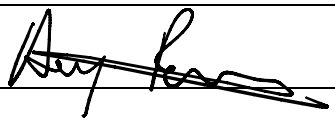

Date Submitted:	18/05/2019

For Completion in the Student Service Centre (SSC)

Received in the SSC by *(name in capitals):*			
Method of Submission *(Handed in to SSC; posted through internal/external mail):*			
*E-thesis Submitted (**mandatory for final theses)***			
Signature:		Date:	

Inclusion of Published Works

Declaration

This thesis contains one or more multi-author published works. In accordance with Regulation 6 (9.1.2) I hereby declare that the contributions of each author to these publications is as follows:

Citation details	e. g. Author 1 and Author 2, Title of paper, Title of Journal, X, XX-XX (20XX)
Author 1	Contribution….
Author 2	Contribution….
Signature:	
Date:	

Citation details	e. g. Author 1 and Author 2, Title of paper, Title of Journal, X, XX-XX (20XX)
Author 1	Contribution….
Author 2	Contribution….

Signature:	
Date:	

Citation details	e. g. Author 1 and Author 2, Title of paper, Title of Journal, X, XX-XX (20XX)
Author 1	Contribution….
Author 2	Contribution….
Signature:	
Date:	

Abstract

This work investigated the reinforcement effects of the addition of silica nanoparticles to a polymer and the aging effects on the characteristics of styrene acrylonitrile (SAN). The nanoparticles that were investigated in this study included hydrophilic silica (HDK-I) and hydrophobic silica (HDK-O), with both having the same surface area and diameter this allowed for study into the nature of the silica and if this had any effect on the aging of the nanocomposites. The final silica nanoparticle used was colloidal MEK-ST, this nanoparticle had a different diameter and surface area to the HDK samples. This allowed for the comparison between the fumed silica samples and the colloidal as well as size of nanoparticle. With regards to quantity of nanoparticle, from studies by Fu *et al* and Feng, a ratio of 10% silica nanoparticle to 90% polymer was used. For ease 0.1g of silica nanoparticle was combined with 0.9g of polymer.

In this study the addition of silica nanoparticles appeared to have negligible reinforcement effects upon the polymers thermal and mechanical properties. The effect of this addition was seen by a limited increase in both the glass transition temperatures and storage moduli of the polymer-silica nanocomposites.

An investigation of the glass transition temperatures of unaged and aged samples revealed, data for the relaxation enthalpies and free volumes of SAN nanocomposites. It was found that upon physical aging of the samples, the HDK-O and MEK-ST nanocomposites exhibited the greater reinforcement compared to the HDK-I, with respect to the DSC, DMA and master curve data. For the thermal effects upon aging of the nanocomposite samples the HDK-O sample exhibited the greatest reinforcement of $+1.8^{O}C$ for 24 hours aged, $+3.5^{O}C$ for 72 hours aged and $+3.5^{O}C$ for 168 hours aged. For the mechanical effects upon aging of the nanocomposite the storage modulus increased by $4.7^{O}C$ for the MEK-ST sample at 24 hours aging while the other samples showed negligible increase. At 72 hours aged, once again the HDK-O and MEK-ST samples exhibited an increase in the storage modulus. At 168 hours aging all samples had similar results. The HDK-I samples were found to have similar results of the unmodified polymer. This suggested that possibly the hydrophobicity of the silica played a role in the reinforcement effects.

Acknowledgements

I would like to thank Dr Valeria Arrighi for her continued support, guidance, and advice throughout my project. Her knowledge and patience were greatly appreciated.

I would also like to thank my grandmother, my parents and my partner for their continual love and support during my studies.

Contents

List of Figures

List of Equations

List of Tables

CHAPTER 1: INTRODUCTION

1.1 Polymer/Silica Nanocomposites

In the past several years there has been a great interest in polymer-inorganic nanocomposites, this is primarily due to their interesting electrical, physical, optical and chemical properties.[1] Many groups have reported the superior properties of these polymer nanocomposites in comparison to their unmodified polymer counterparts, including Patel *et al*[1], Saladino[2] and Feng[3]. These desirable properties lead to applications in both industry and academia, for example coatings, photo-resistant materials, flame-retardant materials and optical devices.[4].

These hybrid materials incorporate the thermal stability and toughness of the inorganic filler nanoparticle and the malleability and ductility of the organic polymer[5]. There are several different types of inorganic nano-filler particles, these include silicon, metal oxide nanoparticles and even some semi-conductors[4].

In this project silica nanoparticles (SiNPs) were chosen for their high mechanical strength, chemical and thermal stability, high surface area and low refractive index[5]. The addition of SiNPs to polymers has been shown to improve the materials insulation properties, augment film mechanical properties as well as reduce thermal degradation at elevated temperatures[5].

The Royal Society of Chemistry (RSC) describes a composite as "a material made by combining two or more materials - often ones that have very different properties"[6]. This includes composite materials such as fiberglass, a composite of plastic and glass woven into fibres which is often used in boat hulls, car bodies, *etc.* Thin carbon fibres are also bound to plastic polymer resins to form a versatile material that is both strong and lightweight. These carbon fibre composites are used in golf clubs and even in aeroplane panels. A composite material has the ability to combine the desirable properties of each different individual material and form a hybrid.

As well as combining polymer resins with carbon fibres other filler particles can be added to change the desired properties of the hybrid. In recent years nanoparticles have drawn great attention from both academia and industry. Nanoparticles are particles that

span the size range of between 1 and 100 nm. It is the smallest unit size that can still behave as a whole entity with respect to its properties and transport[7].

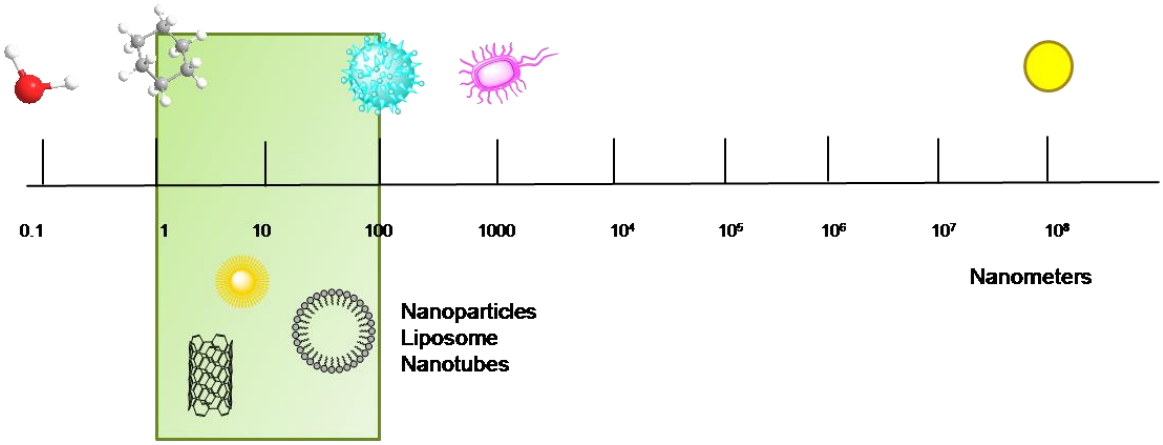

Figure 1.1: Nanoscale Diagram highlighting the differences in size between molecules[8]

Nanoparticles can be seen as a bridge between large bulky materials and atomic/molecular structures. As can be seem from figure 1.2, this had led to an increased interest in their uses and an ever-growing use of them in everyday materials. Within 4 years the number of consumer products using nanomaterials grew from only 54 in 2005, to over 1,000 in 2009.

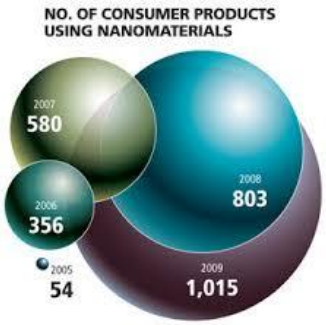

Figure 1.2: Number of products containing nanomaterials per year[9]

1.2 Silica Nanoparticles

Silica is often used in the production of nanocomposites due to its well-ordered structure, high surface area, cost-effective production and the ease at which its surface can be modified. When combined with polymers, silica can improve the thermal and mechanical properties as well as the materials ability to perform under environmental conditions[10]. Silica plays several important roles within industry and nature[11, 12]. Silicon is one of the most abundant elements in the Earth's crust and is commonly found as silica ore[11]. However, in its raw form it is difficult to guarantee the size and purity of the silica, therefore nanoscale silica is often made *via* controlled synthesis routes (e.g. RAFT, NMP, etc.). There are two main types of silica nanoparticles (SiNPs): fumed and colloidal. Both were used in this project.

The surface of an unmodified silica nanoparticle consists of multiple hydroxyl groups (figure 1.3). It is these hydroxyl groups that account for the bonding and interactions of the silica with other compounds and indeed itself.

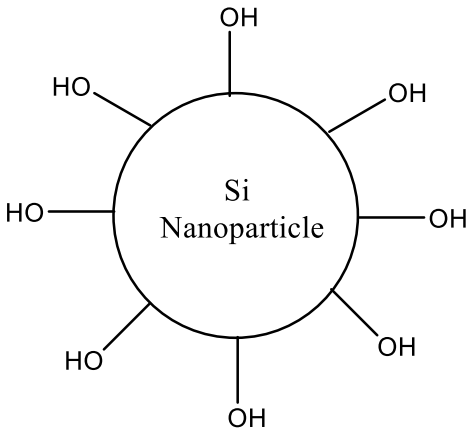

Figure 1.3: Schematic diagram of an unmodified silica nanoparticle

The hydroxyl groups on the surface of the silica accompanied by the large surface area of the SiNPs can lead to the formation of agglomerates. An agglomerate is described as a group or cluster of particles. This is caused by the inter-particle interactions (hydrogen bonding interactions)[13] of the silanol (Si-OH) groups. The silanol groups act as receptive centres and can also form hydrogen bonds with other polar substances[13].

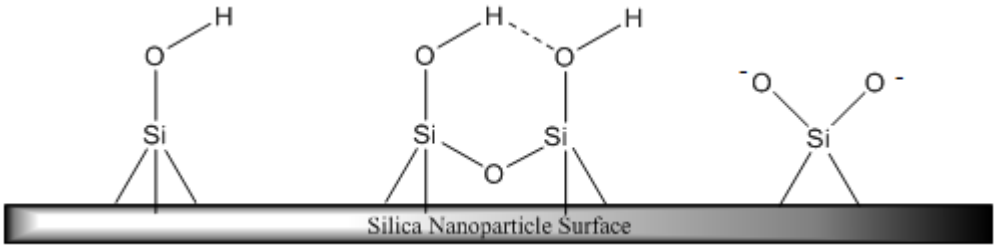

Figure 1.4: Silica nanoparticle surface

Colloidal silica is a stable dispersion of solid silica particles in a charged solution to prevent the silica from escaping the suspension. If not charged, then the silica particles may be able to evaporate out of the solution. It is found to have several applications in semiconductor wafer polishing, coatings, textiles and as an inorganic binder as stated by Lim[12]. Colloidal silica can be prepared *via* numerous methods. These methods as mentioned by Lim[12] include ion exchange, neutralization/electrolysis of aqueous silicates, the hydrolysis and condensation of silane and the direct oxidation of silicon. Colloidal silica is often characterised by its percentage content in solution, pH and particle size.

The second type of silica used in this project was fumed silica. Fumed silica is generally made *via* the high temperature hydrolysis of silicon tetrachloride in a flame. The Wacker Company[13] describe their production of fumed silica as the hydrolysis of pyrogenic silica and hydrogen chloride in a flame at over 1000ºC. Fumed silica is commonly used in rheology control, reinforcing agents, thickeners and flow enhancers. Fumed silica can also be modified in order to make it either hydrophobic or hydrophilic. Unmodified silica is hydrophilic with silanol groups on the surface (figure 1.4). In order to modify the silica, hydrophobic compounds are heated in the presence of a gas, with the purpose of distributing the modifiers homogeneously on the silica particle surfaces. Some typical modifiers include organochlorosilanes, polydimethylsiloxanes and long chain alkylsilanes.

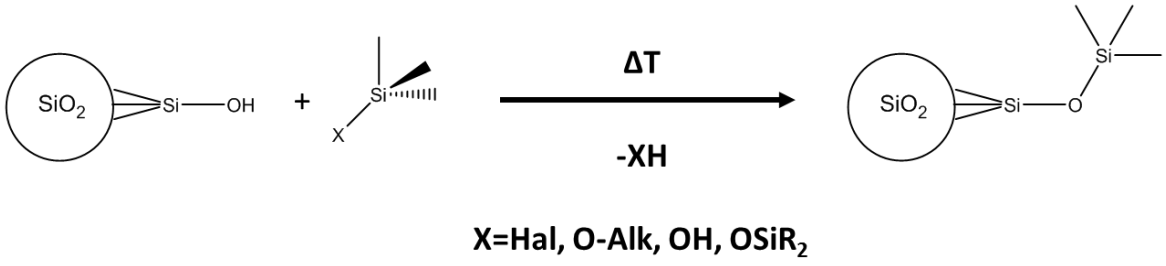

Figure 1.5: Production of hydrophobic silica

1.3 Hydrogen Bonding in Composites

According to IUPAC, a hydrogen bond is an electrostatic attraction between polar groups that occurs when a hydrogen atom is bound to a highly electronegative atom, such as oxygen, nitrogen or fluorine. The small size of the hydrogen molecule permits the attraction of a nearby electronegative atom. Hydrogen bonds can be intramolecular and intermolecular[14].

There are several factors that can affect the strength of hydrogen bonds, these include distances between donor and acceptor groups, bond angles and the number of donor and acceptor groups, as well as temperature and pressure[15].

Within the SiNPs there can be a high degree of aggregation. This comes from the intermolecular hydrogen bonds. If the attraction of the filler-filler is greater than that of the filler-polymer then it can lead to large agglomerates of silica and therefore a non-homogenous composite. Similarly, if the polymer-polymer interactions are greater than the filler-polymer interactions then this again can lead to a non-homogenous composite which is important for the functionality of the materials properties. A non-homogenous material caused by areas of large agglomerates can make the material brittle.

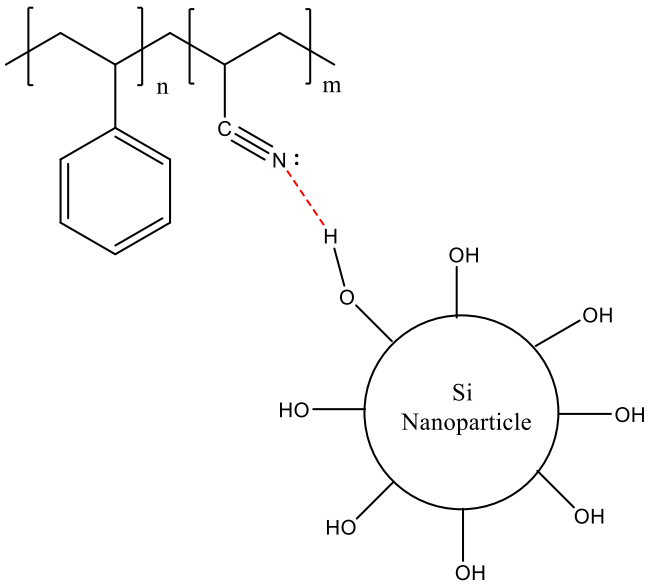

Figure 1.6: Hydrogen bonding of SAN and a SiNP

1.4 Nature of the Glass Transition

1.4.1 The Glass Transition

The glass transition temperature (T_g) is described as the temperature at which an amorphous polymer goes from the glassy state to the rubbery state or *vice versa*. Therefore, it is necessary to know the T_g of a material in order to determine its applications. The glassy state is also synonymous with a non-equilibrium state[16]. Polymer glasses are usually made up of long chains of random conformation which in the liquid state have very high viscosities. Upon cooling, the molecular movement of the chains is too lethargic or the geometry too cumbersome to form a crystalline structure[17]. Therefore, the chain arrangement is random.

When a material is heated through its glass transition the chains go from a high density packing and low free volume state to a situation with greater free volume and lower density of chain packing. A glass transition is observed over a range of temperatures (figure 1.7). From a differential scanning calorimetry (DSC) thermogram the glass transition can be measured.

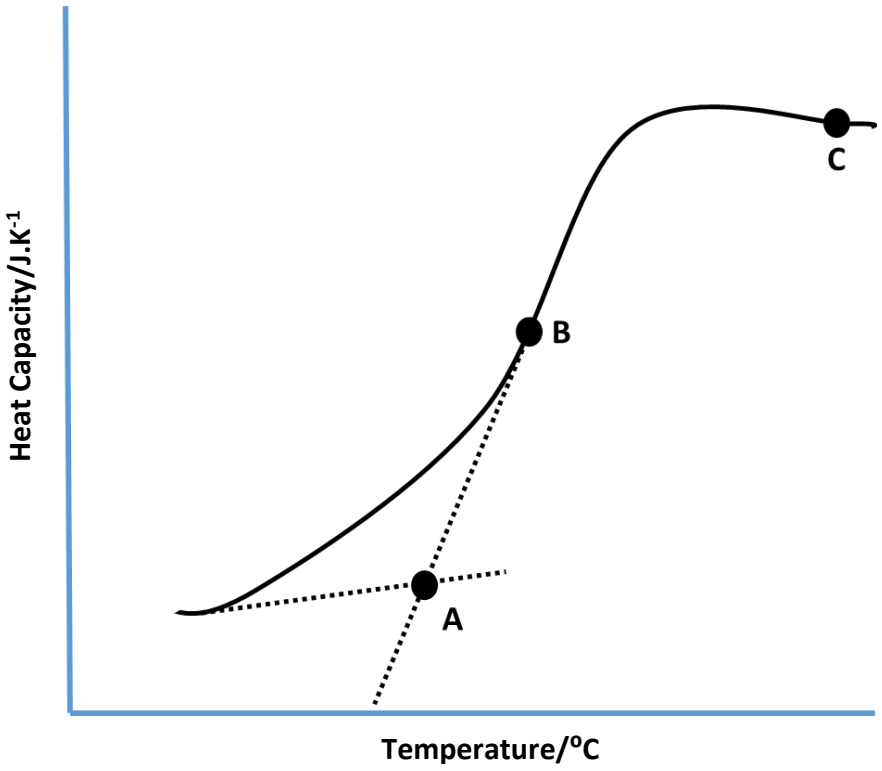

Figure 1.7: Determination of T_g

As the glass transition occurs over a range of temperatures, the midpoint of this transition is taken to be the calculated T_g. This is done by calculating the midpoint (B) from the onset (A) and the endpoint (C). This method for determining the T_g temperature was then used for every aged and unaged sample that was studied.

A general DSC apparatus is composed of a measurement chamber and a computer[18]. Two aluminium pans are heated in the chamber. One pan is left empty to act as a reference cell, while the other is filled with the sample. The samples are then heated; the rate of change for the heat capacities for each cell will be different. This is due to the difference in the contents of the empty pan and the pan containing the sample.[18] It is this change in the heat capacities of the reference cell and the sample cell that is recorded in order to produce the DSC trace.

The heat capacity (C_p) of a substance as the amount of energy required to raise the temperature of the system by 1ºC[19]. This parameter can be calculated if the heat flow and heating rate are known. Heat flow is measured as the quantity of heat supplied per second.

$$\text{Heat Flow} = \frac{heat}{time} = \frac{q}{t} \qquad [1]$$

where q is heat and t is time.

Here the heating rate is defined as the change in temperature over time.

$$\text{Heating Rate} = \frac{\Delta T}{t} \qquad [2]$$

The heat capacity of a system can be calculated as the heat flow over the heating rate:

$$C_p = \frac{\left(\frac{q}{t}\right)}{\left(\frac{\Delta T}{t}\right)} = \frac{q}{\Delta T} \qquad [3]$$

If a polymer is heated at a constant rate it will eventually reach its glass transition temperature. It is at this point that it undergoes a change in its mechanical properties, from a brittle material to an elastic one.

However, there are other methods apart from DSC used to determine the T_g of a polymeric sample. Dynamic Mechanical Analysis (DMA) is perhaps one of the most sensitive techniques used. DMA will be discussed in more detail later on, but in general it measures the response of a material to an applied oscillatory strain, and how that response changes with temperature/frequency. The T_g is commonly measured as the tan δ peak, the onset of the storage modulus or the peak of the loss modulus. It is important to point out that there are several factors in the DMA that may affect the T_g such as, the different modes of oscillation, variable heating rates and frequencies as well as different strains. This can sometimes lead to the T_g being determined by DMA, varying significantly from one reported technique to the next. For these reasons DSC was preferred.

1.4.2 Physical Aging

Hodge defines physical aging as the "structural relaxation of the glassy state toward the metastable equilibrium amorphous state, and it is accompanied by changes in almost all physical properties"[20]. Physical aging is carried out by a process where a glassy polymer is annealed at a temperature below, but close to, it's glass transition temperature and is quenched from the molten state. It has been widely known that amorphous polymers are not in thermodynamic equilibrium when exposed to temperatures below their glass transition temperature[21]. Struik explains that a solid polymer in its glassy state will have higher volumes, entropy, *etc* than it would typically have in the equilibrium state. During physical aging there is a slow and progressive move towards equilibrium, it is this process that is called physical aging[21]. During this approach to equilibrium there is a change and relaxation of chain conformation by molecular motion; this in turn will affect the free volume, enthalpy of relaxation and many other thermal and mechanical properties of a polymer. In this study, time dependence on physical aging will be analysed. The changes that occur during physical aging can greatly impact the performance of a polymer. This is of particular importance when discussing polymer nanocomposites as they have a wide range of uses in industrial applications. The nanoparticles themselves can change many of the properties of a polymer and therefore can also affect the physical aging of the nanocomposite[22]. It

is vital to fully understand and quantify these changes caused by physical aging in polymer nanocomposites in order to help predict a product's properties and to try and optimise their long-term performance (e.g. car tyres).

Many previous investigations into the physical aging of polymer nanocomposites have resulted in ambiguous results. Several studies found a slowing down to the physical aging of polymers by the addition of nanoparticles[23], while others have observed no change[24] or an increase in the aging in comparison to the unmodified polymers[25]. For example, in a paper by Boucher *et al* they observed that the addition of surface functionalised silica and gold nanoparticles actually accelerated the physical aging in the poly (methyl methacrylate) and poly styrene polymers that they were studying. Furthermore they go on to say that the functionalised fillers did not change the molecular mechanism for the physical aging but in fact increased the surface-to-volume ratio for the accelerated physical aging.[25] One further example includes the work of Ramakrishnan *et al*[26] which looked the physical aging in polycarbonate/silica nanocomposites. Here they show that at shorter aging times (2hrs) there is very little deviation from the unaged samples with regards to the change in the heat capacity. However, at longer aging times (1-24 days) a much greater deviation from the unaged sample is seen. They attribute this to the nanocomposites reaching a final equilibrium structural state earlier, most likely caused by the increased mobility of the polycarbonate chains due to the grafting on the silica.[26]

In order to study the changes that occur during physical ageing, experimental studies on enthalpic relaxations and free volume can be carried out. It is worth noting that physical aging of polymer nanocomposites is a reversible process. To reset the polymers thermal history, the sample must be heated to well above its T_g. This cannot be done with chemical aging.

1.4.3 Relaxation Enthalpies

Glassy materials have a wide variety of uses in everyday life, ranging from packaging to automotives. It is therefore important to understand how these glasses are prepared and the processes occurring within them[27]. There have been several studies on the enthalpy of relaxation for many synthetic polymers[20, 28]. These suggest properties such as

mechanical strength, density and gas permeability can be influenced by the physical aging of the samples and therefore can affect the enthalpies of relaxation.

Many glassy products are produced by thermal processing[29]. Through the course of this thermal processing distinct changes to the physical and mechanical properties may occur.

Amorphous materials can age or relax over time, this leads to an alteration in the properties of the material e.g. texture, brittleness, *etc*. These changes in the materials thermal and mechanical properties are attributed to the temperatures at which it is aged, the type of processing it is exposed to and the time allowed for these changes to occur[29]. Upon relaxation two clear changes occur, there is an increase in the density of the packing of the polymer chains and, therefore, there is a decrease in the free volume of the system.

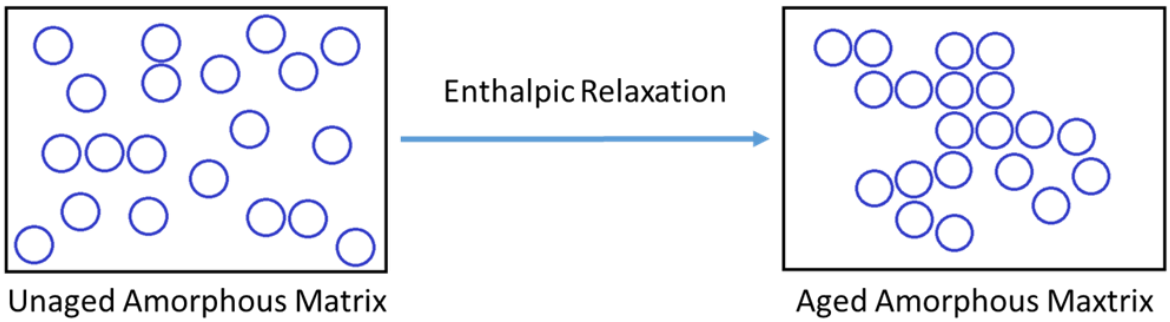

Figure 1.8: Relaxation of polymer chains from an unaged amorphous sample to that of an aged

This relaxation of the polymer chains results in a decrease in the enthalpy of the system, which can be seen from the following equation[30].

By carrying out a DSC scan of the newly aged sample, the enthalpy of relaxation can be observed as an endotherm in the trace.

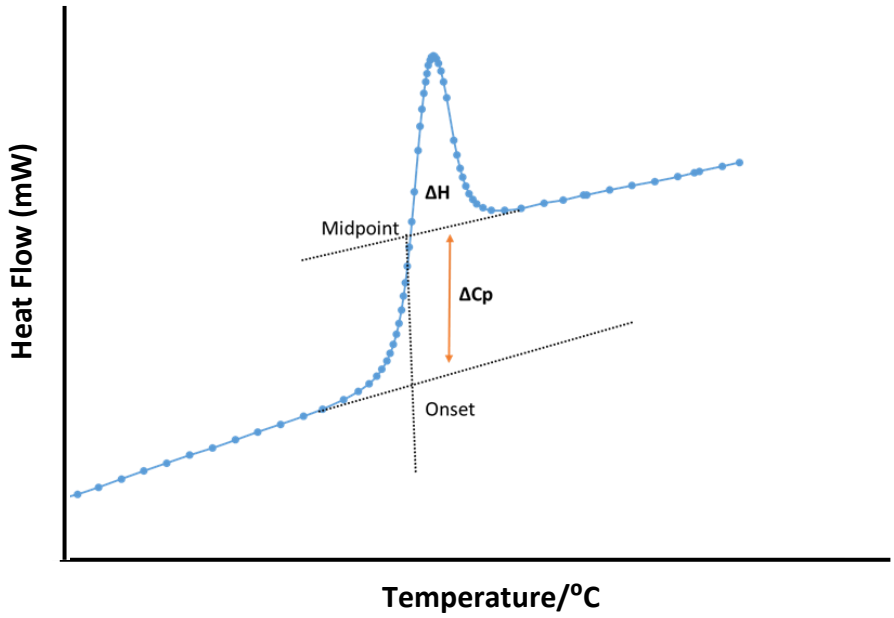

Figure 1.9: Typical DSC trace of an aged polymer nanocomposite

When heated to temperatures higher than the glass transition temperature the amorphous material can be seen to diverge from the equilibrium line of the T_g of the unaged polymer, a greater endothermic peak can be seen for the aged sample, see figure 1.9. The enthalpy of relaxation (ΔH_{relax}) of a sample can be calculated by integrating the area between the peak from an aged sample to the curve of an unaged sample. This allows us to measure the loss in enthalpy between the aged and unaged samples.

$$\Delta H_{relax}(t_a, T_a) = \int_{T\alpha}^{T\beta} [C_p(aged) - C_p(unaged)]dT \qquad [4]$$

C_p = Heat capacity of the sample t_a = Time of aging

T_α = Temperature peak for unaged sample T_β = Temperature peak for aged sample

The longer the length of time the sample is aged for, the greater the magnitude of the enthalpy of relaxation. During the physical aging process several physical and mechanical properties may change. This is dependent on the processing of the nanocomposite, storage temperatures and time allowed for the material to adjust to changes in temperature[28]. The enthalpy and free volume of a polymer decrease over

time. There are have been many studies reporting on the enthalpy of relaxation in synthetic polymers[28, 31]. In a study by Noel *et al*[32], it was shown that the enthalpy of relaxation can provide information about the time-dependent changes in glassy structures. These authors go on to say that the activation energy of relaxation enthalpies is connected to the chain mobility of the polymer in the glassy state. It has also been suggested that the enthalpy of relaxation is closely related to the structure and composition of the nanocomposite.

1.4.4 Cowie-Ferguson Model for Long-term Aging

The Cowie-Ferguson (C-F) model is used to predict the long-term aging in polymer nanocomposites[33, 34]. The enthalpy (H) loss upon aging is given by equation [4].

$$\Delta H(t_a, T_a) = \Delta H(\infty, T_a)[1 - \phi(t_a)] \qquad [5]$$

Where the relaxation is given by:

$$\phi(t_a) = \exp\left[-\left(\frac{t}{t_c}\right)^{\beta}\right] \qquad [6]$$

$\Delta H(\infty, T_a)$ = fully relaxed glass (equilibrium enthalpy at T_a) ϕ=relaxation time

t_a = time of aging T_a = temperature of aging β=parameter of KWW function

Here t_c is defined as a characteristic time, in that $t_a = t_c$ when the polymer has aged to two thirds of the fully aged glass [33]. β is related to the breadth of the distribution of relaxation times, it can have values of $0 < \beta < 1$. If β was found to have a value of 1, this would suggest a markedly sharp and narrow distribution with only one relaxation time[33].

The relaxation time is connected to the parting from equilibrium of the enthalpy (δH) by the following equation:

$$\frac{1}{\tau} = \frac{1}{t_a} \ln\left[1 - \frac{\Delta H(t_a, T_a)}{\Delta H(\infty, T_a)}\right] \quad [7]$$

Here $\delta H = \Delta H(\infty, T_a) - \Delta H(t_a, T_a)$.

τ=characteristic temperature/average relaxation time

In the C-F model $\Delta H(\infty, T_a)$ is regarded as a modifiable parameter, this is due to the fact that this model considers the linear heat capacity extrapolation to be inaccurate. In order to analyse the data, the experimental enthalpies of relaxation at a given aging time and temperature are plotted against the log of the aging time and curve fitted to the C-F model. This allows the thermodynamic characteristics from the $\Delta H(\infty, T_a)$ parameter to be evaluated as well as the kinetic aspects within the $\phi(t_a)$. Both of these elements can be extracted from the C-F model[33].

It should be noted that the C-F model regards the characteristic time, τ, as a constant. This disregards the time dependence of τ[35]. There has been some debate over the validity of these parameters obtained using the C-F model due to the time dependence not being considered.

1.4.5 The Kovacs, Aklonis, Hutchison and Ramos (KAHR) Model for Structural Recovery

The Kovacs, Aklonis, Hutchison and Ramos (KAHR) model is used to describe the structural recovery of a glassy material. One of the important aspects of this model is that it provides a zeroth-order model to structural recovery that captures much of the phenomenology described[36]. According to G. McKenna, the model builds on a set of response equations that are based on a Boltzman-superposition formalism that is linear in the reduced framework[36]. The KAHR model uses the volume departure from equilibrium to obtain the structural recovery parameter. For these equations the stimulus is the thermal history dT/dz where z is the reduced time.

$$\delta = -\Delta\alpha \int_0^z R(z - z') \frac{dT}{dz'} dz' \quad [8]$$

Here, δ is the departure from equilibrium, R(z) is the response function (sum of exponentials) and Δα is the change in the heat capacity (or the change in the coefficient of thermal expansion).

$$z = \int_0^t \frac{d\xi}{a_\delta a_T} \quad [9]$$

the response function as

$$R(t) = \sum_{i=1}^{N} \delta_{i} e^{-t/\tau_i} \quad [10]$$

Here δ_i are prefactors (local departures from equilibrium) and the τ_i are the relaxation times, thought to be related to local molecular dynamics[36]. The temperature dependence can be described in terms of the shift factors; a_T for temperature and a_δ for the structure:

$$\frac{\tau_i(T,\delta)}{\tau_{i,ref}} = a_T a_\delta = e^{-\Theta(T-T_{ref})} e^{\frac{-(1-x)\theta\delta)}{\Delta\alpha}} \quad [11]$$

Here the terms need to be defined clearly, α_T is the first exponential term and α_δ is the second. (T, δ) is defined as the relaxation time at the relevant values of temperature and structure while τ_i is the relaxation temperature at the reference temperature in the reference state[37]. This is often taken as T_r=T_g and that δ=0. The partition parameter , x, where $0 \leq x \geq 1$determines the relative importance of temperature and structure on the relaxation times. In these equations θ is a material constant that characterises the temperature dependence of the relaxation times in equilibrium[38]. KAHR defines θ as, $\theta \approx E_a/RT_g^2$, where R is the gas constant and E_a is the activation energy.

One further importance of this model is that the equations can be applied to both enthalpy and volume experiments. For enthalpy ΔC_p is used in place of Δ_α. It should be pointed out that the response function R(z) doesn't necessarily have to be the same for enthalpy and volume.

Hutchinson explains that the KAHR model allows for the distribution of δ_i to be examined at all instances during the relaxation[38]. He goes on to point out that when relating this to the distribution of free volume it allows for a comparison with the observations obtained from some spectroscopic techniques (e.g. PALS and

photochromic spectroscopy). One further point he makes is that the KAHR model does not try to fit the whole DSC curve, instead it examines the dependence of a characteristic feature of the DSC endotherm (peak endotherm temperature), on experimental conditions and the annealing times, this is proven in several examples[39-41]. Work done by McKenna and Simon highlighted the strength of this model in their experiments regarding polycarbonate material. Here asymmetry of approach and memory experiments were calculated using the KAHR model[37]. They performed experiments at 130, 135 and 140^{O}C in order to determine optimised data for comparison with the KAHR model. From their plot of asymmetry of approach experiments in polycarbonate material aged into equilibrium against time, it is clear to see that the experimental data fits very well with the KAHR model. They went on to further discuss enthalpy of recovery experiments. They found that the model can adequately describe the experimental data[37, 42]. One interesting thing to note in this experiment was that heating scans produced were intriguing, as for particular thermal treatments the scans showed a sub-glass transition peak and a large excess enthalpy peak near to the T_g. The KAHR model was able to replicate both of these features found in the experimental data[42]. In a paper by Grassia and Simon, they look into the effectiveness of the KAHR model regarding the volume relaxation of amorphous polymers. In their experiments they performed continuous cooling and heating experiments, volume relaxation after temperature jump and memory experiments on polystyrene[41]. From their results they were able to fit the KAHR model to their range of experimental data, from this they reported that the equation for the relaxation time is extremely important in order to obtain quantitative descriptions of the experimental data.

It should also be pointed out that the KAHR model does require further refinement. For example, in work done by Medvedev *et al* regarding memory experiments it was found that although the KAHR model did fit acceptably with the experimental data their parameters differed compared to those previously reported by Kovacs[43]. The KAHR model's inability to fit multiple data sets with one single set of parameters is an issue. McKenna and Simon go on to explain that "the models have particular problems capturing the effects of short term aging times after deep quenches, they are not predictive outside of the range of the fitted experimental data, and model parameters are often correlated"[44]. They mention that the main area of focus on refining the KAHR model has been focused on the expression for the relaxation time function. This is

because the original KAHR model does not revert to the WLF or the VFT temperature dependence in equilibrium. McKenna and Simon also offer an explanation as to why the KAHR model has done well previously, they explain that because very little recovery data go into equilibrium, and of that only over a very limited range, therefore the assumption of a linear or Arrhenius temperature dependence in equilibrium is often sufficient to describe the data in such a limited temperature range[44].

1.5.1 Dynamic Mechanical Analysis (DMA)

DMA is a technique often used to characterise a material's viscoelastic properties as a function of time, temperature, frequency, stress or an combination of these parameters[45]. DMA is based on the sinusoidal deformation of a sample. When a sample is exposed to a known stress, it will deform by a given amount. The extent to which a material deforms is related to its stiffness. The stiffness and damping of a material can be measured, these are then conveyed as the modulus and tan δ. We can describe the modulus as having an in-phase and an out-of-phase component as the force used to deform the sample is sinusoidal. The in-phase component is the storage modulus (E') and this describes the elastic properties of a material. The loss modulus (E'') is the out-of-phase modulus and is a measure of the material's viscous response. Tan δ (= E''/E') is also referred to as damping (loss of mechanical energy) or phase lag[46].

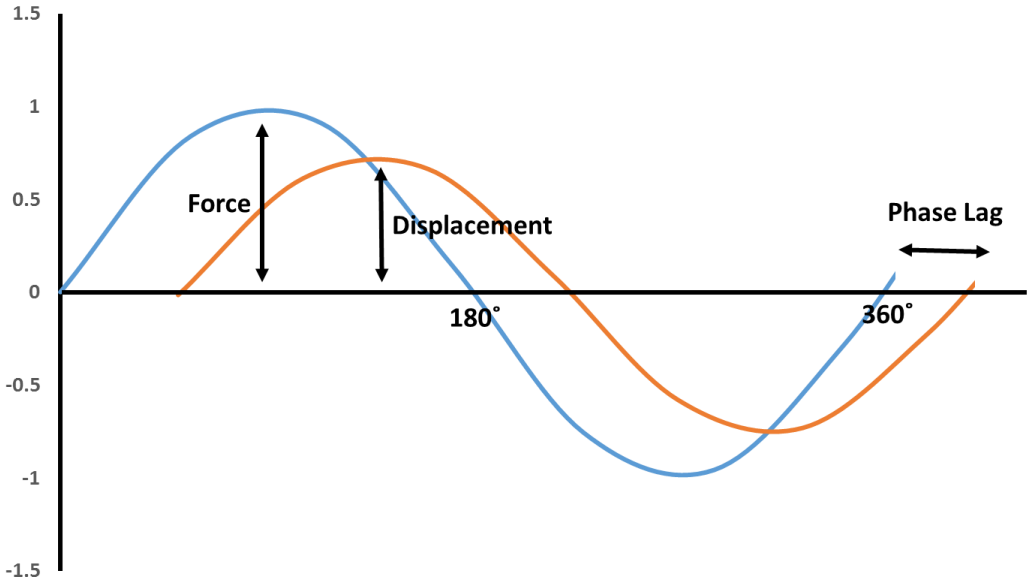

Figure 1.10: DMA in-phase and out-of-phase components

As a material goes through its glass transition, a decrease occurs in the modulus of the material. This is caused by the material becoming less stiff, less glass like and more rubber like. Any changes present in the E', E'' or tan δ curves should relate to changes in the chain dynamics caused by either the presence of the silica, the different aging

times or both. The E' changes are represented by a clear and steady decrease of the modulus, occurring around the T_g. In the case of both the E'' and the tan δ this change occurring around the T_g is expressed by a peak. These peaks represents the molecular reorganisation of the relaxation causing less elastic type behaviour[46]. Upon the addition of nanoparticles to the polymer, one may expect the storage modulus trace to be of higher values. The nanoparticles may act by decreasing the mobility of the polymer chains and therefore greater energy is required to get the nanocomposite to move from the solid state to the mobile.

Using the DMA equipment other types of analyse can be carried out, for example, the production of master curves. Master curves allow for the aging behaviour of materials to be studied at times or temperatures not usually conveniently measured. In order to obtain these master curves a technique known as time-temperature superposition is used.

1.5.2 Time-Temperature Superposition (TTS) and Fractional Free Volume

TTS also known as the method of reduced variables, is a widely used technique applied to determine the temperature dependence of the rheological behaviour of a polymeric liquid. It can also be used to expand the time/frequency arrangement at a given temperature at which the material's behaviour is studied[47]. The Williams-Landel-Ferry model (WLF) states that under certain conditions time and temperature can be interchanged. The DMA measurements allow for data to be collected at a range of different frequencies (1-100 Hz) and over a range of temperatures to predict behaviour at frequencies that are not directly measurable[45]. After the data are collected they can be shifted relative to a reference temperature (often the T_g) in order to create a master curve[48]. This method allows for the production of a master curve composed of data covering substantially wider ranges of time (frequency) and/or temperature than the range of the original data[48].

The WLF equation is derived from the classical model[49] in which the shift factor

$$\mathrm{Ln}(a_T) = \mathrm{Ln}(t_{r1}) - \mathrm{Ln}(t_{r2}) \qquad [12]$$

t_{r1} and t_{r2} are the relaxation times at temperatures T_1 and T_2 respectively.

For the viscosity (η) it is presumed that:

$$Ln(\eta_1) - Ln(\eta_2) = Ln(t_{r1}) - Ln(t_{r2}) \quad [13]$$

When this is combined with the Doolittle viscosity equation[50] we obtain:

$$Ln(\eta) = Ln(A) + B(\nu-\nu_f)/\nu_f \quad [14]$$

here $\nu_f = \nu_f(T_g) + \alpha_f(T-T_g)$ and υ is the free volume fraction of the total volume, the shift factor then converts to:

$$\text{Log } \eta_0(T) = \text{Log } \eta_0 (T_g) - \frac{(B/(2.3).f_g)(T-T_{g)}}{(f_g/\alpha_f)+T-T_g} \quad [15]$$

$f_g = \nu_f (T_g)/ [\nu_f (T_g) + \nu_0 (T_g)$, this is the free volume at T_g

the WLF equation for an arbitrary reference temperature T_0 is:

$$\text{Log}(a_T) = \frac{c_1(T_2-T)}{c_2+T_2-T_1} \quad [16]$$

From a rearrangement of the WLF equation the fractional free volume of a polymer can be calculated, the co-efficients can be determined from a plot of the TTS results. The fractional free volume of a material is the difference between the total volume of the sample and the occupied volume, and its value depends on several factors including temperature and the number of polymer chain ends. The larger the free volume the more space the polymer chains have to move and achieve different conformations. Free volume decreases from the rubbery to the glassy state. Upon cooling the polymer chains begin to have reduced mobility until a critical minimum temperature is reached, the glass transition temperature, and molecular motion is essentially frozen[51].

If $T_{ref} = T_g$ then it gives the WLF equation.

$$\log a_T = \frac{-C_1(T-T_g)}{(C_2+T-T_g)} \quad [17]$$

Ferry described the fractional free volume as:

$$f = f_0 + \alpha_f (T - T_{ref}) \quad [18]$$

By combining the Doolittle equation for free volume, the temperature dependence of the free volume and the definitions of the shift factor viscosity WLF proved:

$$\log a_T = -\frac{[(B/(2.303 f_0))(T - T_{ref})]}{(f_0/\alpha_f + T - T_{ref})} \quad [19]$$

Relating the free volume parameters to the WLF equation parameters gives:

$$C_1 = \frac{B}{(2.303 f_0)} \qquad C_2 = \frac{f_0}{\alpha_f} \quad [20]$$

If the reference condition is the glass transition temperature, then the free volume at the T_g can be expressed as:

$$f_g = \frac{B}{(2.303 C_1{}^g)} \quad [21]$$

1.6 Thermal and Mechanical Properties of Polymer/Silica Nanocomposites

It is well known that the addition of nanoparticles can alter the mechanical properties of a polymer. These alterations can be dependent on the filler type, filler size, and filler composition and distribution. Effective dispersion of the filler particles throughout the polymer matrix is another important factor to consider. The effectiveness of interactions between the polymer and the nanoparticles must also be taken into consideration. For example, if a polymer with no active hydrogen bonding sites was selected, this may lead to ineffective interactions between the polymer and the nanoparticle, leading to poor dispersion. If the nanoparticles do not form an even dispersed sample this can lead to the formation of aggregates. These aggregates can in turn lead to brittleness and fracturing of the polymer sample. There are several properties that can be affected by the addition of nanoparticles, these include the glass transition temperature, the elastic modulus and the tensile strength. There is much debate over the causes of this reinforcement. For example Payne[52] suggested that it is the formation of these agglomerates and the dispersion of the nanoparticles through the system that was responsible for the reinforcement. There is much disagreement as to the first half of this theory. Some groups have seen that above a certain filler composition limit, the addition of filler particles leads to a negative reinforcement effect[53]. Whereas others report that the addition of 2-15 w.t% silica nanoparticles can lead to a positive reinforcement effect and that any greater loading results in the effect being reversed[2].

A second proposed explanation suggests that there is a degree of chain immobility. As previously stated, it is accepted that particle size and loading influence the local (segmental relaxations) dynamics of the polymer matrix. It has been suggested that the areas near the nanoparticles have reduced segmental motion due to the hydrogen bonding interactions between the polymer matrix and the silica nanoparticle. Long *et al*[54] go on further to suggest that this reduced segmental motion near the filler particles leads to the formation of a "bound layer"[53, 55]. This bound layer is described as a glassy region. It is the even dispersion of these glassy regions throughout the polymer that creates the reinforcement effects.

The final suggested reason for the reinforcement effects of filler particles is based on the theory that effective dispersion of the filler particles within the polymer matrix results in

the bridging of the polymer chains by the filler nanoparticles[56]. It is this crosslinking of polymer chains by filler particles that creates a more strengthened polymer matrix[57].

1.6.1 Effect of Silica Nanoparticles on the Glass Transition

At the glass transition temperature, a material's mechanical and thermal properties change due to internal movement of the amorphous polymer chains. Below the T_g the polymer chains are rigid and glassy, once the T_g is approached the polymer chains begin to become more flexible and the material becomes rubbery. If a polymer has a T_g below room temperature it will be flexible, however if its T_g is well above that of room temperature it will be a hard-rigid plastic.

There is much debate over the effect filler nanoparticles have on a polymer. Some researchers have reported a positive reinforcement effect[58] while others have reported no change[59] or negative reinforcement[60]. It is clear that there is still much to be understood regarding the polymer-filler interactions.

In a study carried out by Fragiadakis *et al* it was reported that there was no significant variation in T_g with addition of filler particles[61]. The group reported that the heat capacity (Cp) jump of a poly(dimethylsiloxane)/silica nanocomposite at the glass transition normalised to the fraction of amorphous polymer, ΔCp^{norm}, steadily decreased with increasing filler composition[61]. It is this jump at the T_g that is directly related to the fraction of the polymer participating in the glass transition. This result can be interpreted in terms of a fraction of polymer being immobilized on the surface of the silica nanoparticles[61].

Use of nano-sized filler particles offers a greater reinforcement effect in comparison to macro-sized fillers. This is due to their smaller size (less than 100nm) and increased surface area. Traditionally macro-sized fillers give only moderate changes to the reinforcement (T_g, storage modulus) with negligible effect on the strength of the material due to unfavourable geometry[62]. Nanoparticles disperse within the polymer matrix and allow for greater interactions with the polymer chains thus enhancing any reinforcement effect.

The distribution of the silica nanoparticles within the polymer plays a crucial role. Due to the large number of hydroxyl groups on the surface of the filler particles, agglomerates can form. Rejon *et al* reported that the formation of agglomerates negatively affected the strength of the nanocomposite and a decrease in the glass transition was oberseved[63]. Above a certain size, agglomerates can create larger areas of free volume, this in turn leads to a decrease in the T_g[64]. In a paper by Hamming *et al*, they calculated the size and distribution of agglomerates in polymer nanocomposites and their effect on the glass transition temperature. It was found that the presence and increasing size of agglomerates lead to large negative deviations from the glass transition temperature being observed[64]. A paper by Cabral *et al*[65] reported large-scale agglomeration and corresponding variability in their results of PS-C_{60} nanocomposites. The results showed an increase in the T_g of the samples with the increase of the C_{60} content, above a 4% loading a decrease towards the value of pure PS was observed. This case shows an increase in the T_g to a set point before the loading of the C_{60} negatively affects the nanocomposite.

1.6.2 Effect of Silica Nanoparticles on the Dynamic Mechanical Properties

Dynamic mechanical testing can reveal information related to the mechanical properties (tensile strength, elongation, elastic modulus, toughness, etc.) of a polymer. The technique can provide information on the reinforcement effects of fillers and many papers have investigated the changes in the storage modulus (E'), the loss modulus (E'') and the tan δ [52, 66]. It can therefore be seen that any changes in stiffness or damping of a polymer nanocomposite can be observed by studying any of the storage modulus, loss modulus or tan δ parameters. It is important to stress that the changes observed in these parameters, for a polymer-silica nanocomposite, is not only due to changes in segmental motion (present around T_g) but also as a result of any reinforcement effects of the filler nanoparticles.

Tan δ can also provide information regarding the glass transition temperature. While usually measured by DSC, the DMA technique can allow for the observation of the "mechanical T_g". DMA is more sensitive compared to DSC and can also resolve sub T_g relaxations (β, γ and Δ transitions)[67]. It has been shown in previous studies[68] that the

glass transition temperature measured by DMA is approximately 5-12˚C higher than that observed for DSC. This difference can be explained by the differences in techniques. During DSC measurements the differences in heat capacities are measured between a reference and the polymer sample. For DMA measurements the T_g is assessed both by the change in volume of the sample while it is being heated[67] and the change in the E'/E''/tan δ over different frequencies/temperatures.

There have been extensive studies carried out on polymer-silica nanocomposites using DMA[3, 69, 70]. One of the trends observed for tan δ was the presence of a second relaxation peak. Tsagaropoulos *et al*[53] suggested that this second peak was in fact a second glass transition. This fits with an earlier proposed model of reinforcement, the presence of a loose "bound layer" of polymer chains around the silica nanoparticles. This "bound layer" may lead to restricted motion of the polymer chains. It is logical to assume that this would create regions within the nanocomposite that have a different level of reinforcement that of other regions, some with higher levels of motion than others. This leads to the presence of two glass transitions. In a previous study by Fragiadakis *et al*[61] investigating the glass transition and molecular dynamics in poly(dimethylsiloxane)/silica nanocomposites, the presence of a second glass transition was also observed in the tan δ plot.

However, there is not unified agreement. Other researchers have proposed that the presence of the second tan δ peak is the result of a fraction of the polymer chains not interacting with the filler nanoparticles. These chains will still undergo flow and segmental motion[56].

Furthermore, in work done by Yin *et al* where they studied the aging effects on silver (Ag)/PS nanocomposites, it was observed that the as the aging time increased so did the onset of E'/E'' and tan δ. They also produced master curves and showed that a suppression of the terminal behaviour at low frequencies was not observed, indicating the absence of the formation of a large-scale nanoparticle network[71]. In instances where a slowing down of the physical aging process occurs, this is thought to be due to a slowing down of the polymer segmental dynamics. There has also been reports of no changes observed in the mechanical properties of aged nanocomposites. For example Cangialosi *et al* reported that the addition of silica to PMMA showed no acceleration or deceleration in the physical aging of the nanocomposite[10]. On the final possible

outcome, Boucher *et al* reported a decrease in the onset of the modulus was observed for Poly vinyl acetate/Silica nanocomposites[72]. The proposed theories for the polymer silica nanocomposites mentioned above can also be applied for the aged samples. If the filler particles are in fact reinforcing the polymer and causing a suppression in the physical aging, then an increase in the onset of E', E'' and the peak of tan δ may be observed. However, if the addition of the filler particles resulted in an increase in the physical aging of the polymer, then a decrease in the onset of the E', E'' and peak of tan δ may be seen.

It is clear from the above discussion that the distribution, size and filler composition can dramatically affect the mechanical properties of the polymer-silica nanocomposites. There is once again ambiguity as to the effects of the addition of silica nanoparticles to a polymer. Some studies report an increase in storage modulus and tan δ while others report negligible change or even negative effects.

CHAPTER 2 Experimental

2.1 Materials

Table 2.0: Materials Used and their sources

Chemical	Source	% acrylonitrile	Mw	Hazard
Styrene-Acrylonitrile	Polysciences	23	165,000	Harmful

Table 2.1: Particles used and their sources

Silica Particle	Source	Diameter (nm)	Surface Area (m^2/g)	Particle Type
Hydrophilic Silica (HDK-I)	Wacker	20	240	Fumed
Hydrophobic Silica (HDK-O)	Wacker	20	240	Fumed
A300	Aerosil	7	300	Fumed
MEK-ST	Nissan	10-15	155	Colloidal

Solvents used: Dimethylformamide (DMF), Tetrahydrofuran (THF)

2.2 Methods for the Production of Polymer-Silica Nanocomposites

2.2.1 Dispersion Preparation

Dispersion preparation is one method used for forming polymer-silica nanocomposites. A given amount of polymer and silica nanoparticle are dissolved in a suitable solvent and mechanically stirred for a 0,24, 72 and 168hrs. This provides a quick and easy procedure to prepare dispersions but does have some drawbacks. For one the nanoparticles can often aggregate together and form agglomerates[70]. This is not ideal when trying to obtain homogenous samples. With regards to the quality of the nanoparticles, all samples were bought in and in the case of the colloidal silica a simple weight to volume experiment was carried out to ensure that the solvent suspending the silica had not evaporated and in turn alter the silica % displayed on the canister. Elemental analysis was also carried out by a previous student on the colloidal silica, the results from this agreed with the weight to volume experiment. Results from this showed a 1-2% difference in the experimental silica % to the percentage displayed on the bottle this was considered when calculating the silica content for the SAN nanocomposite samples. The same sample method for the preparation and drying of the nanocomposite samples was kept consistent for each type of silica used. The only real discrepancy may be the number of times the samples were hot pressed. Some samples did not give a solid and flat sample first time and the hot-pressing process had to be repeated several times until a suitable sample was prepared. It may be that this repeated hot pressing of samples aided with the removal of any excess solvent still present in the sample. Finally, with regards to the formation of aggregates, none were visible upon inspection and the samples were taken to be homogenous, in order to fully characterise this further work would be required.

2.3 Production of Polymer-Silica Nanocomposites

The dispersion method was decided to be the preferred choice of preparation due to its short preparation time and simplistic nature. The *in situ* emulsion and CRP techniques all require several steps and in places the synthesis of intermediate reactants is required as well as long reaction times. Previous studies by Feng *et al* have shown successful

production of polymer silica nanocomposites from dispersion techniques[69]. It should be pointed out that other methods for the production of the polymer silica nanocomposites involved the direct, covalent attachment of the polymer chains whereas the dispersion techniques involves the intermolecular bonding interactions, including hydrogen bonding interactions, between the polymer matrix and the silica, there is no chemically grafted attachment of the polymer chain to the silica.

From studying previous literature, Fu et al[73] and Feng[69] both reported that successful, homogenous samples were obtained using compositions of between 2 and 12% silica with poly lactic acid and epoxy resin respectively. From this a composition of 10% silica was decided upon.

A general dispersion technique obtained polymer-silica nanocomposites. The polymer and silica were weighed into a flask and the solvent added. The samples were mechanically stirred for 48hrs. The samples were poured into Teflon film moulds and left to air dry for 2 days before being dried in the oven overnight at 50ºC. The samples did appear to be largely homogenous with little or no visible agglomerates. To confirm this SEM images would have been required, unfortunately this was not available at the time the experiments were carried out.

2.4 Characterisation of Polymer-Silica Nanocomposites

So as to investigate any reinforcement effects of the addition of filler particles to polymers and to investigate the effects of physical aging on styrene acrylonitrile samples, several characterisation techniques were employed.

2.4.1 Fourier Transform Infrared Spectroscopy (FTIR)

A range of 400-4000cm^{-1} was selected on a ThermoScientific Nicolet iS5. FTIR was used in order to confirm the surface modification of the polymer-silica nanocomposites resulting from a bound layer. If any solvent was still present after the hot-pressing process, peaks corresponding to this would be visible in the spectrum. Post hot pressed

samples were analysed. 32 scans were ran for each sample, in order to improve the accuracy of the results.

2.4.2 Differential Scanning Calorimetry (DSC)

DSC measurements were carried out using a TA instruments DSC 2010 Differential Scanning Calorimeter. Samples (10-15mg) were weighed into aluminium pans and sealed. The samples were heated at a rate of 10ºC/min under constant nitrogen flow. Calibration of this instrument was done with an indium metal standard. The glass transition temperature was taken to be the midpoint of the step-like change. Using the TA instruments software, the T_g for the unaged and aged peaks were obtained. For the aging peaks, the software removes the peak associated with the enthalpic relaxations and calculates the T_g.

2.4.3 Dynamic Mechanical Thermal Analysis (DMTA)

The DMA 2980 Dynamic Mechanical Analyser from TA instruments was used in single cantilever mode at a frequency of 1Hz and a heating rate of 5ºC/min. The samples for the DMTA were prepared by hot pressing at 223ºC for 1.5 hrs and allowed to cool for 30-60 minutes. The dimensions of the samples were approximately 10mm in length, 12 mm in width and 2 mm in thickness. It is these dimensions that the computer program (thermal analyser) uses in order to calculate the modulus and tan delta values.

It should also be mentioned that in each run a newly pressed sample was used. Often at the end of the run samples would become fractured or broken and unsuitable for further testing and so therefore had to be repressed. This explains some of the deviations between each sample.

The computer program Thermal Solutions from TA instruments was used to shift the DMA results, according to the TTS method, to produce the master curves.

2.5 Determination of the slope of the master curves

To determine the slope of a curve, the equation of the line must first be found. This can be done by using the format trendline function in excel, it is best expressed as a polynomial function. Once this is found the derivative of the function is found.

$$y = 25.06x^2 - 54.77x + 36.24 \quad [22]$$

$$\frac{dy}{dx} = 50.12x - 54.77 \quad [23]$$

The mid-point of the curve is then found. These coordinates are then used in the equation to give the gradient of the slope.

Mid-point of the curve (7.05, 1.26)

$$\frac{dy}{dx} = 50.12\ (1.26) - 54.77 \quad [24]$$

$$\frac{dy}{dx} = 8.38 \quad [25]$$

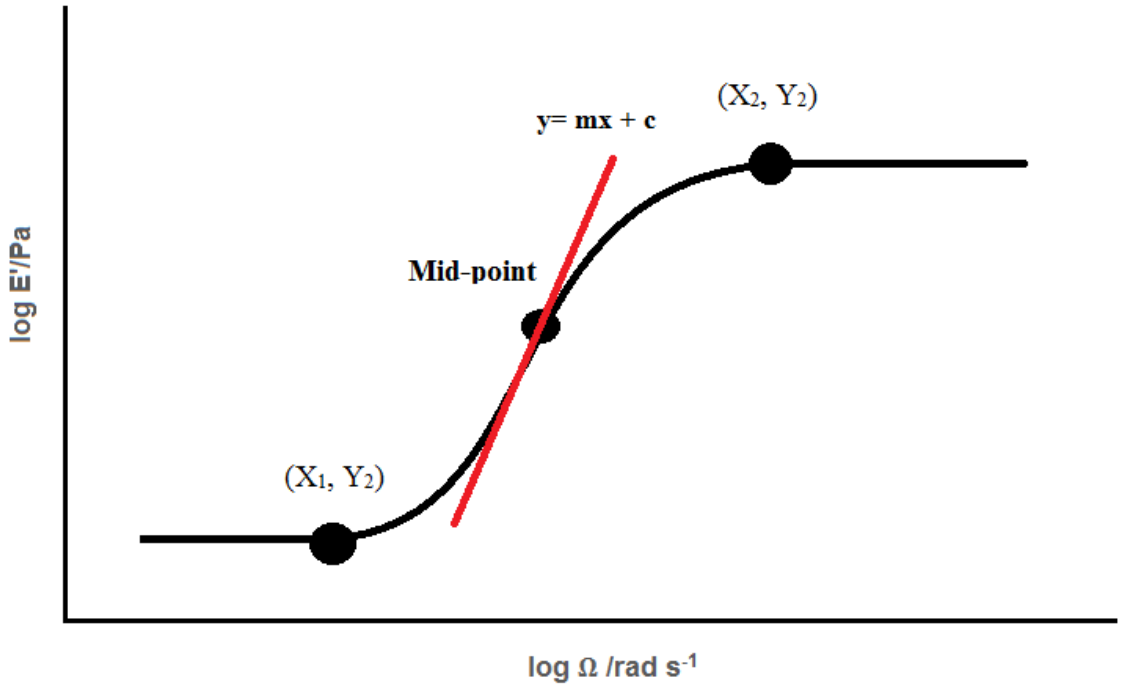

Figure 2.1: Determination of the slope of a curve

CHAPTER 3.0: Results and Discussion

SAN is an important polymer to study due to its many useful properties such as, rigidity, transparency, toughness, resistance to cracking and its processability[74]. SAN is used in many products, for examples in packaging, kitchenware and battery housings.

16 samples were initially prepared using the dispersion technique mentioned in chapter 2. Samples of unmodified SAN, 10% HDK-I/SAN, 10% HDK-O/SAN and 10% MEK-ST/SAN were prepared for each of the 4 aging times (0, 24, 72 and 168hrs). Unfortunately, due to difficulty removing the SAN and its nanocomposites from the moulds some were often broken or deformed. When this occurred, the samples were then heated well above their T_g in order to reset the thermal history and finally repressed.

3.1 Characterisation of SAN/Silica Nanocomposites

3.1.1 Production of SAN/Silica Nanocomposites

Upon the production of the first set of nanocomposites it became clear that this procedure was not the most efficient in which to obtain homogenous samples. A few draw backs were the length of time taken for the samples to fully dissolve and the drying time. In a paper by Yu et al they successfully achieved homogenous samples using solution dispersion techniques alongside sonication[3]. Not only did this improve the time scale for the reaction but it also provided a simple and effective technique. A new set of samples were prepared, the polymer and silica samples were weighed, and the solvent added. This time once the lids were secured the samples were placed in a sonic bath, heated to 60ºC, and left for 60 minutes. This resulted in a fully dissolved solution. To ensure that the samples were fully homogenous they were then mechanically stirred for 4 hrs before being left to dry for 48hrs. The result of this simple adaptation to the method resulted in effective production of 10% silica-polymer nanocomposites. All samples were then characterised.

3.1.2 FTIR of SAN Nanocomposites

In order to fully characterise the SAN/nanocomposites produced the modified and unmodified samples were analysed by fourier transform infrared spectroscopy (FTIR). Figure 3.1 shows the IR spectrum for the modified and unmodified SAN samples, unaged. For the pure SAN there are peaks at 2926cm^{-1} associated with alkyl C-H stretches and clear aromatic ring vibrations present at 1599-1450cm^{-1}. Finally, the presence of a C≡N stretch at 2235cm^{-1} characterises the polymer. In the case of the HDK-I/SAN and HDK-O/SAN nanocomposites a new peak appears at 1060cm^{-1}. According to Feng *et al*[69], this can be attributed to the Si-O-Si stretching vibrations. There may be other peaks associated with the silica nanoparticles that are being masked by the polymer's other vibrations (1042cm^{-1} and 788cm^{-1} relating to the Si-O_2 and Si-O-Si respectively). Similarly, the MEK-ST silica displays a new peak at 1106cm^{-1} relating to a Si-O-Si stretching vibration. This information confirms the formation of SAN/Silica nanocomposites. It does not provide us with any information relating to the dispersion of the silica throughout the polymer matrix.

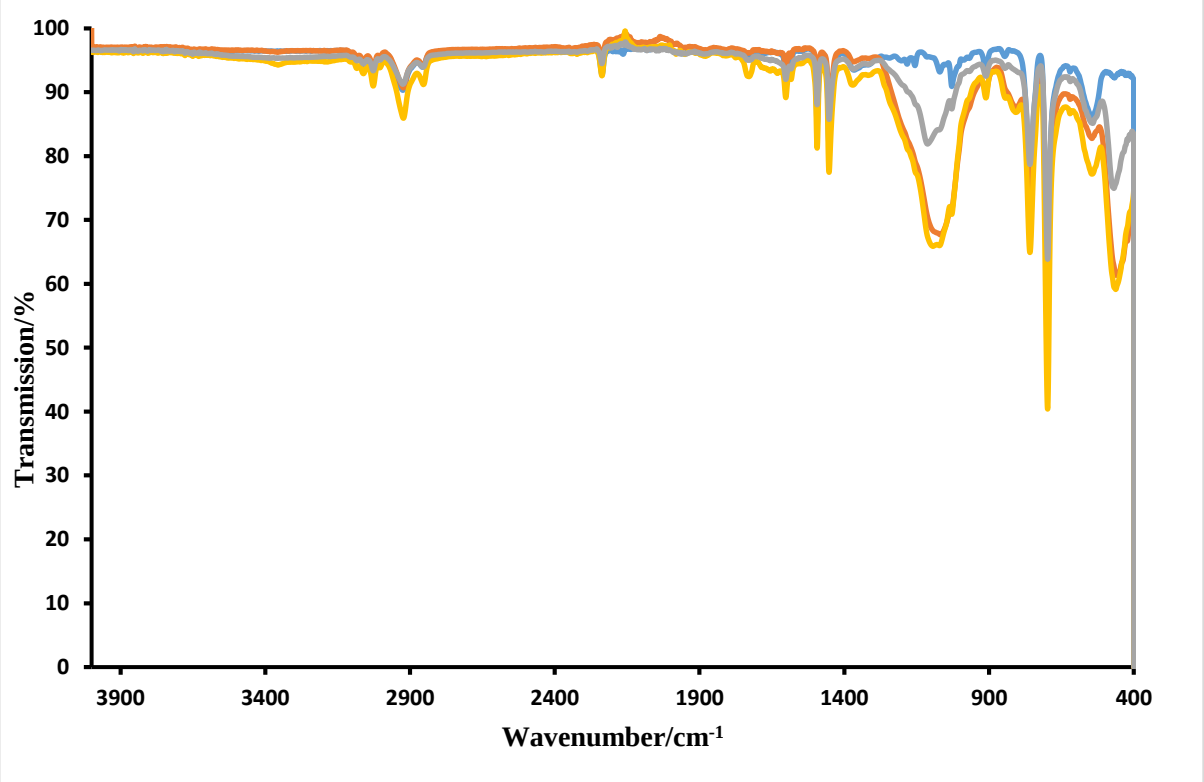

Figure 3.1: FTIR Spectral Data of Unaged SAN-Silica Nanocomposites

(-) Pure SAN, (-) 10% HDK-I/SAN, (-) 10% HDK-O/SAN and (-) 10% MEK-ST/SAN

Similar results are observed for the aged samples. There are obvious C-H alkyl stretches at 3025 cm^{-1} and 2918 cm^{-1}, as well as the aromatic ring vibrations in the region of 1601-14450 cm^{-1}. The C≡N peak at 2235cm^{-1}, also confirms the SAN polymer is present in the sample. Once again, the silica related peaks are detected at 1060 cm^{-1} and 7662 cm^{-1}. As expected, there is no obvious change in the unaged and aged spectra. It would be interesting however to compare an ATR-FTIR spectra with a conventional FTIR spectra. ATR-FTIR is used to see up to a small, measurable depth into the sample. It is known that as a sample ages the silica aggregates have a tendency to migrate to the surface. If this was happening during the aging process of these sample differences could be observed by ATR-FTIR.

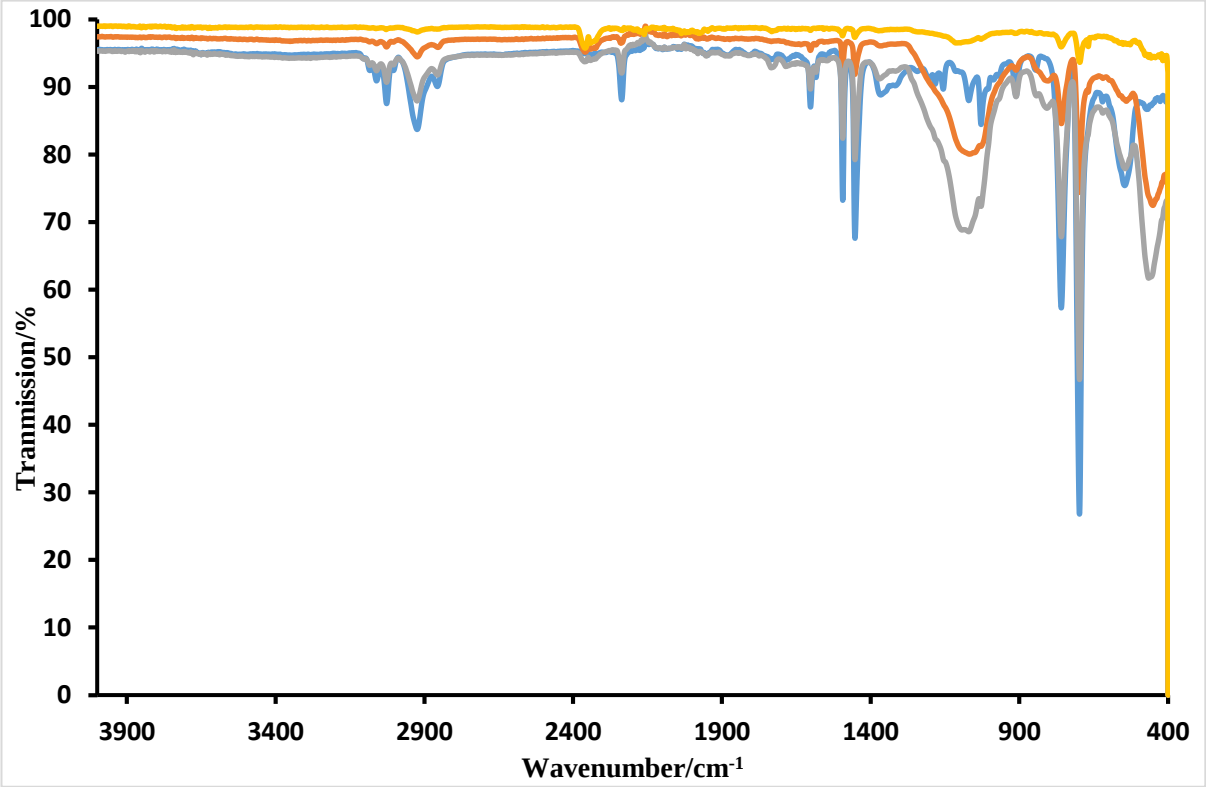

Figure 3.2: FTIR Spectral Data of 24 hr aged SAN-Silica Nanocomposites

(-) Pure SAN, (-) 10% HDK-I/SAN, (-) 10% HDK-O/SAN and (-) 10% MEK-ST/SAN

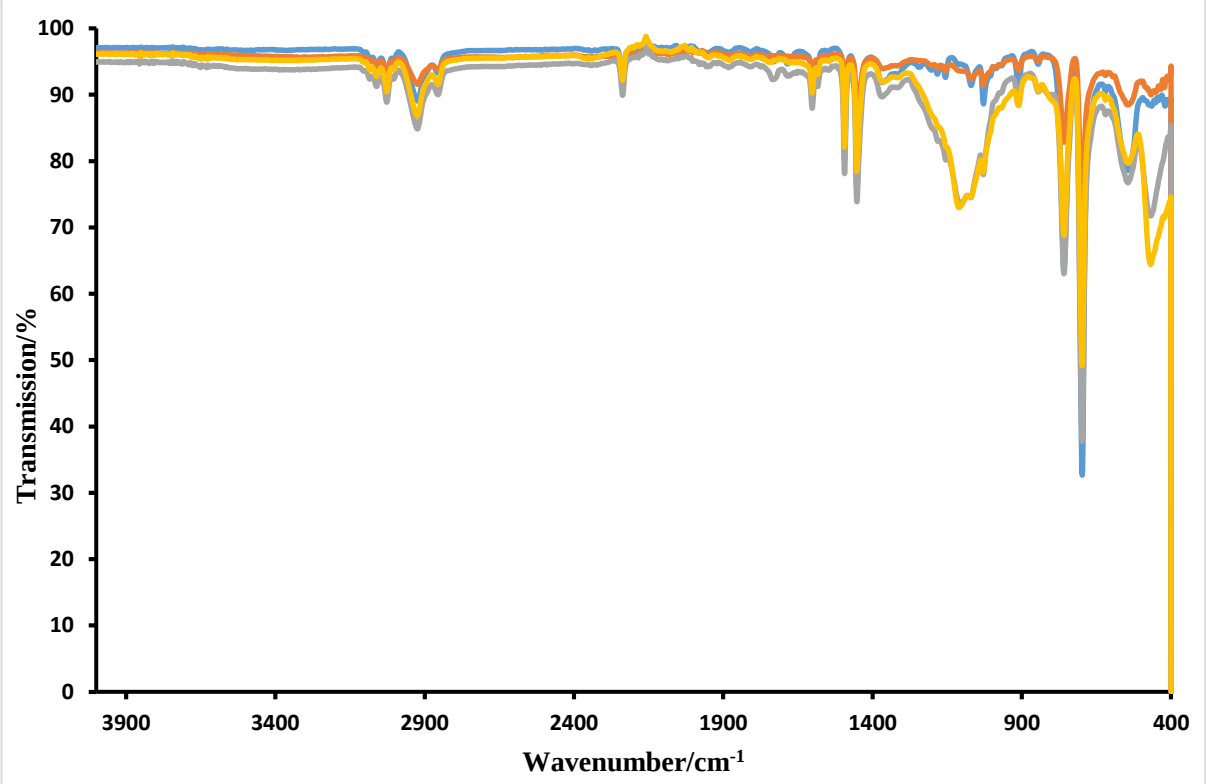

Figure 3.3: FTIR Spectral Data of 72 hr aging SAN-Silica Nanocomposites

(-) Pure SAN, (-) 10% HDK-I/SAN, (-) 10% HDK-O/SAN and (-) 10% MEK-ST/SAN

Table 3.0: FTIR assignments of 72 hr aged SAN/Silica Nanocomposite samples

Wavenumber (cm^{-1})	Assignment
3025-2923	Alkyl CH
2236	C≡N
1601-1452	Aromatic CH
1098	Si-O-Si
1027	$Si-O_2$
758	Si-O-Si

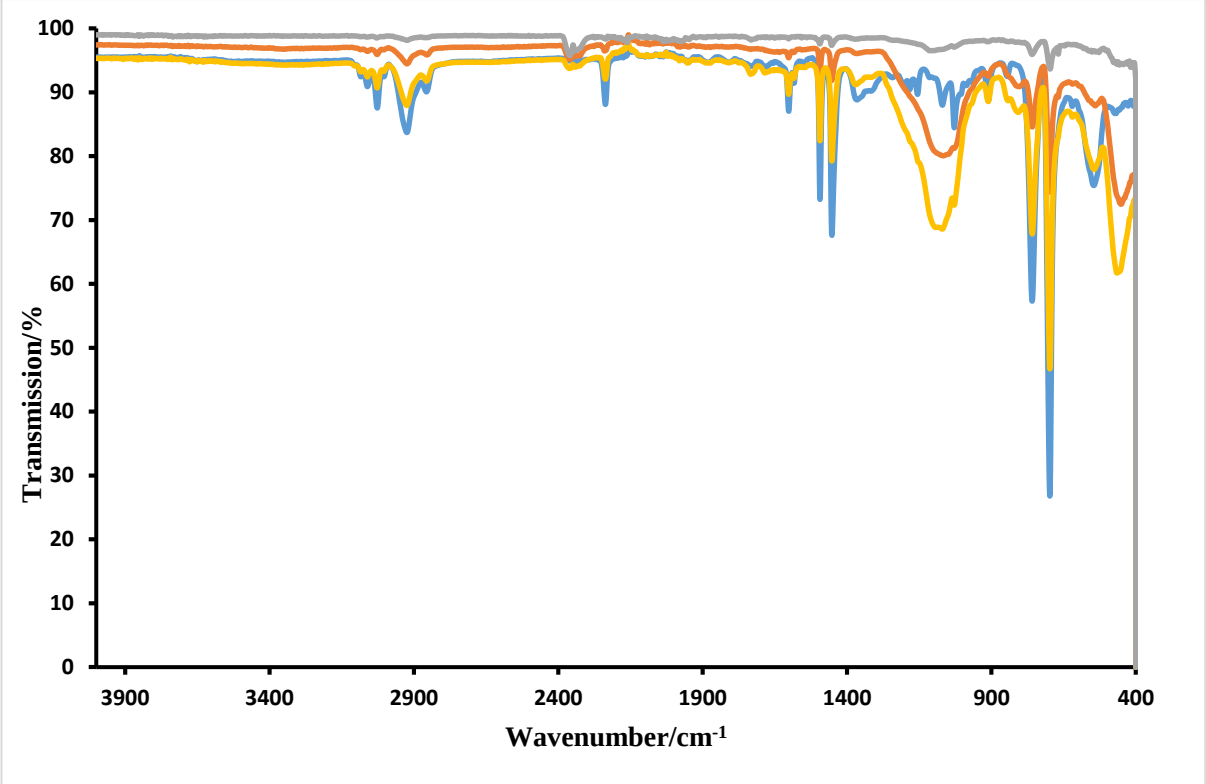

Figure 3.1: FTIR Spectral Data of 168 hr aging SAN-Silica Nanocomposites

(-) Pure SAN, (-) 10% HDK-I/SAN, (-) 10% HDK-O/SAN and (-) 10% MEK-ST/SAN

Table 3.1: FTIR assignments of 168 hr aged SAN/Silica nanocomposites

Wavenumber (cm^{-1})	Assignment
3025-2921	Alkyl CH
2235	C≡N
1601-1449	Aromatic CH
1059	Si-O-Si
1023	$Si-O_2$
757	Si-O-Si

3.2 Thermal Behaviour of Silica Nanoparticles in SAN Nanocomposites

A selection of SAN-silica nanocomposites were produced with differing filler type. There were two fumed silica samples, HDK-I and HDK-O, and one colloidal (Nissan MEK-ST) sample. The 10% silica samples were prepared by dispersing the silica nanoparticles and the polymer in THF and sonicating at 60ºC before being mechanically stirred for 4 hrs. The samples were left to air dry for several days before being dried in the oven at 60ºC overnight. The dried samples were then hot pressed and characterised by DSC mechanical measurements. The aged samples however were put in a vacuum oven at 85ºC ± 5ºC. The samples were aged for times of 0, 24, 72 and 168 Hrs.

As can be seen in figure 3.5 the DSC result shows a general increase in the glass transition temperature of the polymer with the addition of fillers. For the 10% HDK-I/SAN nanocomposite only a negligible increase of +0.8ºC was observed within error but a greater increase in glass transition temperature is seen for the 10% HDK-O/SAN sample. Here an increase of +4.28ºC is observed. In the case of the MEK-ST nanocomposites the greatest increase for all of the samples is observed. In order to achieve a successful sample, the polymer and the silica must form a homogenous solution, the MEK-ST samples were all colloidal, this may have contributed to effective mixing of the sample and in turn led to a greater distribution of the silica throughout the polymer matrix. There are many possible theories for the methods of this thermal reinforcement, Long *et al* suggested that the polymer chain movement is restricted by the presence of the silica nanoparticles[54]. These segmental restrictions can lead to more energy (heat) being required for the chains to go from the glassy state to the rubbery state, hence an increase in T_g. The data obtained for this study does seem to fit this prediction. However a theory by Payne, which suggested that it was the formation of silica agglomerates within the polymer which led to the reinforcement effect[52]. This theory does not seem to fit the resultant data as all of the samples appeared homogenous and no visible large agglomerates were observed. In order to fully confirm that this was the case Scanning Electron Microscope (SEM) images would have proved useful, unfortunately the equipment was not available at the time of this project.

From literature, it was found that the T_g of pure dry SAN at a 26% composition of styrene was 111°C[75]. This clearly differs from the experimental value obtained in this study. The unmodified SAN samples were made straight from the bottle with no solvent

used, it can be presumed that the sample may have absorbed moisture from the air, acting as a plasticiser.

Table 3.2: Glass Transition Temperatures of SAN-Silica Nanocomposites

Polymer Nanocomposite	T_g (°C)	ΔT_g (°C)
SAN	99.5	-
10% HDK-I/SAN	100.3	+0.8
10% HDK-O/SAN	103.8	+ 4.3
10% MEK-ST/SAN	105.4	+ 5.9

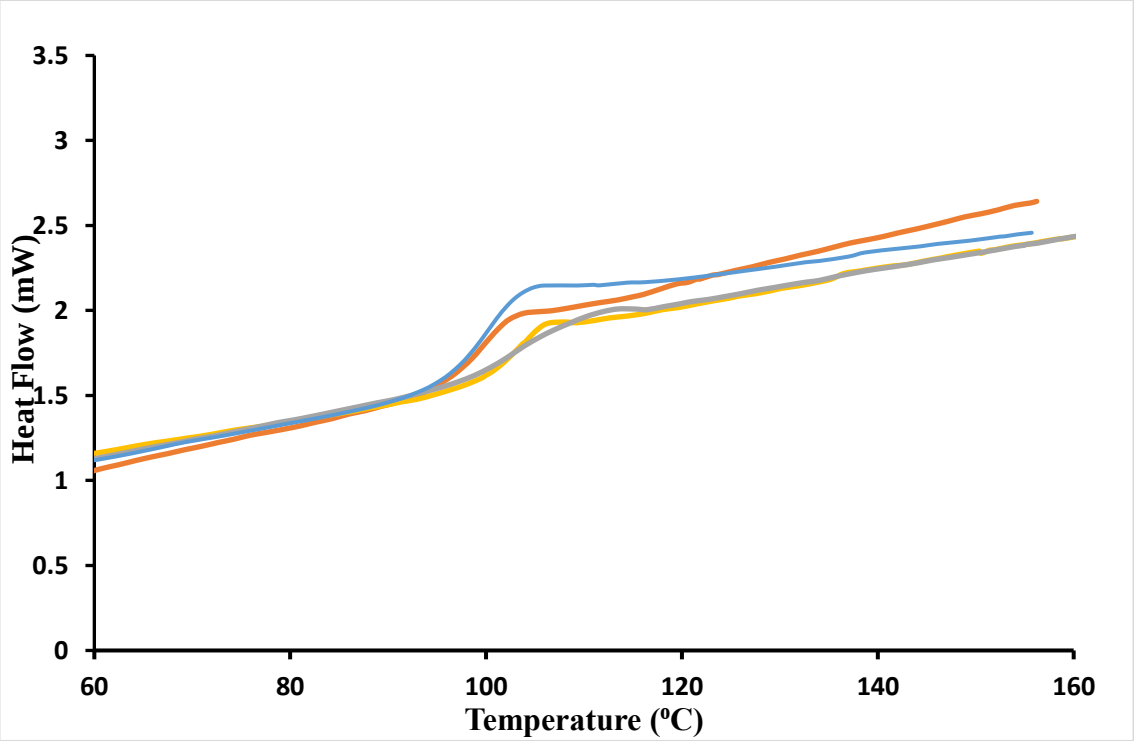

Figure 3.5: DSC Traces of SAN-Silica Nanocomposites Unaged

(-) Pure SAN, (-) 10% HDK-I/SAN, (-) 10% HDK-O/SAN and (-) 10% MEK-ST/SAN

3.3 Mechanical Reinforcement Effects of Silica Nanoparticles in SAN Nanocomposites

Figure 3.6 shows the normalized data for the storage modulus versus temperature curves for the SAN nanocomposites. The data was normalized by taking the average and the standard deviation of the storage modulus data and then combining these with the standardize function in excel. The samples were prepared as described in Chapter 2. There was some difficulty in obtaining identical completely flat and smooth samples each time by hot pressing. This meant that there was some variation in the sample dimensions. In turn, this led to some variations in the modulus at low temperature, to reduce these variations the data was normalised. The results of the unaged mechanical tests can be seen in figure 3.6. At lower temperatures, all the samples were glassy solids and until approximately 100^{O}C where the deviations occur due to the polymer chains beginning to have some translational motion leading to the transitional region at approximately 103ºC. Here the samples begin to exhibit a decrease in their storage moduli. It is in this region that the polymer chains become mobile and the reinforcement effects can be observed. From the data, it can be seen that the HDK-I (hydrophilic) nanocomposite appears to show the greatest reinforcement effect out of all the other filler types. This can be seen, as the HDK-I sample got to the highest temperature before deformation began to occur, $T>T_g$. This shows that the addition of the HDK-I silica to the polymer increased the stiffness in comparison to the unmodified SAN sample. Moving on to the HDK-O (hydrophobic) sample, it does exhibit some positive shifting of the E' compared to the unmodified SAN. The nature of this type of silica makes it less likely to absorb moisture from the atmosphere, and therefore means there is a lower chance of water being absorbed by the sample and therefore acting as a possible plastizer. If the water is only bound by one bond to the matrix then it is not tightly held and easily removed, i.e. by the heating during the DMA run[76]. The MEK-ST sample showed very little change from that of the unmodified SAN polymer. From figure 3.6, the other nanocomposite E' do not exactly match that of the pure SAN. For example, the HDK-I sample has a much flatter and longer rubbery plateau, this is indicative of greater physical crosslinking between the polymer and the filler. The aggregated silica sample, HDK-I silica seemed to show a greater change in the storage modulus of the polymer compared to the colloidal MEK-ST sample. This suggests that the chain dynamics in the transitional region become slightly modified by the presence of the

aggregated silica filler nanoparticles[56]. Zhu *et al* proposes that the aggregated silica forms a fractal structure in the elastic medium of the polymer and that it is this percolation of the silica nanoparticles throughout the matrix and their hydrogen bonding interactions with the polymer that leads to this observed increase in the storage modulus and therefore reinforcement. In the SAN samples the cyano group of the repeating unit can interact with the hydroxyl groups on the surface of the silica. In comparison to the other silica samples the MEK-ST silica has the smallest surface area, as can be seen in table 1.0, this may influence the strength of the intermolecular interactions between the silica and polymer matrix. This implies that the colloidal nature of the MEK-ST silica and the expected improved mixing and therefore greater homogeneity of the nanocomposites does not necessarily mean greater reinforcement. From these results the theory put forward by Payne[52] suggesting that the presence of large silica agglomerates forming between the polymer matrix leads to areas of reinforcement, cannot be disregarded for the purpose of this study. By eye, no large agglomerates were visible in any of the samples, SEM images would be required to fully ascertain this. In the first set of samples where inefficient mixing had occurred the silica/SAN nanocomposites were brittle and fragile with visible large agglomerates formed on the surface of the sample. SEM would have allowed the samples to be analysed in more detail, a fully dispersed sample would appear to have well-spaced "dots" i.e. silica particles, while a poorly dispersed sample with large agglomerates would have large clusters of "dots" unevenly spaced. It is known that both a non-homogenous sample or too high a silica loading can lead to a negative reinforcement effect[77]. Furthermore Yuezhan *et al*[69] reported similar results to this study, they found an increase in the reinforcement and speculated that this was due to the immobilization of the SAN polymer chains by the silica nanoparticles.

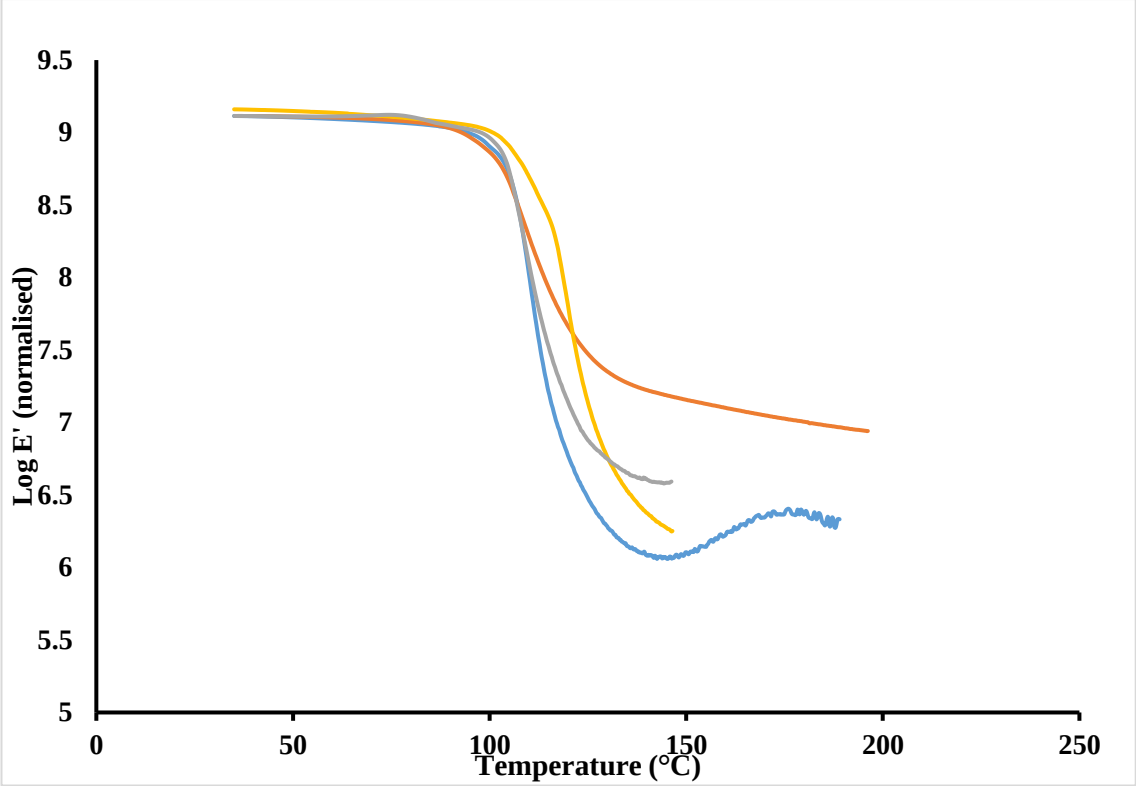

Figure 3.6: Storage Modulus against Temperature Traces for SAN-Silica Nanocomposites Unaged

(-) Pure SAN, (-) 10% HDK-I/SAN, (-) 10% HDK-O/SAN and (-) 10% MEK-ST/SAN

It can be noticed that the T_g of the samples varies if measured by DSC or DMA, the reasons for this variation is that the DMA techniques has many more variables such as various heating temperatures, frequencies and strains that can affect the position at the T_g is observed at.

The loss moduli of pure SAN and its silica nanocomposites can be seen in figure 3.7. For the pure SAN a peak can be seen at 105.8ºC, this is associated with the polymer's glass transition. Only very small changes are seen in peak position with the addition of filler particles are observed. It is clear to see that once again the aggregated HDK-I silica nanocomposite showed an increase in the loss modulus as well as the storage modulus. The HDK-O and MEK-ST samples showed very little deviation from the pure unaltered SAN polymer. A further suggestion for this reinforcement effect was described by Long[54], who suggested that the silica nanoparticles form a bound layer, reducing the segmental motion of the chains.

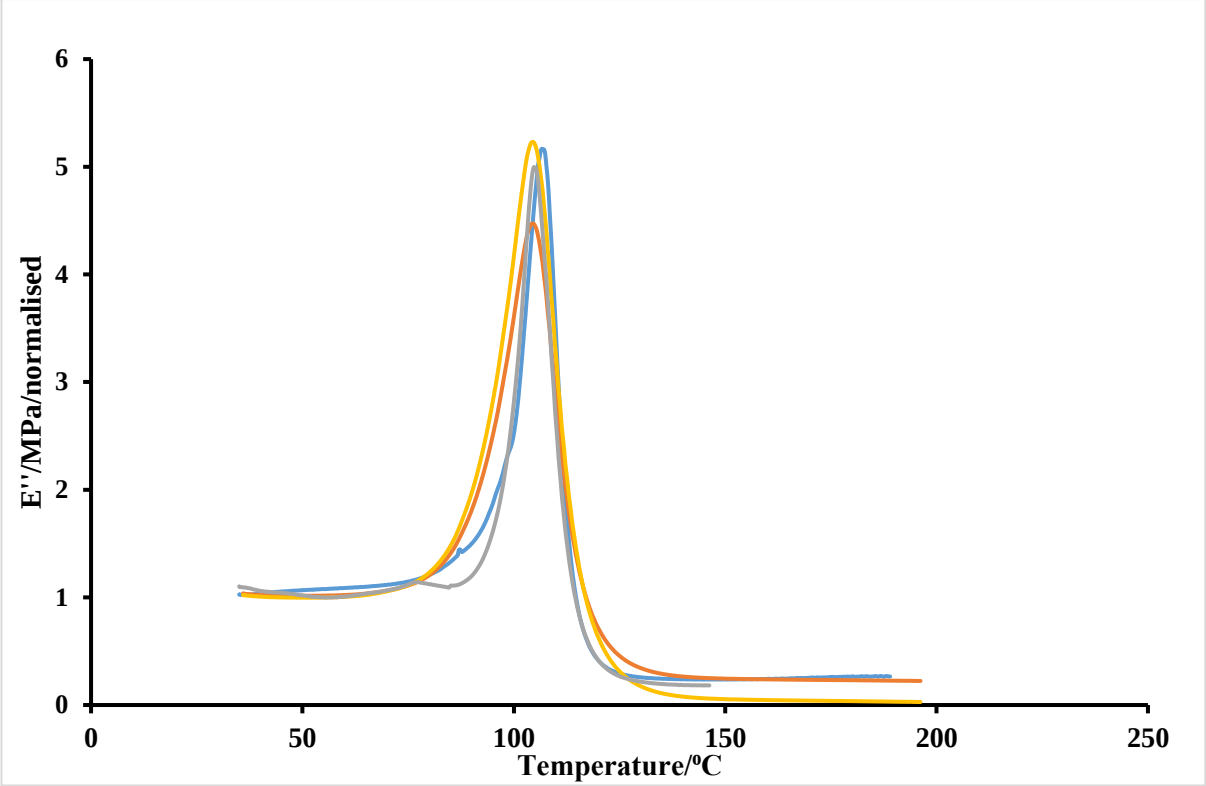

Figure 3.7 Loss Modulus against Temperature Traces for SAN-Silica Nanocomposites unaged

(-) Pure SAN, (-) 10% HDK-I/SAN, (-) 10% HDK-O/SAN and (-) 10% MEK-ST/SAN

Table 3.3: Comparison of T_g between DSC and DMA techniques

Sample	T_g (DSC) (°C)	T_g (E'') (°C)	T_g (Tan δ) (°C)
SAN	99.7	105.8	114.9
10% HDK-I/SAN	100.3	105.6	112.4
10% HDK-O/SAN	103.7	105.3	125.4
10% MEK-ST/SAN	105.4	105.2	115.8

It should also be noted at this point that there is a difference between the T_g values obtained by DSC and DMA. The Cambridge Polymer Group explain that DSC shows changes in the heat capacity through the glass transition which result in a sigmoidal change in heat flow indicating that the T_g has occurred[78]. They go on to say that this technique doesn't have the same sensitivity to accurately assign the glass transition temperature. However, the DMA test involves an oscillatory stress and the polymers

response to this is measured. The storage and loss moduli (elastic and viscous properties respectively) can be sensitive to this and therefore offers a more accurate value[78]. Both values are discussed in this report as both techniques are useful in observing the changes in T_g upon the addition of nanoparticles to polymers.

The loss factor or tan δ is given as the ratio of the loss modulus to storage modulus (E''/E'). This parameter can offer information on whether or not a sample behaves as an elastic material[67]. Figure 3.8 shows a plot of tan delta as a function of temperature. The data was normalised at T= 36°C. The peak maximum is caused by the primary α-relaxation which relates to the glass transition of the pure SAN. In this case, the peak changes upon addition of different fillers. In contrast with previous data, in this report, the HDK-O/SAN nanocomposite showed the greatest increase in comparison with the pure polymer and the MEK-ST sample exhibits a small change in comparison to the pure SAN. This is quite different from the results presented in figure 3.5, this deviance could be due to the different techniques used to measure the T_g. The HDK-I filled sample exhibited a decrease in the tan δ peak. There are a couple of main factors to consider when discussing the causes of changes in the T_g of a polymer. To begin with the possibility of the silica nanoparticles impeding the segmental motion of the polymer chains must be considered.

Lastly, the concept of free volume may explain the effects expressed by the HDK-I/SAN nanocomposite, the addition of filler nanoparticles may lead to an increase in the free volume of the system. This will in turn interrupt the packing of the polymer chains and allow for greater segmental motion at lower temperatures, hence a decrease in the T_g is seen. In the results observed in this study the positive increase in the HDK-O sample may fit with the above theory however it should also be mentioned that the greater the dispersion of the silica throughout the polymer matrix can also lead to greater surface area of the silica to interact with the polymer. If the silica had agglomerated this would have resulted in an overall reduced surface area available for interaction with the polymer. It therefore could be argued that the hydrophobic nanoparticles were better dispersed throughout the sample compared to the others. However, when we look back at the storage modulus and loss modulus data, this is in disagreement with the Tan δ results, in order to further explain this further work would be required.

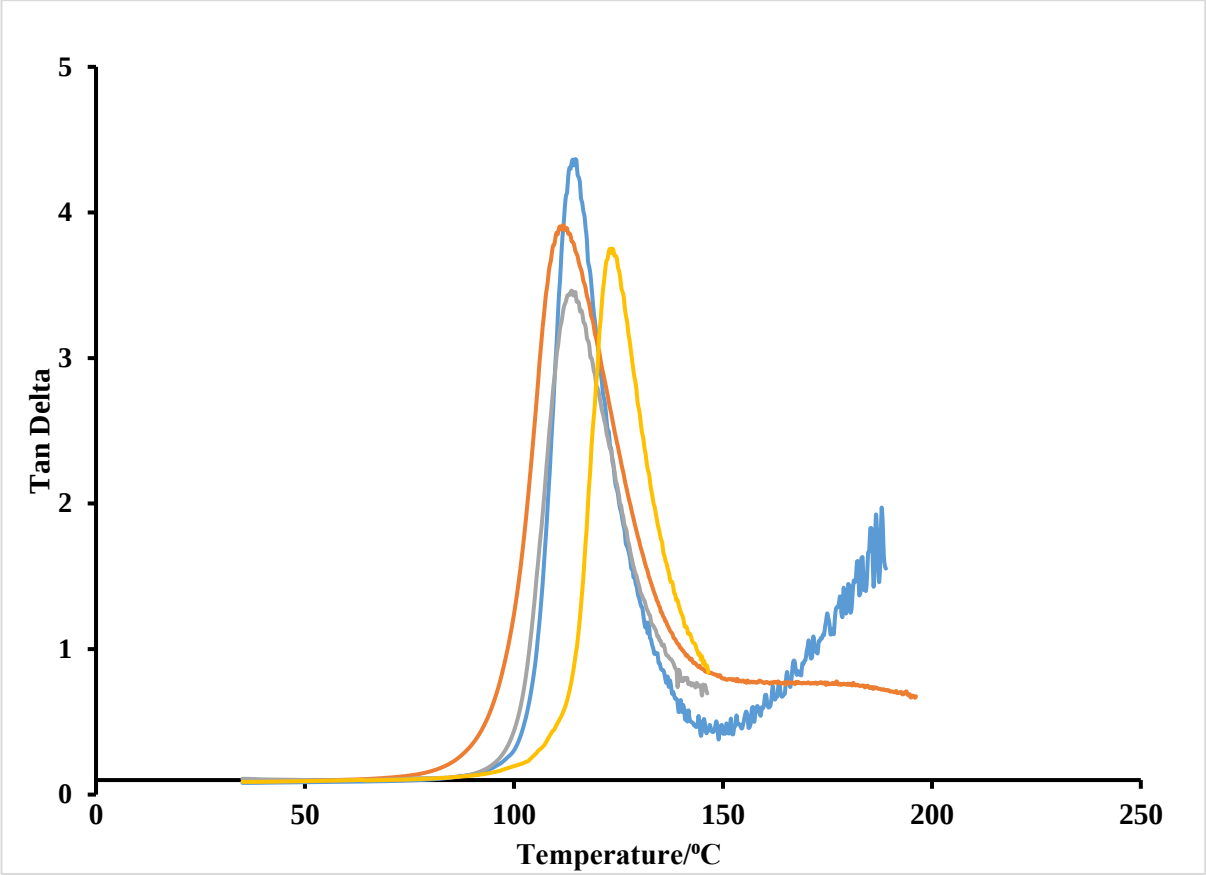

Figure: 3.8 Tan Delta against Temperature Traces for SAN-Silica Nanocomposites unaged

(-) Pure SAN, (-) 10% HDK-I/SAN, (-) 10% HDK-O/SAN and (-) 10% MEK-ST/SAN

3.4 Thermal Reinforcement Effects of Silica Nanoparticles in Physically Aged SAN Nanocomposites

The physical aging of the SAN/Silica nanocomposites was carried out in a vacuum oven at 85ºC ± 5ºC. The samples were aged for times of 0, 24, 72 and 168 Hrs. To first see the effects that the addition of silica has on the physical aging of the samples one must first study aging in the pure unaltered styrene-acrylonitrile samples. It is thought that the local segmental relaxation processes that occur in physical aging of polymer nanocomposites should be similar to that of other systems in which the chains are perturbed[79]. The environment around surrounding the polymer chains, in this case the presence of silica nanoparticles will influence the segmental relaxation of the polymer chains and in turn may affect the T_g, the morphology and the composition. If the interaction is favourable, i.e. attractive bonding interactions then studies have shown a positive thermal effect, thought to be due to a restriction of polymer chain segmental mobility, it may be that this reduction in mobility is linked to the near suppression of physical aging effects. Physical aging involves the relaxation of polymer chains at temperatures close to but below the glass transition temperature, it can therefore be proposed that the presence and interactions of the nanofillers can lead to the polymer chains resisting this chain relaxation, hence the lack of change in T_g of the aged nanocomposite samples.

The conditions at which the polymer samples are aged also play an important role. It is often taken that accelerated aging occurs between 5-20°C below the T_g of the polymer. The further away from the T_g the aging temperature, the slower the aging. Therefore, it is important to note the aging temperature of the samples.

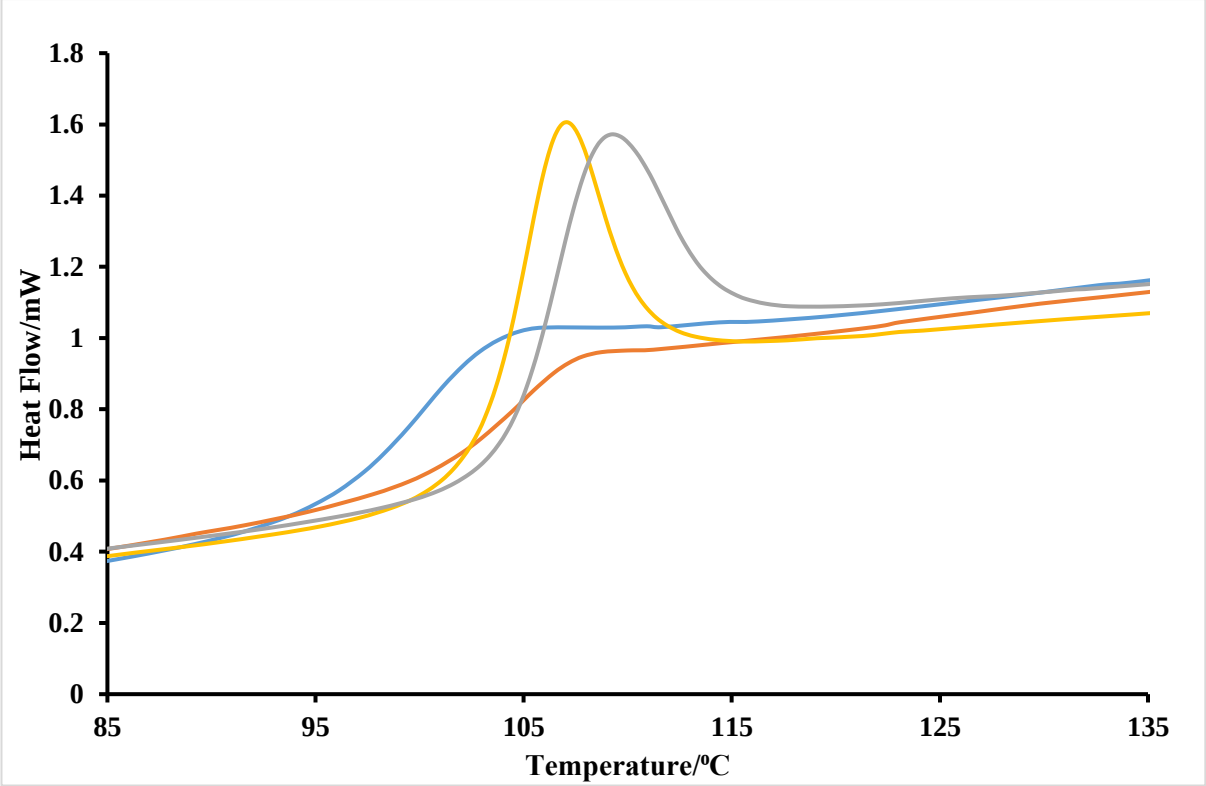

Figure 3.9: DSC Traces of Unmodified Aged SAN Samples (Annealing T=85ºC ± 5ºC)

(-) unaged, (-) aged 24 hrs, (-) aged 72 hrs and (-) aged 168 hrs

It can be seen from the figure 3.9 that there is a clear trend. Aging manifests itself as a peak on top of the step-like change at T_g and this is what is observed in figure 3.9, with increasing ageing time. It is clear that aging has occurred within the samples. Although there is no obvious enthalpic peak at 24 hrs aging, at 72 and 168 hrs clear peaks are observed. In a study by Robertson, the physical aging effects on SAN were investigated. It was reported that when aged 15, 30 and 45°C below the T_g, very little change (2-10°C) in the T_g was observed[80]. This change is similar to the results obtained in figure 3.9. Here the increase in T_g varies from 4.7ºC for the 24hr aged sample to the greatest increase of 6.4ºC for the 168hr aged sample. It could be argued that the 24 hr sample results of the pure SAN are not due to the aging process as the data shows no obvious aging peak. In the unmodified SAN samples this increase in glass transition can be explained in terms of the free volume concept. Struik describes this concept as every system made of particles, molecules, etc all depend on the free volume or in other words the degree of packing of molecular chains[21]. In its glassy state the polymer chains have little or no segmental mobility, this is reflected here in the curves seen for 0 hrs aged.

However, as the polymer is heated through its T_g (100-115°C) the chains begin to have more energy to move and segmental motion increases, i.e. the material becomes rubbery. This increase in chain mobility in turn leads to an increase in the free volume. As the sample is aged it is kept at a temperature close to but below its T_g. Consequently, the mobility of the chains will be low but not zero. As the free volume surpasses its equilibrium a slow and progressive contraction of volume will occur[21]. Physical aging in glassy materials originates from the fact that they are out-of-equilibrium[22]. The physical aging leads to the polymer chains becoming further out-out-of-equilibrium due to the tighter packing of chains because of the slow relaxations. The greater packing of polymer chains leads to a greater amount of thermal energy required to allow segmental motion, hence an increase in the glass transition is observed. This increase in T_g can clearly be seen for the 24, 72 and 168 hr aged samples. This typical endothermic overshoot of the T_g for unmodified bulk aged samples is typical of physical aging behaviour. Boucher *et al* report similar findings in their study of the aging-time dependence of the segmental relaxation time of poly(vinyl acetate) (PVAc)[72].

In this study three different types of silica were investigated. The DSC traces of the 10% HDK-I/SAN nanocomposites are shown in Fig. 3.10. For this sample, aging leads to considerable broadening of the glass transition region and this is evident when comparing the DSC traces of the 10% HDK-I/SAN samples with results in Figure 3.9. It can be difficult to accurately define the T_g in these cases as depending on your point A and point B allocations, the results can vary. A computer programme was used and from this the results are as follows. For the HDK-I aged 24 hrs the mid-point of the curve shifts by +1.2 degrees to higher temperatures compared to the unaged sample, with an increase of +2.3ºC for the 72 hrs ages and finally an increase of +2.3ºC for the 168 hrs aged sample. In the pure SAN aged samples aging clearly affects the appearance of the DSC traces but this is not that evident for the nanocomposite. This suggests that the presence of nanoparticles reduces the thermal effects of aging on SAN. In a study carried out by Lee and Litchtenhan[81] regarding the inclusion of polyhedral oligomeric silsesquioxane (POSS) nano-reinforcements in epoxy, the group noted that the addition of the filler lead to retarded physical aging rate and also shorter time to reach equilibrium. Their aged data often has wider/longer range over which the glass transition is observed. This was also noted in 2003 by Lu *et al*[82] who reported reduced

relaxation times (slower motion) and a much broader glass transition in dispersed silicate epoxy nanocomposites compared to the neat epoxy. The intermolecular interactions between the polymer and the silica play an important role in this suppression of physical aging, this interaction is thought to supress the conformational relaxation processes associated with physical aging[83].

In the case of the 72 hrs ages sample the wide transition observed in Figure 3.10 may be due to the nanocomposite sample having poor dispersion. As previously mentioned, poor dispersion leads to large areas of aggregation of the silica within the nanocomposite. This may in turn lead to phase separation where the sample may show a T_g of the bulk polymer and a close second T_g of the nanocomposite. However, another possibility for this large transitional region may be due to traces of solvent or even decomposition of the sample.

It should also be pointed out that there are other interactions present in the samples which may also contribute to the observed suppression of physical aging, for example dispersion forces and dipole-dipole interactions.

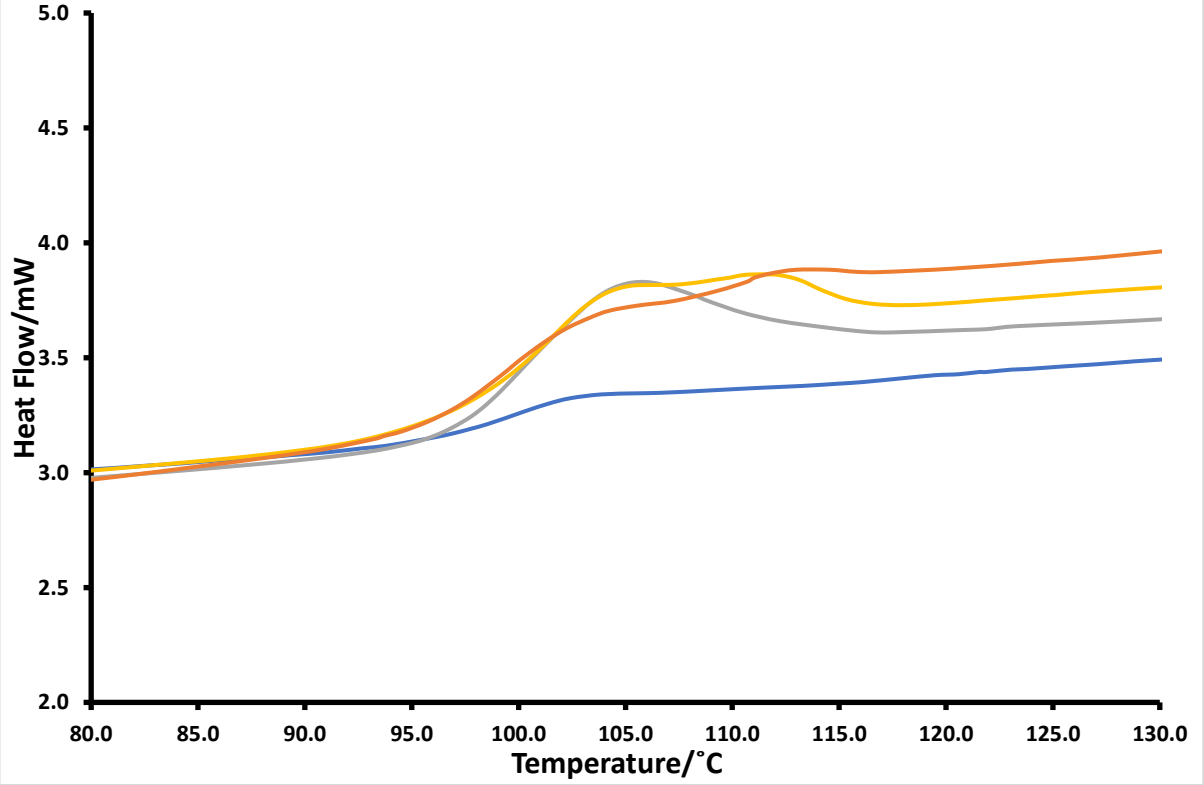

Figure 3.10: DSC Traces of Aged HDK-I/SAN Nanocomposites (Annealing T=85ºC ± 5ºC)

(-) unaged, (-) aged 24 hrs, (-) aged 72 hrs and (-) aged 168 hrs

In figure 3.11 the DSC traces of the aged HDK-O/SAN nanocomposites can be seen. As noted for previous samples there is a shift of the DSC traces to higher temperatures, with increasing aging time. However, it should be pointed out that in all instances at 0 hrs aging the SAN/silica samples showed an increase in T_g compared to the aged samples. Within the results for the aged samples both no change and increases in T_g were observed. This may be explained by solvent still being present in the sample and therefore acting as a plasticiser, in this case tetrahydrofuran (THF), which can be tricky to remove[84]. The data in figure 3,10 exhibit more prominent aging peaks similar to that of the pure polymer.

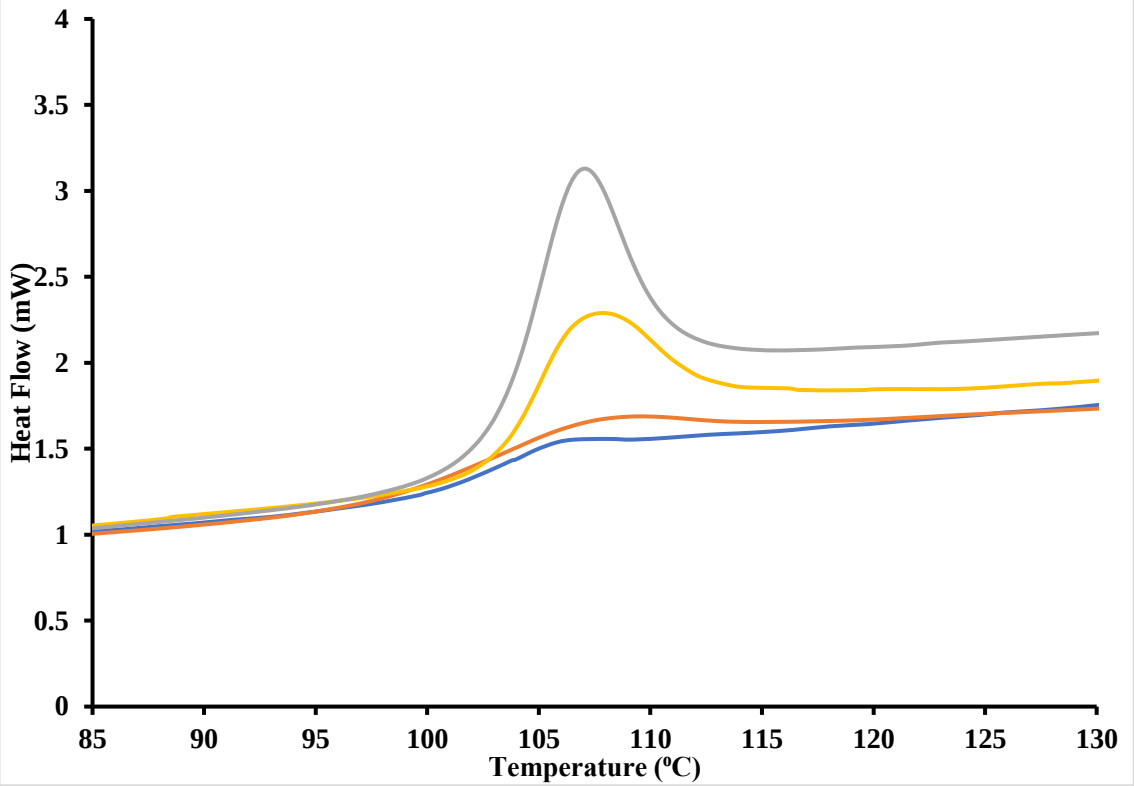

Figure 3.11: DSC Traces for HDK-O/SAN Nanocomposites (Annealing T=85ºC ± 5ºC)

(-) unaged, (-) aged 24 hrs, (-) aged 72 hrs and (-) aged 168 hrs

When comparing the data in table 3.3 for the T_g of the HDK-I and HDK-O samples they appear to be similar. This suggests that there is no large notable difference between hydrophilic silica and hydrophobic silica with regards to thermal properties upon incorporation into SAN. One of the bigger differences between the two DSC traces is

the height of the peak present at T_g. For a more reliable and clearer result the 24hr and 72 hr aged HDK-I samples should be run again. Although this was done in the lab it was extremely difficult to achieve a uniformed sample.

In the MEK-ST nanocomposite samples, figure 3.12, the peak heights are much smaller, this in turn lead to a reduced enthalpy of relaxation. There is an increase in the shift of the curve upon both the addition of the MEK-ST nanoparticle and the increasing aging times. The increase in the shift of the curve is presumed to be associated with the restricted chain mobility and this in turns leads to the higher T_g. For the MEK-ST samples there what appears to be an abnormality at 24 hrs aging. This is shown by a slight decrease in the shift of the curve by $0.5^{O}C$ when compared to the unaged MEK-ST sample. As previously mentioned, this could be down to several factors. The change is also very slight and could fall within experimental error.

Table 3.3 compares the calculated T_g values of all the samples, aged and unaged, modified and unmodified. It also compares these values against the pure unmodified SAN. Table 3.3 shows that compared to the unaged unmodified SAN, all the samples exhibit an increase in the shift of their curve to higher temperatures. For example, at 72 hrs aging the HDK-I nanocomposite had shift of +2.6ºC, whereas the MEK-ST nanocomposite had a shift of +5.7ºC. It should be noted however that the unaged samples also showed an increase in the shift of their curves, the MEK-ST sample had an increase of 2.7ºC, as well as the HDK-I sample which had an increase of +0.3ºC. This increase although small may be due to the increased thermal effects of the MEK-ST and the HDK-I.

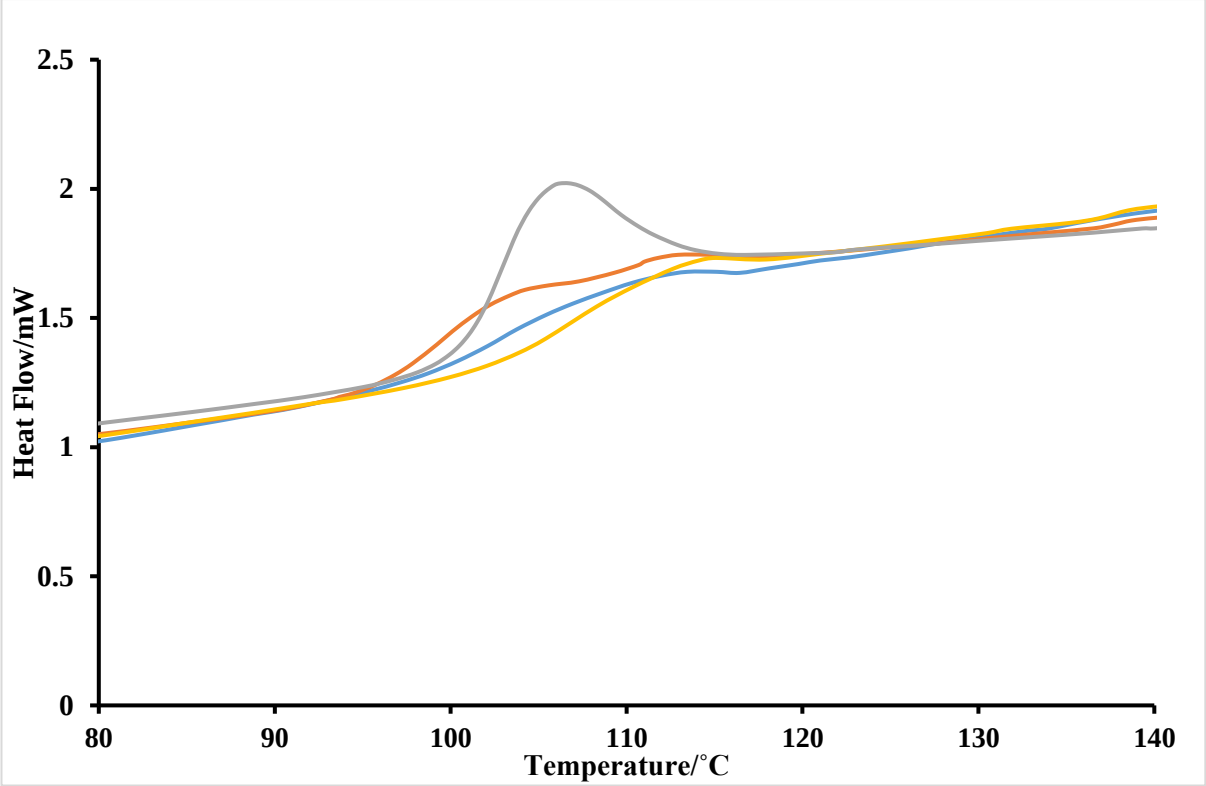

Figure 3.12: DSC Traces of MEK-ST/SAN Nanocomposites (Annealing T=85ºC ± 5ºC)

(-) unaged, (-) aged 24 hrs, (-) aged 72 hrs and (-) aged 168 hrs

The ΔC_p values can be calculated from the above DSC data. When a given amount of heat is supplied to a sample, its temperature will rise by a given amount. The amount of heat required to get a certain temperature increase is the heat capacity (C_p)[85]. The ΔC_p was calculated by integrating the area under the curve for the aged sample minus the integrated area under the curve for the unaged sample. This was done using a computer program as mentioned in the experimental chapter. From table 3.3 for the pure SAN samples, the ΔC_p increases as the aging time increases. This may suggest that as the polymer ages for longer timescales the chains have a chance to slowly relax down and therefore pack more closely together. This increased density of packing may result in the increase in heat energy required for the glass transition to occur. For the HDK-I samples there is a larger increase seen at 72 hrs aging. Figure 3.10 shows the DSC curve for the aged sample, here it can be seen that there is an obvious deviation from the trend. A much wider transition is observed, this resulted in the larger ΔC_p value. However, an increase between the 24hr and 168 hr samples are also seen. Furthermore, the HDK-O samples exhibited an increase in ΔCp as aging time increased. Lastly, the

MEK-ST samples follows the trend seen for figure 3.12, here the greatest increase is observed for the 168hr aged sample, with the 24 hr second and the lower value seen for the 72hr sample. It may be that as it was not the sample used in each instant (due to breakages) differences are seen.

Table 3.3 Comparison of Glass Transition Temperatures of Pure SAN and its Nanocomposites

Sample	Aging Time (Hrs)	T_g (^oC)	ΔT_g (^oC)	ΔT_g compared to Pure SAN (^oC)	ΔC_p (J/g/^oC)
Pure SAN	0	99.7	-	-	-
Pure SAN	24	104.4	+4.7	+4.7	0.21
Pure SAN	72	104.4	+4.7	+4.7	0.30
Pure SAN	168	106.1	+6.4	+6.4	0.39
10% HDK-I/SAN	0	100.0	-	+0.3	-
10% HDK-I/SAN	24	101.2	+1.2	+1.5	0.10
10% HDK-I/SAN	72	102.3	+2.3	+2.6	0.57
10% HDK-I/SAN	168	102.3	+2.3	+2.6	0.39
10% HDK-O/SAN	0	101.5	-	+1.8	-
10% HDK-O/SAN	24	103.3	+1.8	+3.6	0.22
10% HDK-O/SAN	72	105.0	+3.5	+5.3	0.33
10% HDK-O/SAN	168	105.0	+3.5	+5.3	0.46
10% MEK-ST/SAN	0	103.8	-	+2.7	-
10% MEK-ST/SAN	24	103.3	-0.5	+3.6	0.28
10% MEK-ST/SAN	72	105.4	+1.6	+5.7	0.14
10% MEK-ST/SAN	168	104.1	+0.3	+4.4	0.43

3.4.1 Relaxation Enthalpies

Each sample was aged in a vacuum oven for a given amount of time. The samples were then weighed into an aluminium DSC pan and heated from room temperature to 160˚C at a heating rate of 10˚C/min. The runs were carried out on a DSC 2010 Differential Scanning Calorimetry TA instrument. The relaxation enthalpies were calculated from the formula previous mentioned in chapter 2.

To calculate the enthalpic relaxation, $\Delta H_{Relaxation}$, the area under each aged peak was subtracted from that of the unaged sample and then integrated. Figure 3.13 shows a generic DSC trace for an unaged polymer and its aged counterpart.

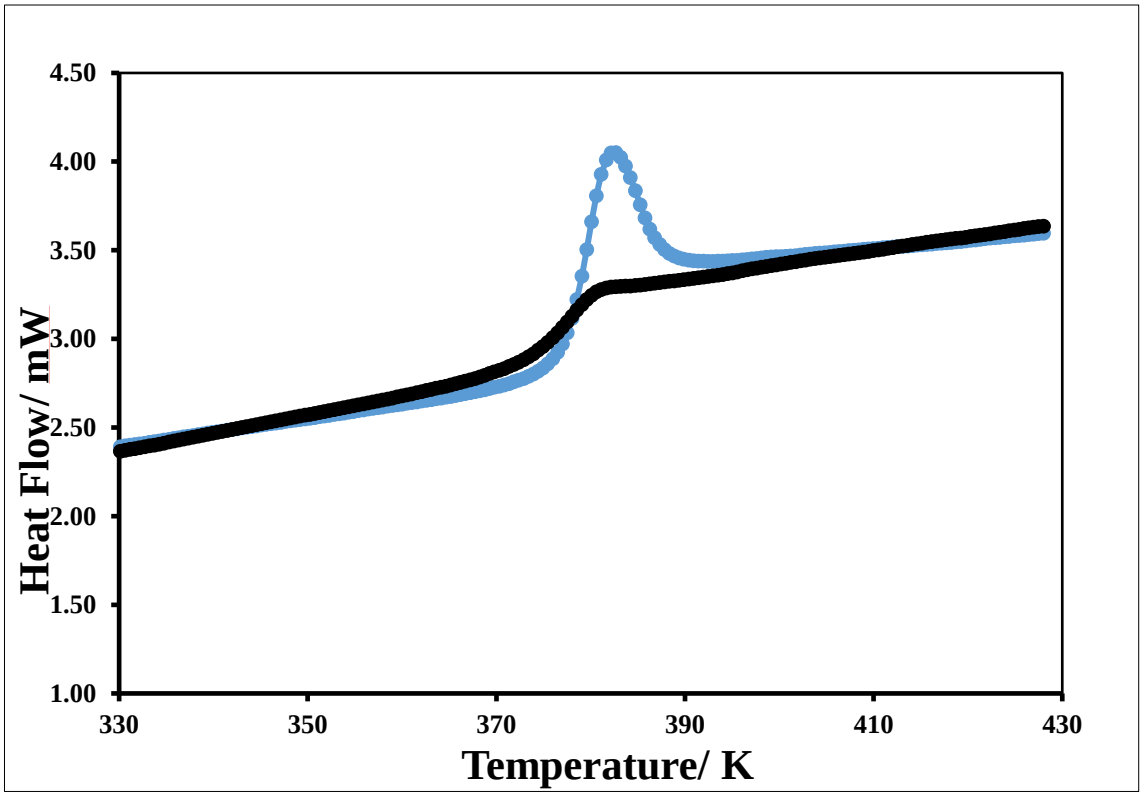

Figure 3.13 DSC traces showing the calculations of Relaxation Enthalpies

Unaged (-) Aged (-)

Below in table 3.4, values of the calculated relaxation enthalpies for all nanocomposite samples have been reported. The unaged samples do not exhibit an endothermic relaxation peak associated with physical aging. Figures 3.10, 3.11 and 3.12 show that

the magnitude of the aging peak increases with increasing time of aging. This in turn relates back to the enthalpic relaxation, which also increases with increased aging time. The pure SAN samples exhibited an increase in their $\Delta H_{relaxation}$ at 72 and 168hrs aging. No value could be obtained for the 24hr aged sample as no clear aging peak could be seen. The HDK-I and HDK-O samples also showed an increase in their $\Delta H_{relaxation}$ when compared to their unaged counterpart. Furthermore, both the HDK-I and HDK-O samples all exhibited a decrease in their $\Delta H_{relaxation}$ compared to the pure SAN samples. Previous studies on the aging effects of polymer nanocomposites also reported results similar trends[86, 87]. It has been suggested that this reduction in the aging effects caused by the presence of the nanofillers is due to the strong polymer-nanoparticle interactions. If strong interactions are present this may cause the polymer chains to have even further reduced segmental motion during the aging process, this may also suggest that the silica nanoparticles have reinforcement effects upon the polymer chains[71].

The MEK-ST silica nanocomposites showed an increase in their relaxation enthalpies, from 0.27(J/s) at 24 hrs aging to 1.55(J/s) at 168hrs aging. At 168 hr aging the MEK-ST sample had an $\Delta H_{Relaxation}$ the same as the pure SAN aged for the same time. This suggests that in this case, the addition of the MEK-ST silica nanoparticles has very little effect on the $\Delta H_{Relaxation}$.

Table 3.4: Calculation of Relaxation Enthalpies for SAN Nanocomposites

Nanocomposite	Aging Time (Hrs)	$\Delta H_{Relaxation}$ (J/s)
Pure SAN	**0**	**-**
Pure SAN	**24**	**-**
Pure SAN	**72**	**1.38**
Pure SAN	**168**	**1.55**
10% HDK-I/SAN	**0**	**-**
10% HDK-I/SAN	**24**	**0.13**
10% HDK-I/SAN	**72**	**0.28**
10% HDK-I/SAN	**168**	**0.80**
10% HDK-O/SAN	**0**	**-**
10% HDK-O/SAN	**24**	**0.67**
10% HDK-O/SAN	**72**	**1.35**
10% HDK-O/SAN	**168**	**1.24**
10% MEK-ST/SAN	**0**	**-**
10% MEK-ST/SAN	**24**	**0.27**
10% MEK-ST/SAN	**72**	**-**
10% MEK-ST/SAN	**168**	**1.55**

3.4.2 Cowie Ferguson Model

From figures 3.14 to 3.17 for the aging data of modified and unmodified SAN samples can been seen. As can be seen, the experimental values (represented by dots) are compared to their Cowie Ferguson (CF) models (solid line). It can be seen that for the pure SAN sample, the enthalpic relaxation does follow a trend similar to that expected from the CF model, figure 3.14. From the calculated CF trend, one would expect to see the ΔH values increase as the log of the aging time increases. In the case of the pure SAN the experimental results seem to match best at 72hrs aging with the 168hrs aging deviating slightly from the line.

The HDK-I/SAN sample does appear to follow the trend of the calculated values. The greatest deviation here from the CF model is the 72 hr aged sample. For the MEK-ST/SAN sample data at 72 hrs aging time were not plotted. This is because, for this sample, a clear aging peak could not be seen (Figure 3.10). However, the values of the CF parameters were obtained from the 24 hr and 168hr aged samples.

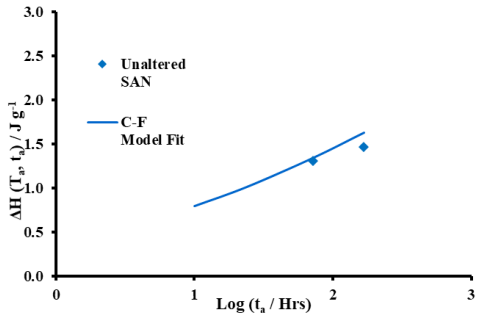

Figure 3.14: Enthalpic relaxation, ΔH, against log of the aging time (t_a) for the SAN samples. Solid line are the CF fits

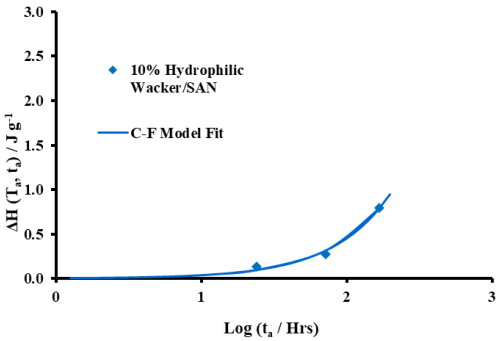

Figure 3.15: : Enthalpic relaxation, ΔH, against log of the aging time (t_a) for the HDK-I/SAN samples. Solid line are the CF fits

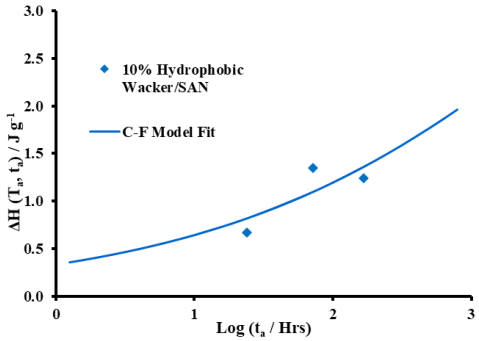

Figure 3.16: : Enthalpic relaxation, ΔH, against log of the aging time (t_a) for the HDK-O samples. Solid line are the CF fits

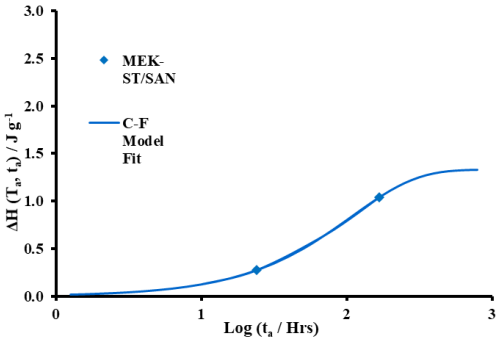

Figure 3.17: Enthalpic relaxation, ΔH, against log of the aging time (t_a) for the MEK-ST samples. Solid line are the CF fits

$$\Delta H(t_a, T_a) = \Delta H(\infty, T_a)[1 - \phi(t_a)] \quad [6]$$

This relaxation enthalpy function is a useful mathematical tool to quantitatively study the physical aging of polymer nanocomposites and takes into account the thermodynamic driving forces[87]. Several parameters can be found as a result of the CF model [6]. The ones discussed in this report are the β and T_c parameters. The values for the enthalpy change of the fully relaxed glass (ΔH (∞)) are also listed. As mentioned in the introduction the β value defines the width of relaxation rates and has values that vary between 0 and 1. If the β was found to be close to one, as seen in table 3.5, this suggests that there is a sharp and narrow distribution with only one relaxation time[35]. Values of β close to zero indicate that the ΔH is non exponential due to a broad distribution of relaxation times[35].

In some cases, such as that seen by Khalifa *et al*, the presence of the silica nanoparticles causes the breadth of the distribution of the aging times to increase and become wider. In Khalifa's experiment it was the interaction between PMMA and cab-o-sil H5 that was being studied. From their results, it could be taken that the silica nanoparticles are interacting with the PMMA chains during the relaxation and leading to longer and broader aging times arising. From the experimental results found for this study of HDK-I, HDK-O and MEK-ST silica, the β values were found to be equal to 0.97 for all samples. This suggests that the aging of the silica nanocomposites is mainly dominated by the faster moving SAN chains.

T_c, which is defined as the characteristic aging time, increased upon addition of silica nanoparticles, except in the case of the MEK-ST where a smaller increase was observed. The T_c of the pure unaltered polymer was found to be 90.5 minutes, however the T_c of the filled samples varied from 109-394 minutes. The T_c data revealed that the rate of the relaxation process was much slower in the HDK-I and HDK-O SAN nanocomposites than in the pure SAN and the colloidal silica samples. This is similar to findings in the aged DMA data (Figures 3.23-2.26). T_c suggest that the incorporation of the HDK-I and HDK-O silica nanoparticles into the SAN polymer matrix leads to longer characteristic aging times and an increase in the relaxation enthalpy of the fully aged samples. These longer characteristic aging times may be due to the hydrogen bonding interactions between the polymer matrix and the silica. This interaction may

encourage the chains to relax more slowly due to their attractive nature. This effect would also be expected to be seen for the MEK-ST sample as it too will have H-bonding interactions. The fact that this is not observed in the data results may be due to experimental error.

Table 3.5 Enthalpic Relaxation Parameters for SAN Nanocomposites from fitting data using CF equation

Sample	ΔH (∞) (J/g)	β	τ_c (min)	Log(t_c/min)
Pure SAN	0.97	0.97	90.5	1.96
10% HDK-I/SAN	2.68	0.97	394.3	2.60
10% HDK-O/SAN	2.47	0.97	345.3	2.54
10% MEK-ST/SAN	1.33	0.97	109.02	2.04

In figure 3.18 the experimental change in enthalpy for each sample at its giving aging time (t_a) and aging temperature (T_a) can be seen. This diagram shows the enthalpic changes that occur below the Tg. The pure SAN ages differently form the HDK-I and HDK-O nanocomposites. The HDK-I samples did have some issues with the DSC data, it was very difficult to see clear aging peaks, therefore affecting the results for the relaxation enthalpies and subsequent calculations. This may explain the lower enthalpy value at Log (t_a) 2.22. The enthalpy values for the HDK-O nanocomposites are higher than that for the pure polymer. In a study carried out on the enthalpy of recovery of PMMA silica nanocomposites by Boucher *et al*[87] a similar trend was also seen. They found that the presence of silica in their PMMA nanocomposites indicated an accelerated structural recovery of the polymer compared to the unmodified PMMA. The MEK-ST silica appears to age similarly to the SAN, with higher $\Delta H(t_a,T_a)$ values.

At 168hr aging the nanocomposite samples will be reaching a final structural state[87]. These results are consistent with the fumed HDK-O and MEK-ST sample showing an acceleration of physical aging and the HDK-I sample showing a suppression in the aging as the aging time increases. Boucher goes on to point out that in the acceleration of physical aging found by their study, the results cannot be due to a change in the segmental motion of the polymer chains as their glass transition temperatures never changed upon the addition of silica. They therefore state that the physical aging is related to the ratio of the area of silica to the volume of PMMA and consequently the

inter-particle distance of silica within the sample[25]. However, the HDK-I sample showing a reduction in the effects of physical aging and the relaxation enthalpy follows the trend reported by many experimentalists[71, 86]. It is interesting to note that Lin *et al*[71] also noticed both a reduction and an increase in the relaxation enthalpies of their PS/silver nanocomposites. Here they suggest that the negligible change in glass transition temperature and the increase in relaxation enthalpies is due to the plasticisation effect of the PS matrix caused by packing constraints of the PS chains due to the presence of the silver nanoparticles. They go on to suggest that there are not strong particle-polymer interactions as the PS chains were not grafted to the Ag nanoparticles. Finally, they offer an explanation as the suppression effect on physical aging shown by their second sample, they suggest that the anti-plasticization effects and an increase in the chain barrier between nanoparticles leads to a slowing down of the physical aging. It should be noted that the parameters used for the calculation of the $\Delta H(t_a,T_a)$ reply upon the accuracy and fitting of the Cowie-Ferguson model. From figures 3.14-3.17 the experimental data does deviate slightly from the model. This in turn may have a cascading effect on the calculations for the enthalpy. It is interesting to note that the previous DSC data leant towards an argument for positive reinforcement of the polymer nanocomposite however the C-F model may suggest otherwise. It should be pointed out that the changes in the T_g, E', E'' and tan δ are all relatively small.

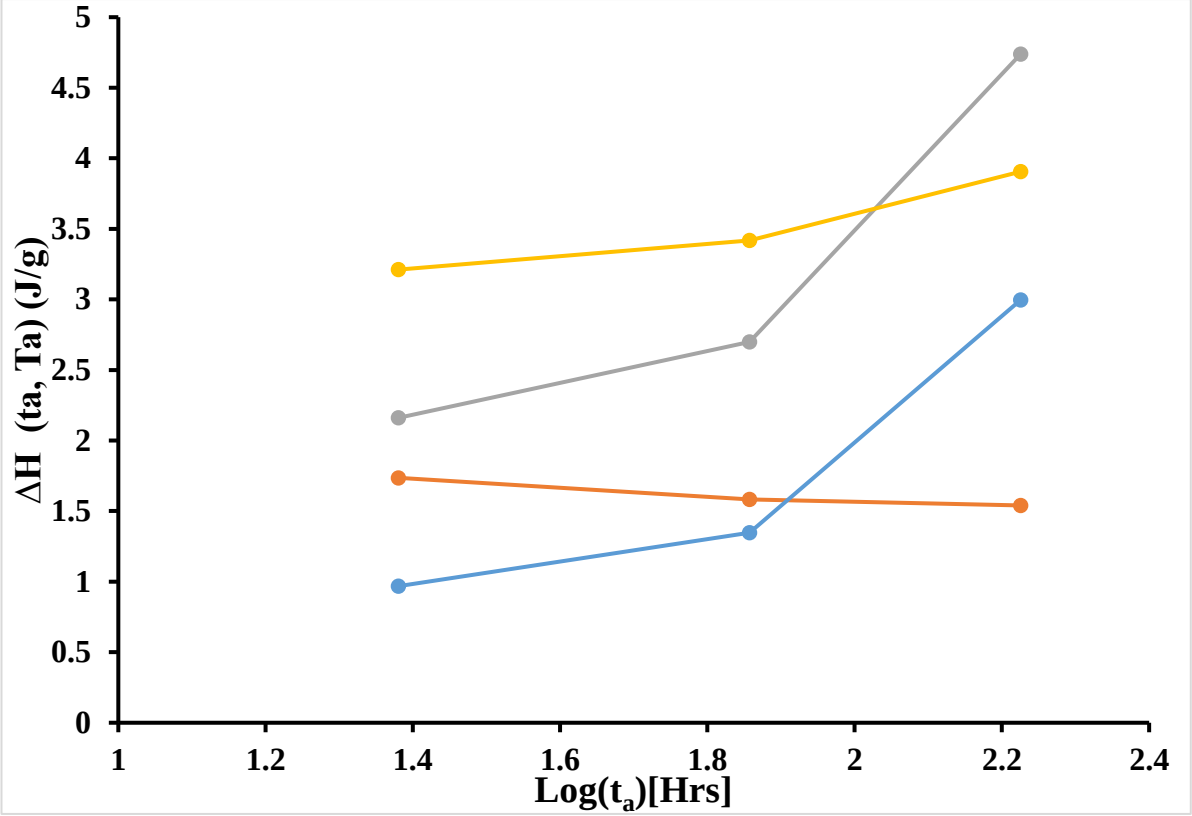

Figure 3.18: Enthalpic Change for each sample at their given Aging time (t_a) and aging Temperature plotted against log of the aging time (t_a)

(-) Pure SAN, (-) 10% HDK-I/SAN, (-) 10% HDK-O/SAN and (-) 10% MEK-ST/SAN

3.5 Mechanical Reinforcement Effects of Silica Nanoparticles in the Physical Aging of SAN Nanocomposites

Figures 3.19-3.22 show the viscoelastic response of SAN and its silica nanocomposites over an aging range. At the lower temperatures, the storage modulus of the samples is constant, as the temperature approaches the T_g region the polymer chains begin to have more motion and a change in the shifting of the storage modulus was observed. Firstly, the unaged data, here there is little deviance from the unmodified polymer. The unmodified polymer had an E' temperature of 109.5^{O}C, the HDK-I sample was 110^{O}C, the HDK-O sample was 117.7^{O}C and the MEK-ST was 109.7^{O}C. This larger shift in the HDK-O sample may be due to the interactions of the HDK-O particles with the SAN however it may also be caused by any deformations or imperfections in the sample. Secondly the 24 hrs aged samples, for the unmodified sample had an E' temperature of 111.7^{O}C. This showed an increase of +2.2^{O}C compared to the unaged sample. Furthermore, the HDK-I and HDK-O samples exhibited a small negligible decrease of 0.31 and 1.2 ^{O}C respectively. The greatest shift observed was for the MEK-ST samples. Here there was an increase of 4.7^{O}C. When looking at the 72 hrs aged samples there is once again a slight increase for the HDK-O and MEK-ST samples. The pure SAN showed very little change from previous samples with an E' of 108.5^{O}C. The HDK-O and MEK-ST samples were found to have a value of 112.7 and 117.3^{O}C. The value obtained for the HKD-I sample of 103.4^{O}C was a decrease of 5^{O}C. This larger change may be due to deformations in the sample or the presence of excess solvent as mentioned for figure 3.10. At 168 Hr aging, there is very little difference in the storage moduli for the samples. However, it is also clear to see that the HDK-I sample exhibits a clear rubbery plateau further verifying that in the case of this sample, a greater cross-linked polymer-filler network is formed. In terms of this study, the increase noted in both the MEK-ST and HDK-O samples suggests that effective cross-linking can lead to increases in the reinforcement of the polymer nanocomposite. This is in agreement with Holt[88] who attributed their increase in modulus to the formation of a large-scale nanoparticle network. The RSC state that cross-linking "makes the whole structure more rigid and less elastic"[6]. Previously in the storage modulus, loss modulus and tan delta for the unaged samples, the HDK-O appeared to have the greatest reinforcement effect out of the other two silica filled samples. However, in the aging data it can be seen that there are some differences, for example at the 72 hrs aging time it was not the

hydrophobic samples that exhibit the greatest increase in T_g but the colloidal MEK-ST samples. The least amount of variation in moduli is observed at 168 Hrs aging, at this point the samples will have reached their aging plateau, i.e. the chains will not relax any further at point. It must be asked why we see such conflicting experimental results, in some cases as above we see an increase in reinforcement in the HDK-O samples and a very little change in the MEK-ST samples for the 0 Hr aging yet in the aging experiment we observe a greater increase in the MEK-ST samples compared with others. It is not easy to identity a clear-cut reason for the discrepancies seen. In the case of the 168 hrs aging where little change is observed, the reinforcement effects appear to disappear upon aging. One explanation for this may be that the aging causes a redistribution of the particles within the nanocomposite. However further experiments would need to be carried out. There are a number of variables involved that must also be taken into account, for example the quality of the nanoparticles, the methods of preparations and drying of the samples, how well the nanoparticles dispersed within the polymer matrix, the formation of aggregates and the hot pressing of the samples[88]. The curves at 24 hrs, 72 hrs and 168 hrs all show similar properties of that of the unaged, unmodified SAN. the greatest difference from this was seen for the 72 hrs HDK-I sample, where a longer, flatter rubbery plateau was seen. This suggests that a non-covalent cross-linked network may have formed between the polymer and the filler particles. Furthermore, the HDK-O sample at 168 hrs aging showed some deviation from the unmodified polymer. Here much lower values for E' were observed. The unaged samples showed the greatest change compared to the pure SAN.

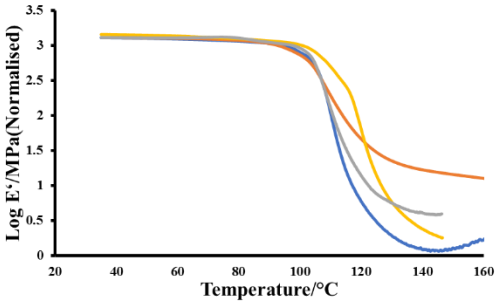

Figure 3.19: Log of normalised Storage Modulus of Unaged SAN/SAN Nanocomposite against Temperature

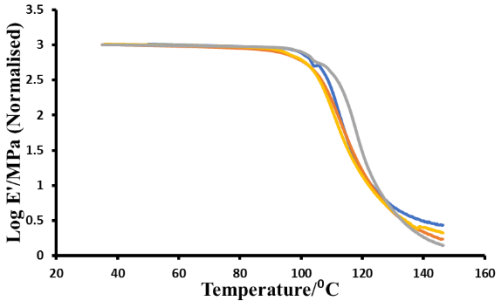

Figure 3.20: Log of normalised Storage Modulus of 24hrs Aged SAN/SAN Nanocomposite against Temperature

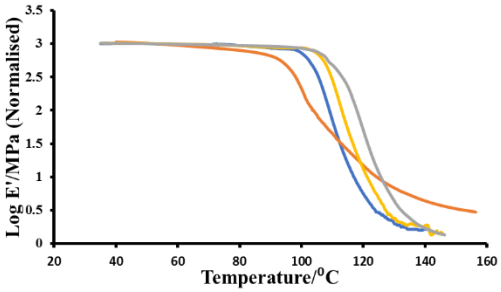

Figure 3.21: Log of normalised Storage Modulus of 72hrs Aged SAN/SAN Nanocomposite against Temperature

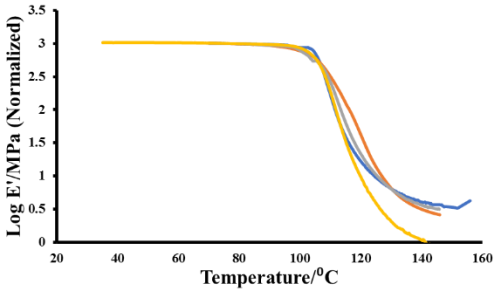

Figure 3.22: Log of normalised Storage Modulus of 168hrs Aged SAN/SAN Nanocomposite against Temperature

(-) Pure SAN, (-) 10% HDK-I/SAN, (-) 10% HDK-O/SAN and (-) 10% MEK-ST/SAN

The aging data for the loss modulus can be seen in figures 3.23-3.26. It once again mirrors that of the storage modulus data for the aged samples. At 24 Hr aging the MEK-ST sample shows the greatest increase in the loss modulus, with the HDK-I sample displaying very similar results to that of the unmodified silica. The HDK-O shows a decrease in the loss modulus at 24 Hr aging but shows an increase at both the 72 Hr and 168 Hr aging. At 168 Hr aging the samples all exhibit a slight increase in loss modulus compared to the pure SAN. The nanocompoistes all display similar proerties to that of the unmodifeid SAN.

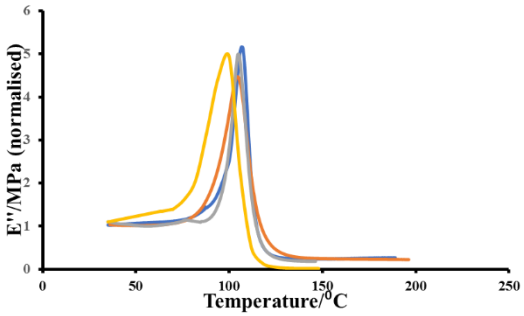

Figure 3.23: Log of normalised Loss Modulus of Unaged SAN/SAN Nanocomposite against Temperature

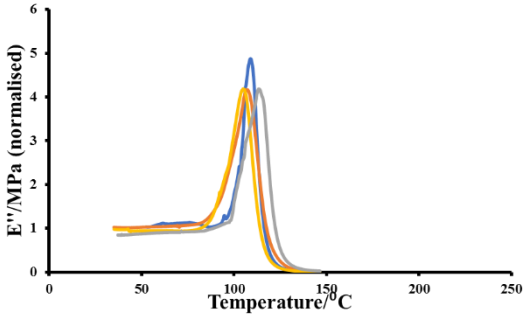

Figure 3.24: Log of normalised Loss Modulus of 24 hrs aged SAN/SAN Nanocomposite against Temperature

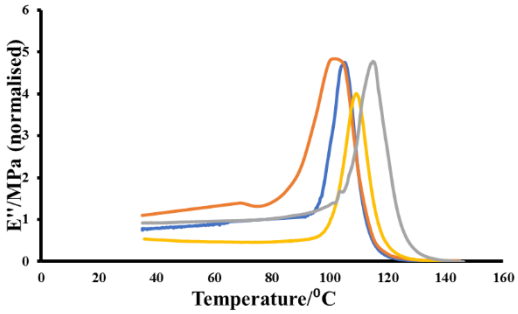

Figure 3.25: Log of normalised Loss Modulus of 72 hrs aged SAN/SAN Nanocomposite against Temperature

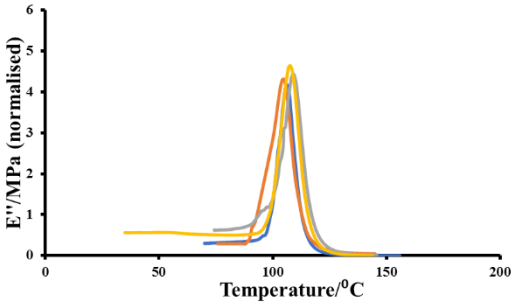

Figure 3.26: Log of normalised Loss Modulus of 168 hrs aged SAN/SAN Nanocomposite against Temperature

(-) Pure SAN, (-) 10% HDK-I/SAN, (-) 10% HDK-O/SAN and (-) 10% MEK-ST/SAN

The tan delta data associated with the aging experiments can be seen in figures 3.27-3.30. The data does follow a similar trend with the DSC data obtained for the glass transition temperatures of the SAN nanocomposites. For example, at 24 Hr and 72 Hr aging times the tan delta data suggests that the MEK-ST sample showed the greatest increase, and when consulting the DSC data it was found that the MEK-ST samples also showed an increase in T_g of +4.5ºC and +5.7ºC respectively. The majority of the data does fit that found by the DSC experiments. However, the HDK-O samples did exhibited some differences in T_g measured. This may be due to deformation in the sample or unevenness may lead to slight discrepancies being observed. For example, at 0hr aging the HKD-O sample T_g, measured by Tan δ, was found to be 124.0ºC, at 24 hrs this was then found to be 114.9ºC. This is a decrease of 9.1ºC. As mentioned previously this may be due to the fact that some of the samples had snapped and new ones were made, i.e. the same sample was not always used each time. Different deformations/flaws may be present in this new sample leading to the inconsistent results.

Table 3.6: T_g of SAN-Silica nanocomposites determined by DMA

Sample	Aging Time (Hrs)	T_g (°C)
Pure SAN	0	114.1
10% HDK-I/SAN	0	113.6
10% HDK-O/SAN	0	124.0
10% MEK-ST/SAN	0	115.6
Pure SAN	24	117.2
10% HDK-I/SAN	24	118.7
10% HDK-O/SAN	24	114.9
10% MEK-ST/SAN	24	121.1
Pure SAN	72	112.6
10% HDK-I/SAN	72	110.0
10% HDK-O/SAN	72	114.8
10% MEK-ST/SAN	72	123.3
Pure SAN	168	114.0
10% HDK-I/SAN	168	124.2
10% HDK-O/SAN	168	115.1
10% MEK-ST/SAN	168	116.5

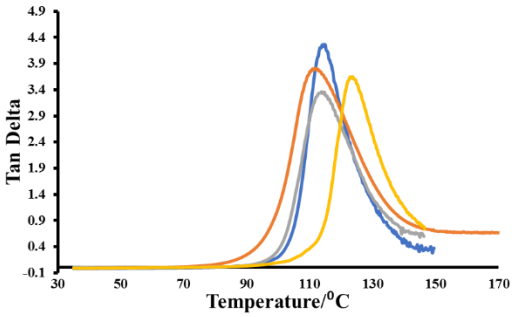

Figure 3.27: Log of normalised Tan Delta of Unaged SAN/SAN Nanocomposite against Temperature

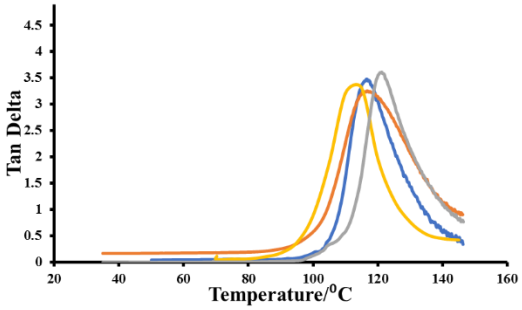

Figure 3.28: Log of normalised Tan Delta of 24 hrs Aged SAN/SAN Nanocomposite against Temperature

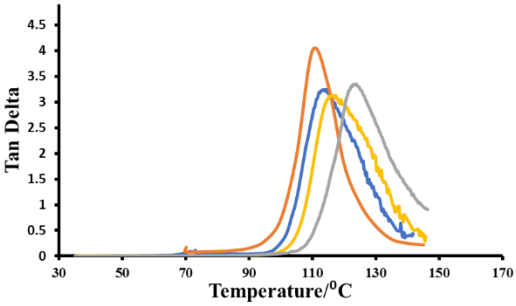

Figure 3.29: Log of normalised Tan Delta of 72 hrs Aged SAN/SAN Nanocomposite against Temperature

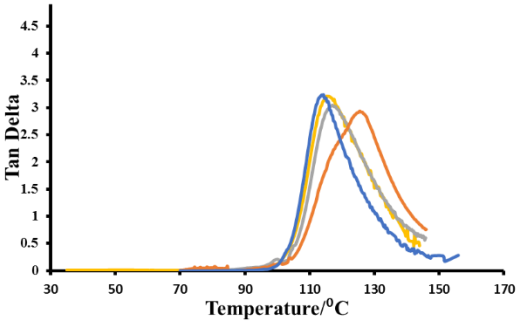

Figure 3.30: Log of normalised Tan Delta of 168 hrs Aged SAN/SAN Nanocomposite against Temperature

(-) Pure SAN, (-) 10% HDK-I/SAN, (-) 10% HDK-O/SAN and (-) 10% MEK-ST/SAN

3.5.1 Master Curves

The dynamic properties of polymers and their nanocomposites are affected by temperature and the frequency of the dynamic loading[67]. Using the time-temperature superposition principles for the storage modulus, master curves were obtained. This principle relies on the notion that relaxation times relating to a given relaxation process have the same temperature dependence[67]. Thus, master curves provide information on the viscoelastic properties of the material. As mentioned in chapter 1, the Williams-Landel-Ferry equation was used to analyse the master curve data.

The slope of all the master curves were calculated using the method mentioned in the experimental chapter. The reinforcement effect was taken to be the difference in slope of the aged and unaged samples. If the sample exhibited a reinforcement effect, then one would expect the value of the slope to decrease. This change in slope would show a wider transitional region and therefore a change in the movement of the polymer chains. A steeper slope may show a clearer transitional region and therefore no filler effect.

Table 3.7: Slopes of Master Curves for SAN Nanocomposites

Sample	Aging Time (Hrs)	G' Slope
Pure SAN	0	0.719
Pure SAN	24	0.639
Pure SAN	72	0.676
Pure SAN	168	0.426
10% HDK-I/SAN	0	0.341
10% HDK-I/SAN	24	-
10% HDK-I/SAN	72	0.530
10% HDK-I/SAN	168	0.422
10% HDK-O/SAN	0	0.458
10% HDK-O/SAN	24	0.565
10% HDK-O/SAN	72	0.534
10% HDK-O/SAN	168	0.461
10% MEK-ST/SAN	0	0.544
10% MEK-ST/SAN	24	0.561
10% MEK-ST/SAN	72	0.375
10% MEK-ST/SAN	168	-

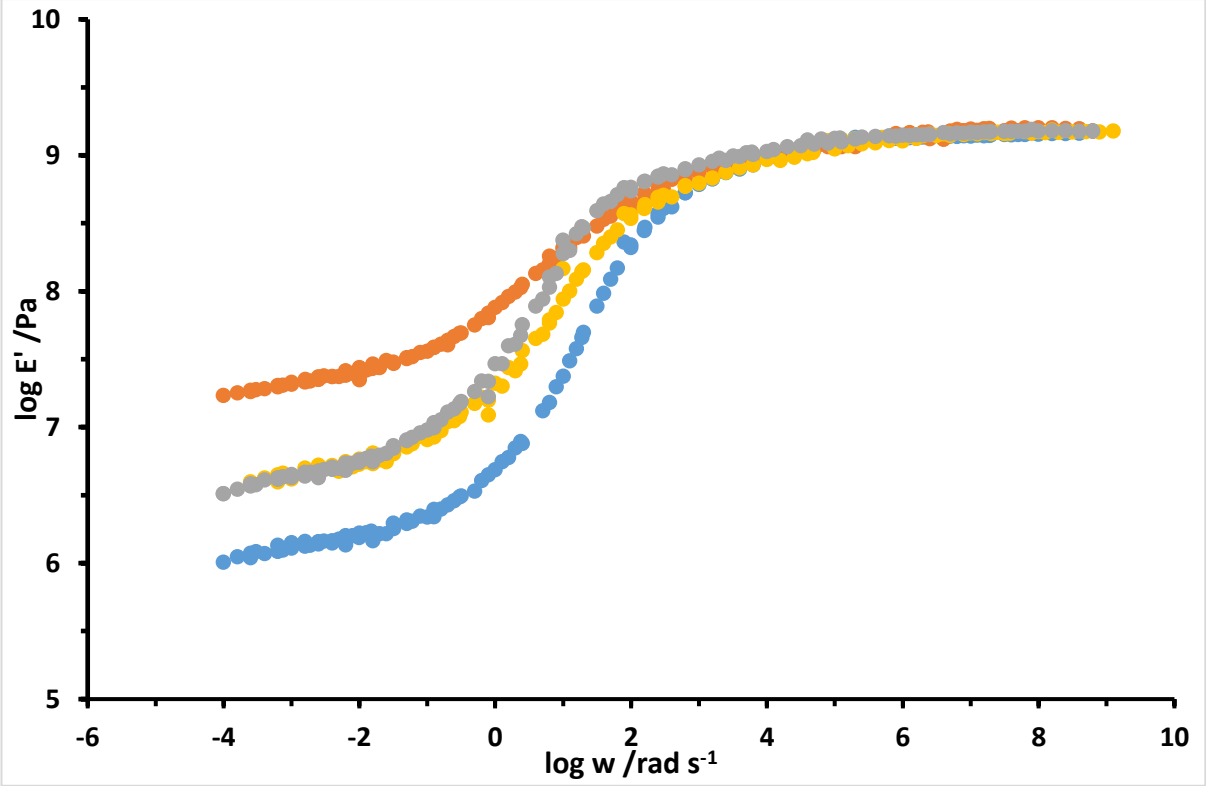

Figure 3.31: Master curve data for the unaged aged SAN/Silica Nanocomposites (○) Pure SAN, (○) 10% HDK-I/SAN, (○) 10% HDK-O/SAN and (○) 10% MEK-ST/SAN

Figure 3.31 shows the master curves for the unaged SAN and silica/SAN nanocomposites. The data has been normalized to the highest value of the modulus at high frequency. The curves were shifted using a reference temperature of 100ºC, which also corresponds to the DSC glass transition temperature of the pure SAN. As shown in figure 3.31there are three main regions to a master curve[89]. At low frequencies (long times) the samples all appear to have a low modulus and therefore act as rubbers. As the frequency increases (shorter times) the modulus begins to increase, this process starts around the T_g of the polymer. At higher frequencies, the modulus levels out and reaches a plateau: this is the glassy state. At high frequency, only small changes in the storage moduli are expected and therefore data have been normalized to the highest E' value measured among all the samples. Any changes in mobility due to the presence of the filler particles are observed in the rubbery plateau region, at low frequencies. In the nanocomposite samples, there was a small increase in the storage moduli. This suggests to an extent the silica nanoparticles are restricting the motion of the polymer chains. The

increase was greatest in the HDK-O silica samples. With the MEK-ST filler sample with very similar results. As can been seen from figure 3.31and table 3.8, the HDK-I sample showed the greatest deviation.

Table 3.7 shows the change in the slope of the master curves. In the unaged samples, all of the samples containing silica nanoparticles exhibited a smaller slope compared to that of the pure SAN. This suggests that the slopes are steeper and therefore a smaller transitional region. This in turn hints at a possible restriction of polymer chain movement.

Data plotted in figure 3.31 indicate that, compared to the pure SAN, addition of 10% silica caused an increase in the storage moduli above the glass transition temperature (at low frequency). By measuring the amount of decrease in the storage modulus of each sample, across the T_g region, a measure of the reinforcement effects of silica nanoparticles on SAN can be monitored.

It is clear from table 3.8 that compared to the neat SAN sample, there is a variation in the reinforcement seen, depending on the type of silica used. In the case of the HDK-I sample there is a positive reinforce of 1.17 Pa observed while in the HDK-O and MEK samples exhibit a slight positive reinforcement of 0.53 Pa and 0.50 Pa respectively.

Table 3.8: Amount of decrease in E' across the T_g region as a measure of reinforcement for the unaged nanocomposites

Sample	Δ E' (Pa)	Δ E' $_{\text{Nanocomposite- SAN}}$ (Pa)
Pure SAN	2.91	-
10% HDK-I/SAN	1.74	-1.17
10% HDK-O/SAN	2.38	-0.53
10% MEK-ST/SAN	2.41	-0.50

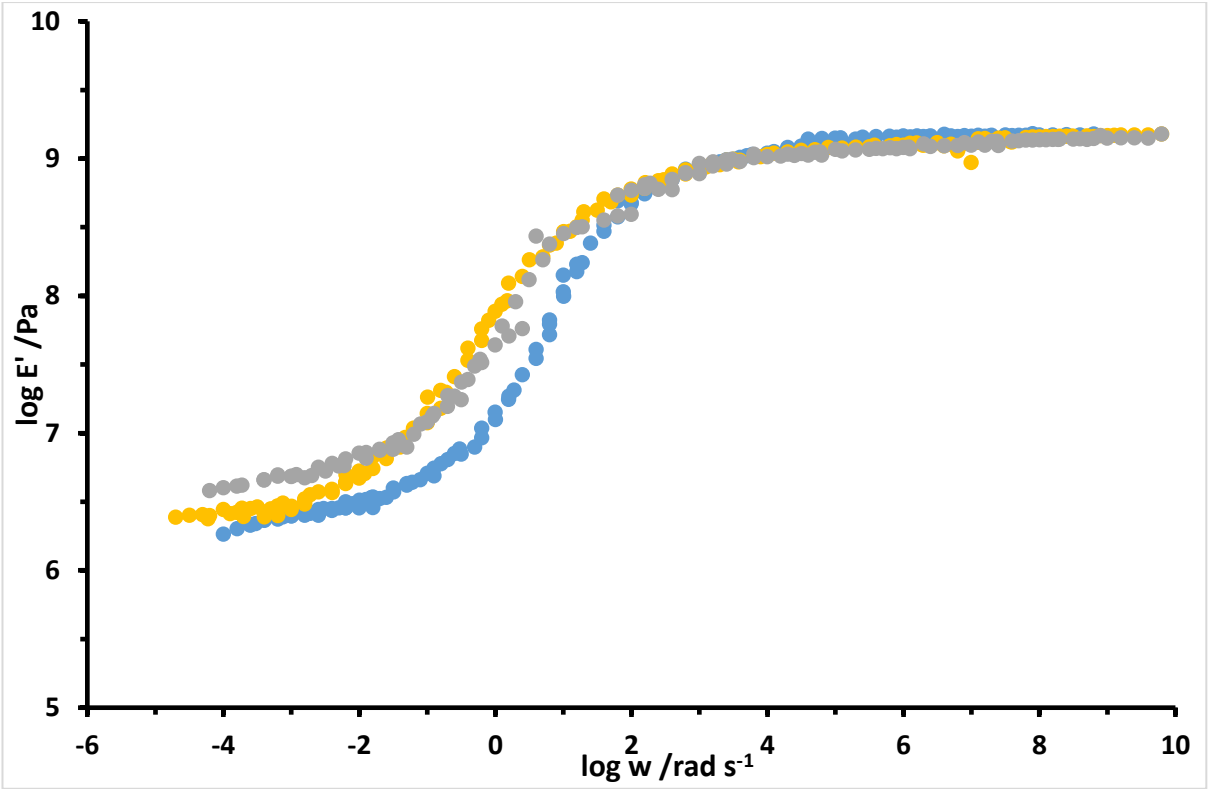

Figure 3.32: Master curve data for the 24 Hr aged SAN/Silica Nanocomposites (Aged at85^{O}C ± 5^{O}C)

(○) Pure SAN, (○) 10% HDK-I/SAN, (○) 10% HDK-O/SAN and (○) 10% MEK-ST/SAN

Cowie mentions that SAN exhibited an increase in the steepness of the slope of the samples as they aged[90]. The aged samples were compared against the unaged samples. Figure 3.32 shows the master curves obtained for samples that were aged for 24 hr at 85^{O}C ± 5^{O}C. Compared to the unaged data of figure 3.31, small differences can be observed among the samples at low frequency. Based on the unaged data, the largest reinforcement should have been measured for the 10% HDK-I/SAN sample. Unfortunately, the frequency data for this sample was collected up to 115^{O}C, too close to the samples glass transition to be of use for generating a master curve. These are not present in figure 3.32.

The aged samples exhibited very little change in the slope ranging from 0.565 to 0.561 Pa (table 3.7). The HDK-O and MEK-ST samples exhibited a slight decrease in the slope suggesting possible positive reinforcement effect, in this instance it should be noted that the increase is relatively small and may be due to experimental error.

Table 3.9 shows the change in E' across the T_g region as a measure of reinforcement. When compared to the aged unmodified SAN sample both the HDK-O and MEK-ST samples exhibited a slight positive reinforcement effect of 0.12 and 0.35 Pa respectively. When the change in E' are compared for the aged and unaged nanocomposite samples, the HDK-O sample shows a negative reinforcement effect with an increase in the E' of +0.20Pa. The aged MEK sample showed very little change from that of its unaged counterpart.

Further investigation looked at the difference between the aged filled samples and the unaged unmodified SAN, once again very little increase ranging from 0.21 to 0.56 Pa. When comparing with the unaged SAN, there is a larger difference in the slope of the curves for the aged filled samples. This may suggest that the presence of the silica nanoparticles is slowing the relaxation of the polymer chains compared to that of the unfilled sample. The HDK-O sample showed little change in the slope of the master curve suggesting that the presence of the filler particles has little effect on the SAN aging on this time scale. The MEK-ST sample also exhibited a decrease in slope of 0.561 Pa. This also correlates to the ΔE' values seen in table 3.9.

Table 3.9: Amount of decrease in E' across the T_g region as a measure of reinforcement for the 24 hr aged nanocomposites

Sample	Δ E' (Pa)	Δ aged-unaged (nanocomposite) (Pa)	Δ E' aged nanocomposite-unaged SAN (Pa)
Pure SAN	2.70	-0.18	-0.21
10% HDK-I/SAN	-	-	-
10% HDK-O/SAN	2.58	+0.20	-0.33
10% MEK-ST/SAN	2.35	-0.06	-0.56

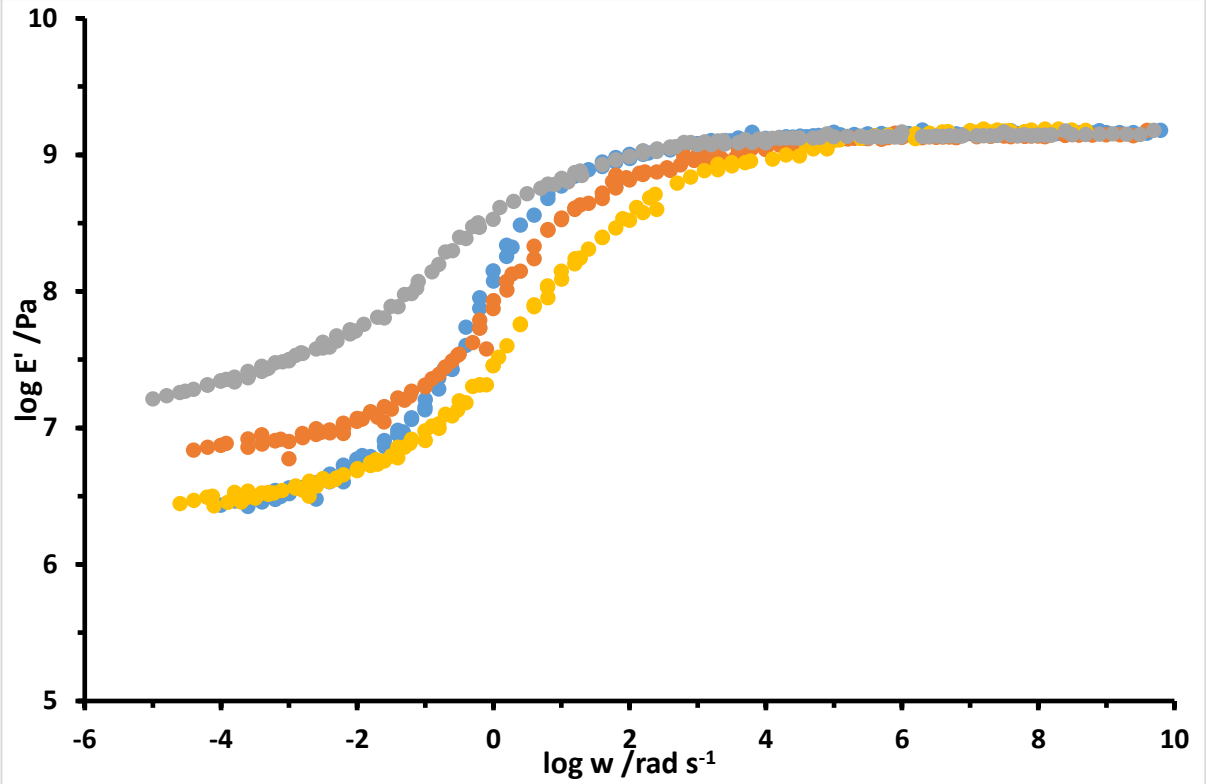

Figure 3.33: Master curve data for the 72 Hr aged SAN/Silica Nanocomposites (Aged at85^{O}C ± 5^{O}C)

(○) Pure SAN, (○) 10% HDK-I/SAN, (○) 10% HDK-O/SAN and (○) 10% MEK-ST/SAN

The master curves for the 72 hour aged samples are compared in Figure 3.33. In this instance, the 10% HDK-O/SAN sample showed a much larger transitional region but reaches values of rubbery plateau close to those of the pure SAN. This suggests little reinforcement whereas larger transitional region suggests that the polymer chains have a larger range of frequency under which they are slightly mobile.

There is much greater variation in the 72 hr aged data compared to that of the 24 hr. Table 3.10 shows that when compared to the 72 hr aged SAN samples the aged nanocomposites the fumed silicas were found to show a slight negative reinforcement of 0.50 Pa for the HDK-I and 0.21 Pa for the HDK-O. When we also look at the slope of the curve in table 3.7 further evidence for this is found. The slope of HDK-I aged 72hrs shows a decrease in the steepness of the slope by 0.146 Pa. Due to deformities in the 24 hr sample it was not clear to see the true change in reinforcement over time. This

sample provided much more reliable data. The HDK-O sample also showed a negative reinforcement for the 72 hr aging, notably less significant than that of the HDK-I.

The MEK-ST sample showed the greatest positive reinforcement when considering our two parameters of slope and ΔE'. A change of -0.71 Pa was seen for the ΔE' and a decrease in the slope was also found to be 0.301 Pa. This may suggest that the addition of silica nanoparticles to the polymer does provides reinforcement for the polymer chains by restricting movement through intermolecular interactions. When comparing to the unaged unaltered SAN samples all of the 72 hr aged samples exhibited a change in slope. This is more significant to the MEK and the HDK-I samples as they showed the greatest decrease of 0.146 and 0.301 respectively. When comparing the slope of the modified samples to the unaged, unmodified sample it is clear to see that as the samples age there is a decrease in the value of the slope of the master curves. This decrease is due to the samples aging. When compared against its unaged counterpart and the unmodified unaged SAN the MEK-ST sample exhibited the greatest decrease in the slope. Suggesting that in this case the MEK-ST sample suppressed the physical aging effects to a small degree. This agrees with the storage modulus data obtained in figure 3.21.

Table 3.10: Amount of decrease in E' across the T_g region as a measure of reinforcement for the 72 hr aged nanocomposites

Samples	ΔE' (Pa)	Δ E' aged-unaged (nanocomposite) (Pa)	Δ E' aged nanocomposite-unaged SAN (Pa)
Pure SAN	2.62	-0.29	-0.29
10% HDK-I/SAN	2.24	+0.50	-0.67
10% HDK-O/SAN	2.59	+0.21	-0.32
10% MEK-ST/SAN	1.70	-0.71	-1.21

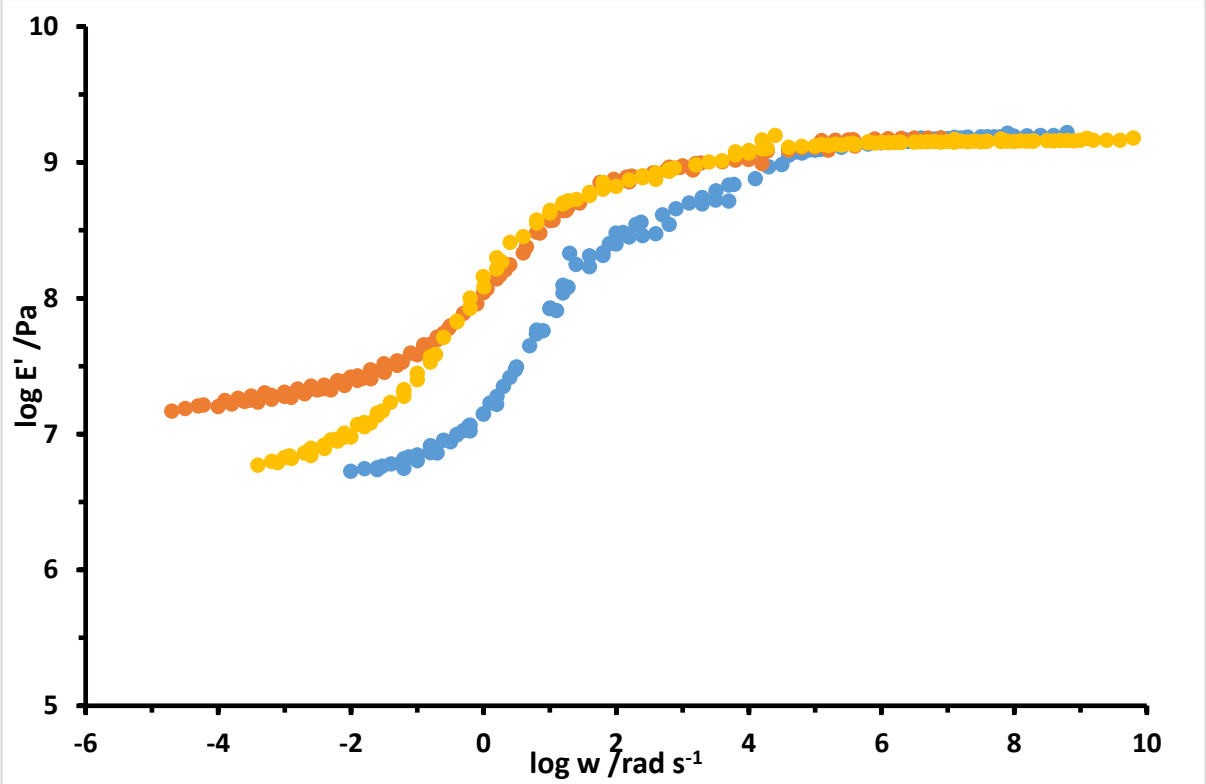

Figure 3.34: Master curve data for the 168 Hr aged SAN/Silica Nanocomposites (Aged at85^{O}C ± 5^{O}C)

(○) Pure SAN, (○) 10% HDK-I/SAN, (○) 10% HDK-O/SAN and (○) 10% MEK-ST/SAN

Finally, the 168 hour aged samples were investigated. Figure 3.34 shows the changes between the samples, there appears to be a lack of uniformity. The MEK-ST sample was removed from the figure the results as this sample was extremely difficult to obtain reliable results for. This could be as previously mentioned due to deformation of the sample but if mixing of the filler nanoparticle was unsuccessful this may have led to aggregates forming. This would have led to concentrated areas of filler particle which may cause inaccuracies in the results. Overall this suggests that regardless of the filler type over the range of temperatures studied no or little reinforcement effects were observed. One improvement that should be made is the process by which the moulds are produced to ensure uniformed and flat samples are obtained each time.

Table 3.11 shows the change in E' for the 168hr aged samples. From this it can be seen that when compared to the pure SAN aged 168hrs the HDK-I sample once again exhibits a positive reinforcement effect. The HDK-O sample was very similar to that of

SAN. When comparing the 168hr aged samples with the unaged SAN sample the HDK-I sample has the greatest reinforcement effect, -1.06 Pa. The MEK-ST also showed a positive reinforcement of -0.59 Pa.

All three 168 hrs aged samples have similar values of the slope for their master curves. This is quite different when compared to the slopes of the curves at 24hr and 72 hrs aging. This deviation between the aged samples may be due to the relaxation effects but it may also be related to the fact that the samples were often repressed between aging sessions. This change in the samples' dimensions and reversal of the physical aging may contribute to the differing values observed. When the filled samples are compared to their unaged counterparts an increase in the reinforcement is observed. When compared to the pure unaged SAN, the filled samples also showed an increase in the reinforcement of the samples.

Table 3.11: Amount of decrease in E' across the T_g region as a measure of reinforcement for the 72 hr aged nanocomposites

Sample	ΔE' (Pa)	Δ E' aged- unaged (nanocomposite) (Pa)	Δ E' aged nanocomposite-unaged SAN (Pa)
Pure SAN	2.37	-0.54	-0.54
10% HDK-I/SAN	1.85	+0.11	-1.06
10% HDK-O/SAN	2.32	-0.06	-0.59
10% MEK-ST/SAN	-	-	-

3.5.2 Shift Factors

By plotting a graph of the log of the shift factors (α_T) vs temperature, the constants C_1 and C_2 can be calculated, as well as providing information that allows the fractional free volume of the sample to calculated.

In order to estimate how successful, the shifting has been a comparison between the calculated values using the WLF method and the experimental values was carried out. Figure 3.35 shows the plots for the unaged samples. The dots represent the experimental values and the solid lines represent the calculated shift values.

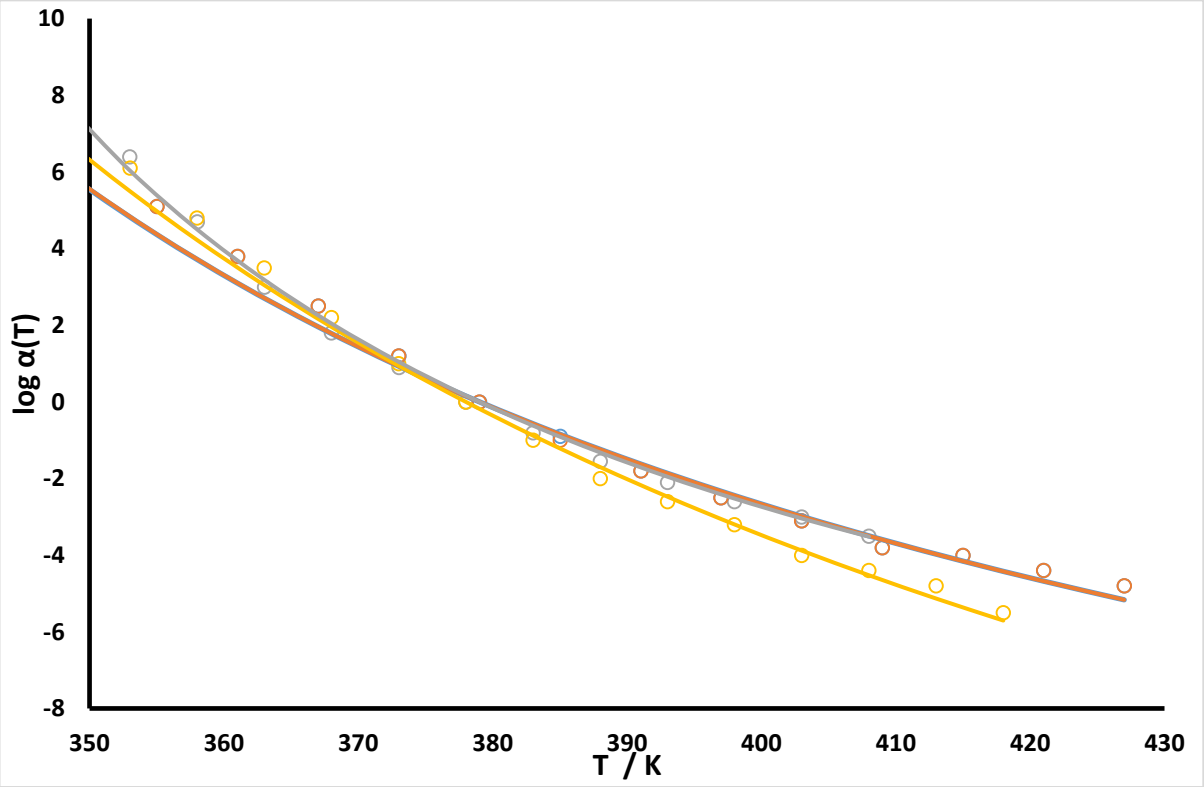

Figure 3.35: Shift Factor plot and WLF fit for Pure SAN samples

(○) Unaged SAN (experimental), (○) 24 hrs aged (experimental), (○) 72 hrs aged (experimental) and (○) 168 hrs aged (experimental)

(-) Unaged SAN (WLF), (-) 24 hrs aged (WLF), (-) 72 hrs aged (WLF) and (-) 168 hrs aged (WLF)

It is clear to see from Figure 3.35 that the aged SAN samples experimental values all appear to have a good correlation with their WLF predicted values. This suggests that the shifting of the data for the construction of the master curves were successful. It is

vital that this correlation is a good fit in order to have accurate results for fractional free volume calculations as well as C_1 and C_2 parameters to be calculated.

3.5.3 Fractional Free Volume

The Williams-Landel-Ferry parameters obtained by the shift factors of the master curves can be used to estimate the fractional free volume, f_0, and the thermal expansion coefficient of the free volume, $_T$, as show in equations [16]-[25] found in chapter one. The reference temperature was chosen to be the temperature at which the data intersects the x-axis.

Table 3.12 shows the C_1 and C_2 constants for the WLF equation as well as the calculated fractional free volume and the thermal expansion coefficient. It should be pointed out that values for the 24-hr aged 10% HDK-I/SAN and 168 hr aged samples were not included. The C_1 and C_2 constants for the pure polymer and the nanocomposites are all relatively close to the literature values[91]. For both the polymer and the nanocomposites the C_1 and C_2 parameters varied from 10.573 to 56.217 for the C_1 values and from 59.099 to 280.580 for C_2. Very little change in the C_1 and C_2 parameters may have suggested that due to the silica being dispersed and not grafted to the polymer a limited formation of a 3D network between the polymer and the silica. However, there does appear to be a good variation, this therefore suggests a relatively good formation of a 3D network between the nanocomposites and silica.

The fractional free volume also shows very limited variation. In each sample, there is very little change, from 0.0077 to 0.0411. There was no significant change in free volume when the SAN was dispersed with either the aggregated or colloidal silica samples. This suggests that as the chains relax, the presence of the silica nanoparticles does not affect the relaxation process during the physical aging. If the polymer-silica interaction was very strong a decrease in free volume may be expected, for example in grafted nanocomposites. In a study by Khlifa it was reported that a decrease in free volume was observed for the physical aging of PMMA/Silica nanocomposites. In this study the silica was chemically grafted to the PMMA.

Table 3.12 WLF parameters for aged SAN/Silica Nanocomposites

Sample	Aging Time (Hrs)	C_1	C_2	Ref. Temp (K)	T_g (K)	f_0	α_T
Pure SAN	0	19.004	128.555	379	374	0.0228	1.7×10^{-4}
Pure SAN	24	18.934	127.913	379	378	0.0229	1.8×10^{-4}
Pure SAN	72	26.411	145.117	379	378	0.0164	1.3×10^{-4}
Pure SAN	168	13.968	86.159	379	380	0.0310	3.6×10^{-4}
10% HDK-I/SAN	0	10.573	59.099	379	374	0.0411	6.9×10^{-4}
10% HDK-I/SAN	24	-	-	-	375	-	-
10% HDK-I/SAN	72	30.397	163.779	379	375	0.0143	8.7×10^{-5}
10% HDK-I/SAN	168	27.638	149.452	379	376	0.0157	1.1×10^{-4}
10% HDK-O/SAN	0	19.004	128.555	379	374	0.0228	1.8×10^{-4}
10% HDK-O/SAN	24	26.112	139.644	379	375	0.0166	1.2×10^{-4}
10% HDK-O/SAN	72	21.765	116.620	379	375	0.0199	1.7×10^{-4}
10% HDK-O/SAN	168	27.004	128.555	379	376	0.0161	1.3×10^{-4}
10% MEK-ST/SAN	0	19.004	128.554	379	376	0.0228	1.7×10^{-4}
10% MEK-ST/SAN	24	23.639	133.633	379	377	0.0184	1.4×10^{-4}
10% MEK-ST/SAN	72	56.217	280.580	379	378	0.0077	2.7×10^{-5}
10% MEK-ST/SAN	168	-	-	379	377	-	-

CHAPTER 4: Conclusions

The successful production of SAN nanocomposites was confirmed by the FTIR and DCS data as presented in Chapter 3. The influence of silica nanoparticles on both the thermal and mechanical properties of SAN nanocomposites was investigated with the use of DSC and DMA. The samples were prepared by the dispersion of the silica nanocomposites throughout the polymer at a composition of 10%. It was seen from the DSC data that the addition of silica nanoparticles to SAN had a very small but positive thermal effect on the pure polymer. In essence the positive thermal effect is describing how the addition of silica nanoparticles led to a small but noticeable increase in the T_g (thermal effect) of the nanocomposite and how, compared to the unaltered, aged SAN, the addition of the silica nanocomposites suggests a suppression of aging. Both the Wacker and MEK-ST silica had similar surface areas; therefore, the effects of reinforcement were taken to be due to the successful dispersion of the filler throughout the polymer matrix and this dispersion leading to the hydrogen bonding of the polymer chains with the silica nanoparticles. However, in the mechanical reinforcement effects studied by DMA for the unaged samples found that the HDK-O samples expressed the greatest positive reinforcement effect. The other nanocomposites exhibited very little change from the pure polymer for the unaged study. It was also found that the HDK-I sample expressed the largest rubbery plateau, suggesting the greatest cross-linking of the silica and polymer occurred within this sample. For example, the intermolecular interactions between the hydrogen of the silica nanoparticle and the nitrogen of the SAN (page 6).

Upon the physical aging of the SAN nanocomposites, a different trend was observed. At 24 and 72 Hr aging it was the MEK-ST sample which exhibited the greatest increase in stiffness of the samples closely followed by the HDK samples. This increase in stiffness is referring to the changes observed in the storage and loss moduli of the samples as well as the tan delta values. These refer to the mechanical effects that silica nanoparticles and aging have on the polymer. For example, in figure 3.20 where the storage modulus changes upon the addition of nanoparticles and a move of T_g values to higher temperatures. This suggests that the nanocomposites have a greater stiffness compared to that of the unalter polymer. When compared with the relaxation enthalpy data it was found that the MEK-ST sample reached its $\Delta H (\infty)$ quickest out of the silica samples. It is also known that physical aging causes an increase in the stiffness and

brittleness of a polymer, this result may be related to the MEK-ST reaching its fully relaxed state quicker than that of the other samples. The HDK samples once again exhibited very little deviance from the pure SAN and at 72Hr aging even expressed negative reinforcement.

From the relaxation enthalpy data, the Cowie-Ferguson model could be utilized in order to check the reliability of the results. The experimental values were found to fit well with the predicted in the case of the pure polymer. However, the experimental values, particularly the HDK-O samples, deviated greatly from the experimental values. It is clear to see here that some improvements in the method were required. Firstly, ensuring that only the one sample is aged and tested with no substitutes being used would remove one source of error. Secondly, being able to repeat the test several times would provide much more reliable data. Due to breakages and repair work being carried out on the equipment this was made very difficult to do with the time restraints. With regards to the relaxation enthalpy function, the MEK-ST sample showed similar values to that of the pure polymer whereas the Wacker samples both exhibited an increase in relaxation enthalpies.

Generation of master curves from the TTS data was used in order to calculate shift factors and fractional free volume. The shift factors were found to fit well to the Williams-Landel-Ferry equation and were taken to be accurate. Using the parameters obtained from the WLF equation the fractional free volume was found for each sample. All the filled nanocomposite samples expressed a slight decrease in free volume, this may be the result of the silica and the polymer interacting successfully, suggesting a uniformed structure is produced.

To summarize, this study aimed to investigate the reinforcement effects of filler nanoparticles in polymer-silica nanocomposites and the effects of physical aging on SAN nanocomposites. When we consider the reinforcement effects of the addition of silica nanoparticles, one would expect the silica to enhance the thermal and mechanical properties of the polymer. This is one of the reasons silica nanoparticles are so popular in industry. This study found that the addition of silica nanoparticles to SAN led to a small but positive reinforcement effect. For example in figure 3.5 a general increase in the T_g of the polymer could be seen upon the addition of filler nanoparticles as well as in figure 3.6 where a both the HDK-I and HDK-O samples both exhibited an increase in

the storage moduli of the samples upon the addition of filler nanoparticles. This was proposed to be due to the HDK-I and HDK-O silica samples aggregating to form a fractal structure in the elastic medium of the polymer. It also suggests that the colloidal nature of MEK-ST, which in that instance showed little deviation from the unaltered polymer, does not always lead to increased reinforcement. With respect to the physical aging effects on nanocomposites the addition of silica nanoparticles does, to a small degree regarding the samples used in this study, suppress the aging effects. This can be seen from the DMA and master curve data. For example, figures 3.2-3.4 it is clear to see that the filler samples all show a suppression in aging compared to the unfilled counterpart. This may suggest that the dispersion of the silica nanoparticle throughout the polymer matrix, led to the silica nanoparticles restricting the movement of the polymer chains through intermolecular interactions.

5.0 Further Work

One explanation for the reinforcement effects seen in polymer nanocomposites depends on the successful dispersion of the silica throughout the polymer matrix, in order to confirm that the samples were fully homogenous scanning electron microscopy could be carried out in order to confirm the lack of large agglomerates and the even dispersion of the silica. Unfortunately, due to time constraints this was not carried out. It would be interesting to look at trying to control the dispersion of the silica nanoparticles throughout the polymer matrix. One method for this may be the sol-gel reaction. The sol-gel process has been widely used to synthesise pure silica nanoparticles as it allows the user to control particle size, distribution and morphology through systematic monitoring of the reaction parameters[92].

Furthermore, unless any large abnormalities were seen the samples were only ran once on the DSC and DMA. Further repetition of the experiments could be carried out to verify the results. It may also be worth purchasing a new bottle of SAN from the same manufactures and repeating the experiments to see if the difference between the previously reported T_g and the experimental was due to water being absorbed.

As previously mentioned the HDK-O samples showed the greatest indifference compared to the pure SAN, in order to confirm whether the theory of the plasticizer effect of absorbed water is true, further time and care could be taken to try and obtain clearer H^1 NMR data to see if any solvent or moisture is present. Before preparation all the silica and polymer samples were dried in an oven overnight to try and reduced the effect of extra moisture however this does not mean that during the production or drying of the nanocomposite none was absorbed.

A further study could be done into nanoparticle loading and its impact in the percolation and confinement of the polymer matrix. This field offers a large area of expansion into the effects of nanoparticles on polymers. For example, work done by Shin *et al* looked the effect of interphase percolation on mechanical behaviour of nanoparticle-reinforced polymer nanocomposite with filler agglomeration[93]. Here they studied the correlation between inter-particulate distances of two neighbouring nanoparticles and the resulting elastic modulus of the nanocomposite. This would be interesting work to apply to the samples in this study.

References

1. Patel, S.; Bandyopadhyay, A.; Vijayabaskar, V.; Bhowmick, A. K., Effect of acrylic copolymer and terpolymer composition on the properties of *in-situ* polymer/silica hybrid nanocomposites. *J Mater Sci* **2006,** *41*, 927-936.
2. Saladino, M. L.; Motaung, T. E.; Luyt, A. S.; Spinella, A.; Nasillo, G.; Caponetti, E., The effect of silica nanoparticles on the morphology, mechanical properties and thermal degradation kinetics of PMMA. *Polymer Degradation and Stability* **2012,** *97*, 452-459.
3. Yu, F.; Huang, H.-X., Simultaneously toughening and reinforcing poly(lactic acid)/thermoplastic polyurethane blend via enhancing interfacial adhesion by hydrophobic silica nanoparticles. *Polymer Testing* **2015,** *45*, 107-113.
4. Zhang, J.; Liu, N.; Wang, M.; Ge, X.; Wu, M.; Yang, J.; Wu, Q.; Jin, Z., Preparation and Characterization of Polymer/Silica Nanocomposites via Double In Situ Miniemulsion Polymerization. *Journal of Polymer Science Part a-Polymer Chemistry* **2010,** *48* (14), 3128-3134.
5. Ribeiro, T.; Baleizao, C.; Farinha, J. P. S., Functional Films from Silica/Polymer Nanoparticles. *Materials* **2014,** *7*, 3881-3900.
6. Chemistry, R. S. o. Composite Materials. http://www.rsc.org/Education/Teachers/Resources/Inspirational/resources/4.3.1.pdf.
7. T.C., P.; Mathew, L.; Chandrasekaran, N.; Raichuran, A. M.; Mukherjee, A., Biomimetic Synthesis of Nanoparticles:

Science, Technology & Applicability Biomimetics, Learning from Nature: 2010; pp 1-20.
8. Nikalje , P. A., Nanotechnology and its Applications in Medicine. *Med Chem* **2015,** *5*.
9. Ocsial http://ocsial.com/en/.
10. Lee, D. W.; Yoo, B. R., Advanced silica/polymer composites: Materials and applications. *Journal of Industrial and Engineering Chemistry* **2016,** *38*, 1-12.
11. Education, T. J. N. A. F.-O. o. S. 10 Most Abundant Compounds in the Earth's Crust. http://education.jlab.org/faq/index.html.
12. Mi Lim, H.; Lee, J.; Jeong, J.-H.; Oh, S.-G.; Lee, S.-H., Comparative Study of Various Preparation Methods of Colloidal Silica. *Scientific Research Engineering* **2010,** *2*, 998-1005.
13. Silicones, W., There's more to it than you think.

HDK - Pyrogenic Silica 2008.
14. McNaught, A. D.; Wilkinson, A., *Compendium of Chemical Terminology*. 2 ed.; Blackwell Scientific Publications: Oxford, 1994.
15. Lutz, H. D., Structure and strength of hydrogen bonds in inorganic solids. *Journal of Molecular Structure* **2003,** *646* (1–3), 227-236.
16. Gibbs, J. H.; DiMarzio, E. A., Nature of the Glass Transition and the Glassy State. *The Journal of Chemical Physics* **1958,** *28* (3), 373-383.
17. University, C. W. R. Thermal Properties of Polymers. http://plc.cwru.edu/tutorial/enhanced/files/polymers/therm/therm.htm.
18. Berlin, H. U. Z., Investigation of Polymers with Differential Scanning Calorimetry. Berlin, H. U. Z.; I, M.-n. F.; Physik, I. f., Eds. Humbolt Universitat Zu Berlin, 2016.
19. Atkins, P. W.; De Paula, J., *Atkins' Physical chemistry*. Oxford University Press: Oxford; New York, 2014.
20. Hodge, I. M., Effects of Annealing and Prior History on Enthalpy Relaxation in Glassy Polymers. *Macromolecules* **1982,** *16*, 898.
21. Struik, L. C. E., Physical Aging in Plastics and Other Glassy Materials. *Polymer Engineering and Science* **1977,** *17* (3), 165-173.
22. Cangialosi, D.; Boucher, V. M.; Alegria, A.; Colmenero, J., Physical aging in polymers and polymer nanocomposites: recent results and open questions. *Soft Matter* **2013,** *9* (36), 8619-8630.

23. Priestley, R. D.; Ellison, C. J.; Broadbelt, L. J.; Torkelson, J. M., Structural Relaxation of Polymer Glasses at Surfaces, Interfaces, and In Between. *Science* **2005,** *309* (5733), 456-459.
24. Cangialosi, D.; Boucher, V. M.; Alegría, A.; Colmenero, J., Enhanced physical aging of polymer nanocomposites: The key role of the area to volume ratio. *Polymer* **2012,** *53* (6), 1362-1372.
25. Boucher, V. M.; Cangialosi, D.; Alegria, A.; Colmenero, J.; Gonzalez-Irun, J.; Liz-Marzan, L. M., Accelerated physical aging in PMMA/silica nanocomposites. *Soft Matter* **2010,** *6* (14), 3306-3317.
26. Ramakrishnan, V.; Harsiny, S.; Goossens, J. G. P.; Hoeks, T. L.; Peters, G. W. M., Physical aging in polycarbonate nanocomposites containing grafted nanosilica particles: A comparison between enthalpy and yield stress evolution. *Journal of Polymer Science Part B: Polymer Physics* **2016**.
27. Cernosek, Z.; Holubova, J.; Cernoskova, E.; Liska, M., Enthalpic Relaxtion and the Glass Transition *Journal of Optoelectronics and Advanced Materials* **2002,** *4* (3), 489-503.
28. Haque, K.; Kawai, K.; Suzuki, T., Glass Transition and enthalpy relaxation of amorphous lactose glass. *Carbohydrate Research* **2006,** *341*, 1884-1889.
29. Haque, M. K.; Kawai, K.; Suzuki, T., Glass transition and enthalpy relaxation of amorphous lactose glass. *Carbohydrate Research* **2006,** *341* (11), 1884-1889.
30. Newman, A., Using Thermal Techniques for Amorphous Materials. **2012**.
31. Anzai, M.; Hagiwara, T.; Watanabe, M.; Komiyama, J.; Suzuki, T., Relationship between enthalpy relaxation and water sorption of ball-milled potato starch. *Journal of Food Engineering* **2011,** *104* (1), 43-48.
32. George, R. M., Freezing proceseses used in the food industry. *Trends in Food Science & Technology* **1993,** *4* (5), 134-138.
33. Cowie, J. M. G.; Arrighi, V., Physical Aging of Polymer Blends. In *Polymer Blends Handbook*, 2nd ed.; Springer: 2014; pp 1357-1394.
34. Cowie, J. M. G.; Ferguson, R., Physical aging studies in poly(vinyl methyl ether). 1. Enthalpy relaxation as a function of aging temperature. *Macromolecules* **1989,** *22* (5), 2307-2312.
35. Wungtanagorn, R.; Schmidt, S. J., THERMODYNAMIC PROPERTIES AND KINETICS OF THE PHYSICAL AGEING OF AMORPHOUS GLUCOSE, FRUCTOSE, AND THEIR MIXTURE. *Journal of Thermal Analysis and Calorimetry* **2000,** *54*, 9-35.
36. Pochiraju, V. K.; Tandon, P. G.; Schoeppner, G., *Long Term Durability of Polymer Matrix Composites*. Springer: new york, 2011; Vol. 1, p 247-251.
37. McKenna, G. B.; Simon, S. L., Time Dependent Volume and Enthalpy Responses in Polymers. American Society for Testing and Materials, 2000; pp 18-46.
38. Hutchinson, J. M., *Physcial ageing of polymers*. elsevier science ldt: 1995; Vol. 20.
39. Hutchinson, J. M.; Ingram, D.; Pappin, A. J., Enthalpy Relaxation in Polymer Glasses: Evaluation and Interpretation of the Tool-Narayanaswamy Parameter x for Poly(vinyl chloride). Macromolecules: 1992; Vol. 2, pp 1084-1089.
40. Ramos, A. R.; Hutchinson, J. M.; Kovacs, A. J., Isobaric thermal behavior of glasses during uniform cooling and heating. III. Predictions from the multiparameter KAHR model. Journal of Polymer Science: Polymer Physics Edition: 1984; Vol. 22, pp 1655-1696.
41. Grassia, L.; Simon, S. L., Modeling Volume Relaxation of Amorphous Polymers: modification of the equation for the relaxation time in the KAHR model. In *Polymer*, Elsevier: 2012; Vol. 53, pp 3613-3620.
42. Schultheisz, C. R.; McKenna, G. B., Volume Recovery, Physical Aging and the Tau-Effective Paradox in Glassy Polycarbonate following Temperature Jumps. Proceedings North American Thermal Analysis Society: 1997; Vol. 25th Annual meeting, pp 336-373.

43. Medvedev, G. A.; Starry, A. B.; Ramkrishna, D.; Caruthers, J. M., Stochastic Model for Volume Relaxation in Glass Forming Materials: Local Specific Volume Model. Macromolecules: 2012; Vol. 45, pp 7237-7259.
44. McKenna, G. B.; Simon, S. L., 50th Anniversary Perspective: Challenges in the Dynamics and Kinetics of Glass Forming Polymers. Macromolecules: 2017; Vol. 50, pp 6333-6361.
45. Elmer, P. Introduction to DMA. www.perkinelmer.co.uk/CMSResources/Images/44-74546GDE_introductiontoDMA.pdf.
46. Technologies, T., What is Dynamic Mechanical Analysis, DMA? 2016; pp 1-2.
47. van Gurp, M.; Palmen, J., Time-Temperature superposition for Polymeric Blends. DSM Research: 1998.
48. Instruments, T., Guidelines for using TTS. In *TA Instruments*, 2016.
49. Ferry, J.; Myers, H., Viscoelastic Properties of Polymers. *Journal of The Electrochemical Society* **1961,** *108*, 142.
50. Lee, M. H.; Han, D. H.; Cho, B.; liquids, T. t. d. o. t. d. e. p. f. p.; -, J.; Sci., J.-J. A. P.; 50, V.-.; 10, I.-.; PB - Wiley Subscription Services, I., A Wiley Company; 1097-4628, S.-.; http://dx.doi.org/10.1002/app.1993.070501016, U.-.; 10.1002/app.1993.070501016, D.-.; 1803, S.-.; 1806, E.-.; 1993, P.-. The temperature dependence of the doolittle equation parameter for polymer liquids. *Journal of Applied Polymer Science* **1993,** *50* (10).
51. Markovitz, H., Thomas G. Fox 1921–1977. *Rheologica Acta* **1978,** *17* (3), 207-209.
52. Payne, A. R., Effect of Dispersion on the Dynamic Properties of Filler-Loaded Rubbers. *Journal of Applied Polymer Science* **1965,** *9*, 2273-2284.
53. Tsagaropoulos, G.; Eisenburg, A., Direct observation of two glass transitions in silica-filled polymers. Implications to the morphology of random ionomers. *Macromolecules* **1995,** *28* (1), 396-398.
54. Berriot, J.; Montes, H.; Lequeux, F.; Long, D.; Sotta, P., Evidence for the Shift of the Glass Transition near the Particles in Silica-Filled Elastomers. *Macromolecules* **2002,** *35* (26), 9756-9762.
55. Bogoslovov, R. B.; Roland, C. M.; Ellis, A. R.; Randell, A. M.; Robertson, G. C., Effect of Silica Nanoparticles on the Local Segmental Dynamics inPoly(vinyl acetate). *Macromolecules* **2007,** *41*, 1289-1296.
56. Zhu, Z.; Thompson, T.; Wang, S.-Q.; von Meerwall, E. D.; Halasa, A., Investigating Linear and Nonlinear Viscoelastic Behavior Using Model Silica-Particle-Filled Polybutadiene. *Macromolecules* **2005,** *38* (21), 8816-8824.
57. Chen, F.; Clough, A.; Reinhard, B. M.; Grinstaff, M. W.; Jiang, N.; Koga, T.; Tsui, O. K. C., Glass Transition Temperature of Polymer–Nanoparticle Composites: Effect of Polymer–Particle Interfacial Energy. *Macromolecules* **2013,** *46* (11), 4663-4669.
58. Korwin, R. S.; Masui, H., Effect of silica and water content on the glass transition of poly(ethylene glycol) monomethylether–silica gel–lithium perchlorate ormolytes. *Thermochimica Acta* **2005,** *433* (1–2), 157-162.
59. Khlifa, M.; Youssef, A.; Zaed, A. F.; Kraft, A.; Arrighi, V., Synthesis of Polystyrene Grafting Filler Nanoparticles:

Effect of Grafting on Mechanical Reinforcement *International Journal of Chemical, Molecular, Nuclear, Materials and Metallurgical Engineering* **2014,** *8* (12), 1358-1362.
60. Mélé, P.; Marceau, S.; Brown, D.; de Puydt, Y.; Albérola, N. D., Reinforcement effects in fractal-structure-filled rubber. *Polymer* **2002,** *43* (20), 5577-5586.
61. Fragiadakis, D.; Pissis, P., Glass transition and segmental dynamics in poly(dimethylsiloxane)/silica nanocomposites studied by various techniques. *Journal of Non-Crystalline Solids* **2007,** *353* (47–51), 4344-4352.
62. Xanthos, M. *FUNCTIONAL FILLERS FOR PLASTICS:FROM MICRO- TO NANO- TO BIO-COMPOSITES*.

63. Rejón, L.; Saldivar-Guerrero, R.; Castillo-Ocampo, P., CHARACTERIZATION OF NANOCOMPOSITES PRODUCED WITH

THERMOSETTING RESINS AND SILICA NANOPARTICLES *Proceedings of the Polymer Processing Society 24th Annual Meeting* **2008**, 1-5.
64. Potente, H.; Flecke, J., The Division of Agglomerates in Molten Environment of Polymers: A Physical Model for Mathematical Description A2 - Pourdeyhimi, Behnam. In *Imaging and Image Analysis Applications for Plastics*, William Andrew Publishing: Norwich, NY, 1999; pp 257-266.
65. Sanz, A.; Wong, H. C.; Nedoma, A. J.; Douglas, J. F.; Cabral, J. T., Influence of C60 fullerenes on the glass formation of polystyrene. *Polymer* **2015,** *68*, 47-56.
66. Sternstein, S. S.; Zhu, A.-J., Reinforcement Mechanism of Nanofilled Polymer Melts As Elucidated by Nonlinear Viscoelastic Behavior. *Macromolecules* **2002,** *35* (19), 7262-7273.
67. Moussa, K.; Johnston, K.; Nebel, A.; Langford, R.; Kraft, A.; Arrighi, V., Influence of Aggregation and Grafting on Thermal and Dynamic Mechanical Properties of Polymer-Silica Nanocomposites. **2015**.
68. Dittanet, P.; Pearson, R. A., Effect of silica nanoparticle size on toughening mechanisms of filled epoxy. *Polymer* **2012,** *53* (9), 1890-1905.
69. Feng, Y.; Wang, B.; Wang, F.; Zheng, G.; Dai, K.; Liu, C.; Chen, J.; Shen, C., Effects of modified silica on morphology, mechanical property and thermostability of injection-molded polycarbonate/silica nanoparticles. *Journal of Reinforced Plastics and Composites* **2013,** *33* (10), 911-922.
70. Fu, S.-Y.; Feng, X.-Q.; Lauke, B.; Mai, Y.-W., Effects of particle size, particle/matrix interface adhesion

and particle loading on mechanical properties

of particulate–polymer composites. *Composites: Part B* **2008,** *39*, 933–961.
71. Lin, Y.; Shangguan, Y.; Qiu, B., Segmental dynamics and physical aging of

polystyrene/silver nanocomposites. *RSC Advances* **2014,** *4* (39), 20086-20093.
72. Boucher, V. M.; Cangialosi, D.; Alegria, A.; Colmenero, J., Time dependence of the segmental relaxation time of poly(vinyl acetate)-silica nanocomposites. *Physical Review E* **2012,** *86* (4).
73. Fu, S.-Y.; Feng, X.-Q.; Lauke, B.; Mai, Y.-W., Effects of particle size, particle/matrix interface adhesion

and particle loading on mechanical properties

of particulate–polymer composites. *Composites: Part B* **2008,** *39*, 933–961.
74. Federation, B. P. Styrene Acrylonitrile (SAN) & Acrylonitrile Styrene Acrylate (ASA). http://www.bpf.co.uk/plastipedia/polymers/SAN.aspx.
75. Cameron, N.; Cowie, J. M. G.; Ferguson, R.; Gómez Ribelles, J. L.; Más Estellés, J., Transition from miscibility to immiscibility in blends of poly(methyl methacrylate) and styrene–acrylonitrile copolymers with varying copolymer composition: a DSC study. *European Polymer Journal* **2002,** *38* (3), 597-605.
76. Bregg, R. K., *Frontiers in Polymer Research*. Nova Science Publishers: 2006.
77. Tsagaropoulos, G.; Eisenberg, A., Dynamic Mechanical Study of the Factors Affecting the Two Glass Transition Behavior of Filled Polymers. Similarities and Differences with Random Ionomers. *Macromolecules* **1995,** *28* (18), 6067-6077.
78. Group, C. P. *Glass Transition by DMA*; 2014.
79. Koerner, H.; Opsitnick, E.; Grabowski, C. A.; Drummy, L. F.; Hsiao, M.-S.; Che, J.; Pike, M.; Person, V.; Bockstaller, M. R.; Meth, J. S.; Vaia, R. A., Physical aging and glass

transition of hairy nanoparticle assemblies. *Journal of Polymer Science Part B: Polymer Physics* **2016,** *54* (2), 319-330.
80. Robertson, C. G.; Wilkes, G. L., Physical aging behavior of miscible blends of poly(methyl methacrylate) and poly(styrene-co-acrylonitrile). *Polymer* **2001,** *42* (4), 1581-1589.
81. Lee, A.; Litchtenhan, J., Viscoelastic Responses of Polyhedral Oligosilsesquioxane Reinforced Epoxy Systems. *Macromolecules* **1998,** *31* (15), 4970-4974.
82. Lee, C.-H.; Liu, J.-Y.; Chen, S.-L.; Wang, Y.-Z., Miscibility and Properties of Acid-Treated Multi-Walled Carbon Nanotubes/Polyurethane Nanocomposites. *Polym. J* **2006,** *39* (2), 138-146.
83. Rittigstein, P.; Torkelson, J. M., Polymer–nanoparticle interfacial interactions in polymer nanocomposites: Confinement effects on glass transition temperature and suppression of physical aging. *Journal of Polymer Science Part B: Polymer Physics* **2006,** *44* (20), 2935-2943.
84. University, R. Solvents and Workup: Reaction Solvents. http://chem.rochester.edu/~nvd/pages/tips/_workup.php (accessed 24/03/2017).
85. Centre, P. S. L. Differential Scanning Calorimetry. http://www.pslc.ws/macrog/dsc.htm (accessed 30/04/2017).
86. Amanuel, S.; Gaudette, A.; Sternstein, S. S., Enthalpic relaxation of silica–polyvinyl acetate nanocomposites. *Journal of Polymer Science Part B Polymer Physics* **2008,** *46* (24), 2733-2733.
87. Boucher, V. M.; Cangialosi, D.; Alegría, A.; Colmenero, J., Enthalpy Recovery of PMMA/Silica Nanocomposites. *Macromolecules* **2010,** *43* (18), 7594-7603.
88. Holt, A. P.; Sangoro, J. R.; Wang, Y.; Agapov, A. L.; Sokolov, A. P., Chain and Segmental Dynamics of Poly(2-vinylpyridine) Nanocomposites. *Macromolecules* **2013,** *46* (10), 4168-4173.
89. Baeza, G. P.; Dessi, C.; Costanzo, S.; Zhao, D.; Gong, S.; Alegria, A.; Colby, R. H.; Rubinstein, M.; Vlassopoulos, D.; Kumar, S. K., Network dynamics in nanofilled polymers. *Nat Commun* **2016,** *7*.
90. M. G. Cowie, J.; J. McEwen, I.; Matsuda, S., Stress relaxation and physical ageing in a blend of poly(styrene-co-acrylonitrile) and poly(methyl methacrylate). *Journal of the Chemical Society, Faraday Transactions* **1998,** *94* (23), 3481-3486.
91. Douglas, J. F.; Freed, K. F., The meaning of the "universal" WLF parameters of glass-forming polymer liquids. *The Journal of Chemical Physics* **2015,** *142*.

92. Rahemen, I. A; Padevettan, V.; Synthesis of Silica Nanoparticles by Sol-Gel: Size-Dependent Properties, Surface Modification and Applications in Silica-Polymer Nanocomposites- A Review, *The Journal of Nanomaterials*, 2012, **15**
93**.** Shin, H., Yang, S., Choi, J., Chang, S., Cho, M.; Effect of interphase percolation on mechanical behaviour of nano-particle-reinforced polymer nanocomposite with filler agglomeration: A multiscale approach; Chemical Physical Letters, 2015, 635, P80-85

Appendix I

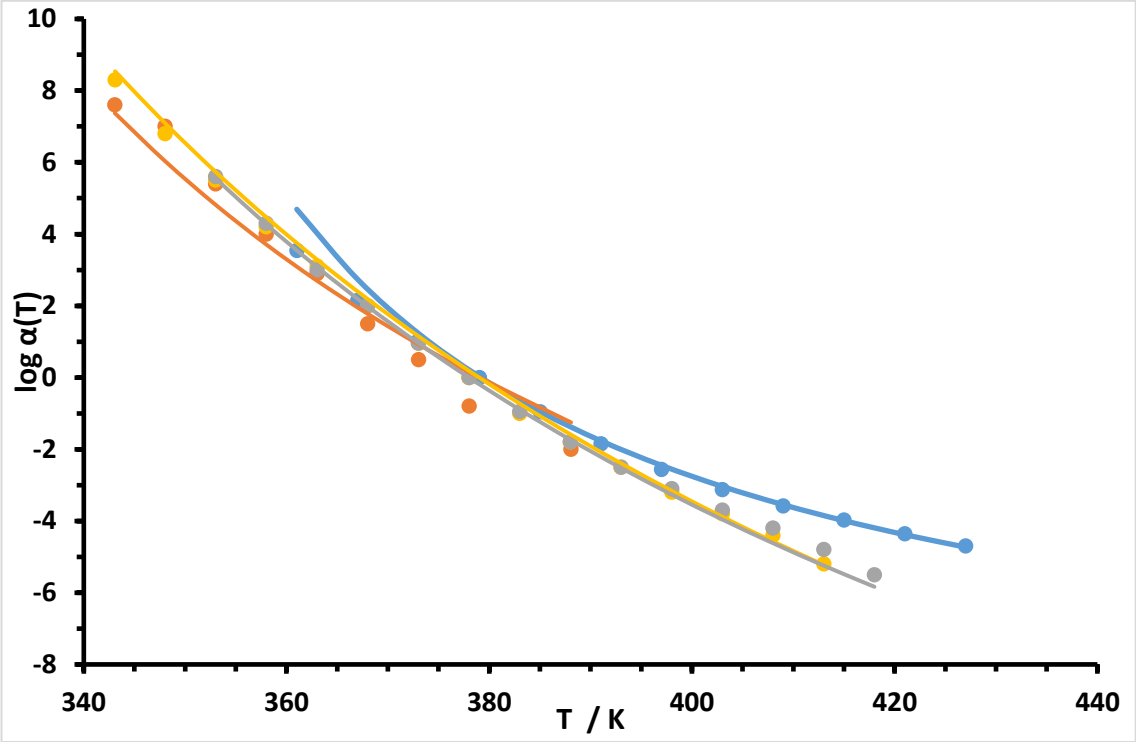

Figure 3.36: Shift Factor plot and WLF fit for HDK-I nanocomposite samples

(○) Unaged SAN (experimental), (○) 24 hrs aged (experimental), (○) 72 hrs aged (experimental) and (○) 168 hrs aged (experimental)

(-) Unaged SAN (WLF), (-) 24 hrs aged (WLF), (-) 72 hrs aged (WLF) and (-) 168 hrs aged (WLF)

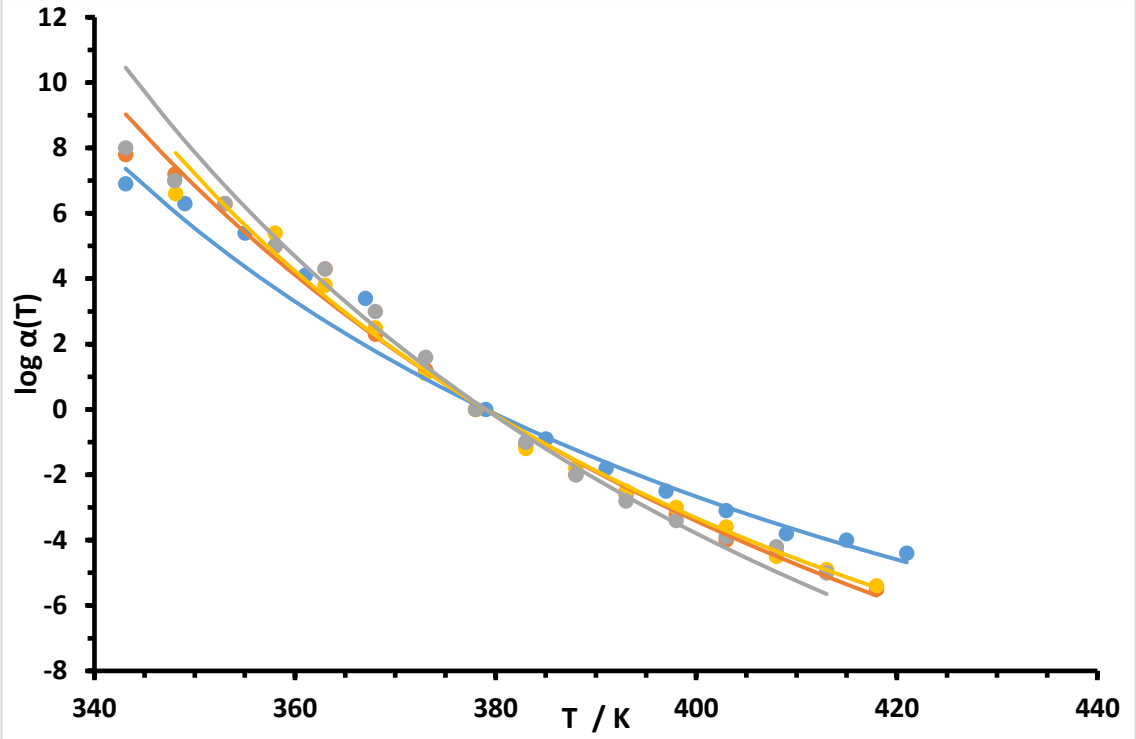

Figure 3.37: Shift Factor plot and WLF fit for HDK-O Nanocomposite samples

(○) Unaged SAN (experimental), (○) 24 hrs aged (experimental), (○) 72 hrs aged (experimental) and (○) 168 hrs aged (experimental)

(-) Unaged SAN (WLF), (-) 24 hrs aged (WLF), (-) 72 hrs aged (WLF) and (-) 168 hrs aged (WLF)

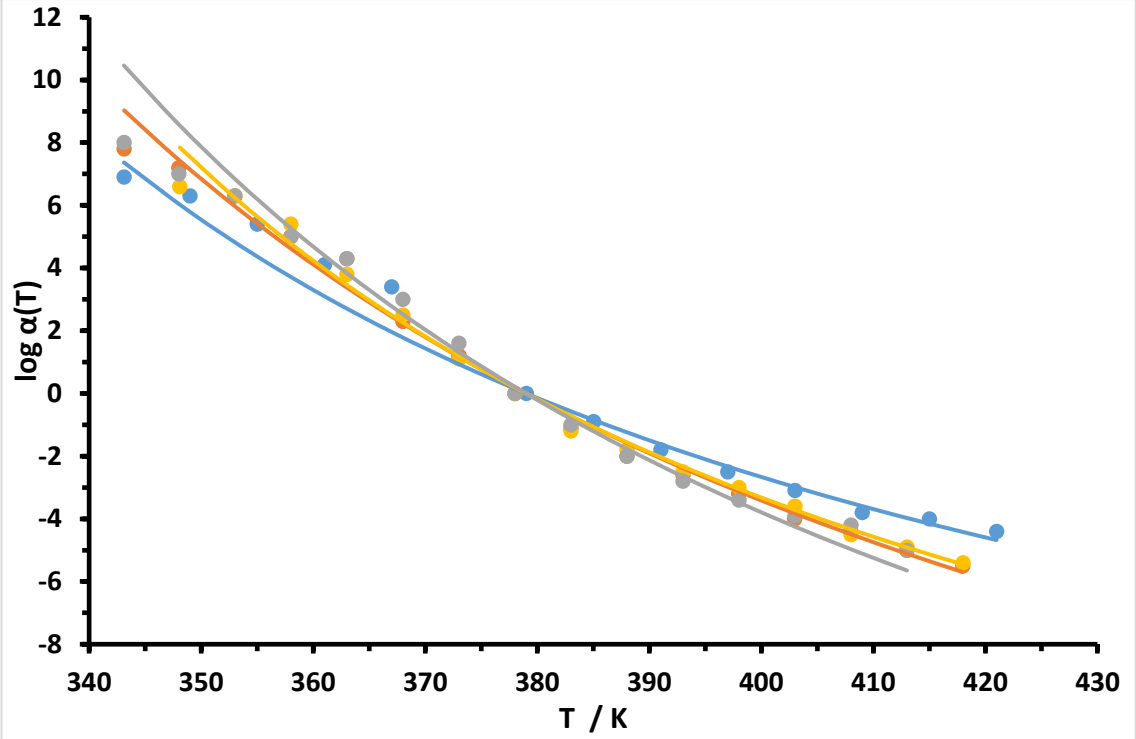

Figure 3.38: Shift Factor plot and WLF fit for MEK-ST Nanocomposite samples

(○) Unaged SAN (experimental), (○) 24 hrs aged (experimental), (○) 72 hrs aged (experimental) and (○) 168 hrs aged (experimental)

(-) Unaged SAN (WLF), (-) 24 hrs aged (WLF), (-) 72 hrs aged (WLF) and (-) 168 hrs aged (WLF)